



PONTIFÍCIA UNIVERSIDADE CATÓLICA DO RIO GRANDE DO SUL
FACULDADE DE BIOCÊNCIAS
MESTRADO EM BIOLOGIA CELULAR E MOLECULAR

BRUNO COUTO GIACOBBO

**2-((QUINOLIN-4-IL)OXI)-FENILACETAMIDAS: SÍNTESE, CARACTERIZAÇÃO
ESTRUTURAL E ATIVIDADE INIBITÓRIA SOBRE O CRESCIMENTO DO
*MYCOBACTERIUM TUBERCULOSIS***

Porto Alegre

2016

BRUNO COUTO GIACOBBO

**2-((QUINOLIN-4-IL)OXI)-FENILACETAMIDAS: SÍNTESE, CARACTERIZAÇÃO
ESTRUTURAL E ATIVIDADE INIBITÓRIA SOBRE O CRESCIMENTO DO
*MYCOBACTERIUM TUBERCULOSIS***

Dissertação apresentada ao Programa de Pós-Graduação em Biologia Celular e Molecular da Faculdade de Biologia da Pontifícia Universidade Católica do Rio Grande do Sul.

Orientador

Prof. Dr. Pablo Machado

Porto Alegre

2016

BRUNO COUTO GIACOBBO

**2-((QUINOLIN-4-IL)OXI)-FENILACETAMIDAS: SÍNTESE, CARACTERIZAÇÃO
ESTRUTURAL E ATIVIDADE INIBITÓRIA SOBRE O CRESCIMENTO DO
*MYCOBACTERIUM TUBERCULOSIS***

Dissertação apresentada ao Programa de Pós-Graduação em Biologia Celular e Molecular da Faculdade de Biologia da Pontifícia Universidade Católica do Rio Grande do Sul.

BANCA EXAMINADORA:

Prof. Dr. Alex Fabiani Claro Flores - FURG

Profa. Dra. Áurea Echevarria - UFRRJ

Profa. Dra. Fernanda Bueno Morrone - PUCRS

Porto Alegre

2016

AGRADECIMENTOS

Agradeço aos meus orientadores Prof. Dr. Pablo Machado e Dra. Kenia Pissinate, pela oportunidade de desenvolver este trabalho, pelos ensinamentos dados durante a realização do mesmo e pela confiança depositada.

Agradeço a todos os meus colegas do Centro de Pesquisa em Biologia Molecular e Funcional, pela colaboração e amizade.

Agradeço a todos meus amigos e familiares pelo apoio durante estes 2 anos do curso.

Agradeço a todos os colaboradores externos, por disponibilizarem tempo e recursos para a realização deste trabalho.

Agradeço ao Programa de Pós-Graduação em Biologia Celular e Molecular da PUCRS.

Agradeço a Pontifícia Universidade Católica do Rio Grande do Sul.

Agradeço a CAPES pela bolsa de estudos o que me permitiu realizar o curso de Mestrado.

LISTA DE FIGURAS

Figura 1. Incidência da Tuberculose (WHO, 2015).....	12
Figura 2. Estrutura e constituintes celulares do granuloma da TB. (Ramakrishnan L, 2012).....	13
Figura 3: Estrutura geral dos compostos quinolínicos e sua numeração.....	18
Figura 4. Estruturas químicas de fármacos utilizados para o tratamento da tuberculose contendo o núcleo quinolínico: a) Levofloxacina; b) Ofloxacina; c) Gatifloxacina; d) Moxifloxacina; e) Sirturo™.	20
Figura 5. Exemplo de compostos apresentados por Beena, <i>et al.</i> , (2012). a) MIC: 0,78 µM; b) MIC: 0,78 µM; c) MIC: 0,78 µM; d) MIC: 66,1 µM.....	21
Figura 6. a) Estrutura do GSK358607A(QOA) MIC: 0,70 µM; b) Estrutura do GSK749336A(QOA), MIC: 0,25 µM; c) GW857165X (QOA) MIC: 3,3 µM.....	22
Figura 7. Estratégia geral para a identificação de potenciais compostos antituberculose a partir de composto líder GSK358607A identificado em estudos de triagem fenotípica que culminaram na descoberta do composto 5s.....	23

SUMÁRIO

1	INTRODUÇÃO	11
1.1	TUBERCULOSE	11
1.2	PATOGÊNESE	12
1.3	TRATAMENTO.....	14
1.4	RESISTÊNCIA AOS FÁRMACOS.....	15
1.5	QUINOLINAS	18
1.6	RELAÇÃO ESTRUTURA QUÍMICA ATIVIDADE BIOLÓGICA (SAR)	22
2	JUSTIFICATIVA	25
3	OBJETIVOS	27
3.1	OBJETIVOS ESPECÍFICOS	27
4	ARTIGO CIENTÍFICO	28
5	CONSIDERAÇÕES FINAIS	90
6	REFERÊNCIAS BIBLIOGRÁFICAS	91

LISTA DE ABREVIações

ATP – Adenosina 5'-trifosfato
ACN – Acetonitrila
CYP3A4 – Citocromo P3A4
CPBMF – Centro de Pesquisa em Biologia Molecular e Funcional
CCD – Cromatografia de Camada Delgada
CLAP – Cromatografia Líquida de Alta Precisão
CFU – Unidades Formadoras de Colônia
DNA – Ácido Desoxirribonucleico
DMAP – 4-(Dimetilamino)piridina
DMF – Dimetilformamida
DMSO – Dimetil Sulfóxido
FDA – *Food and Drug Administration*
FTIR – Espectroscopia de Infravermelho
GSK – GlaxoSmithKline
HIV – Vírus da Imunodeficiência Humana
HTS – *Hight Troughtput Screening*
HCl – Ácido Clorídrico
HRMS – Espectrometria de Massas de Alta Resolução
INH – Isoniazida
INCT-TB – Instituto Nacional de Ciência e Tecnologia em Tuberculose
K₂CO₃ – Carbonato de Potássio
M. tuberculosis – *Mycobacterium tuberculosis*
MIC – Concentração Inibitória Mínima
MeOH – Metanol
MTT – Brometo de (3-(4,5-dimetiltiazol-2-il)-2,5-difeniltetrazólio)
NaHCO₃ – Bicarbonato de Sódio
NB3 – Nível de Biossegurança 3
OMS – Organização Mundial da Saúde
QOA – Quinoloxiacetamida
RIF – Rifampicina
RMN – Ressonância Magnética Nuclear

SIDA – Síndrome da Imunodeficiência Humana

SAR – Relação Estrutura-Atividade

TB – Tuberculose

TB-MDR – Tuberculose Resistente a Múltiplas Drogas

TB-XDR – Tuberculose Extensivamente resistente a drogas

UV – Ultravioleta

Resumo

A tuberculose (TB) é uma doença infecciosa causada principalmente por *Mycobacterium tuberculosis* e é um dos problemas de saúde pública mais devastadores no mundo. Além disso, tratamentos de XDR-TB e MDR-TB são limitados e os medicamentos recomendados frequentemente não estão disponíveis, ressaltando uma necessidade urgente de novas alternativas anti-TB. No presente estudo, uma série de 2-(quinolin-4-iloxi)acetamidas foi sintetizada para posterior avaliação da concentração inibitória mínima (MIC) frente a cepas de *Mycobacterium tuberculosis* (Mtb). Além disso, um estudo preliminar da relação estrutura-atividade (SAR) também foi realizado. Os compostos sintetizados foram avaliados no ensaio *in vitro* frente ao *M. tuberculosis* cepas H37Rv e isolado clínico resistente a fármacos. Os compostos mais ativos frente ao *M. tuberculosis* H37Rv (MIC < 1 μ M) foram selecionados para estudos de viabilidade em células Vero. Os resultados mostraram que o volume molecular e a hidrofobicidade na porção *N*-arilamida, o efeito doador ligação de hidrogênio na porção acetamida e o receptor na posição 4 do anel quinolínico representam três grupos farmacofóricos importantes para a ação antimicobacteriana. Além disso, os compostos sintetizados **6a**, **6h**, **12d-f**, e **12i-n** foram ativos frente a cepa resistente aos medicamentos (MIC \geq 0,001 μ M) com desprovida citotoxicidade aparente para Vero (IC₅₀ \geq 20 μ M). Portanto, estes dados indicam que esta classe de compostos pode apresentar candidatos para o desenvolvimento futuro, e oferecer alternativas de medicamentos para o tratamento da tuberculose.

Palavras-chave: *Mycobacterium tuberculosis*, antitubercular, quinolina, 2-(quinolin-4-iloxi)acetamidas, SAR.

Abstract

Tuberculosis (TB) is an infectious disease caused mainly by *Mycobacterium tuberculosis* and is one of the most devastating public health problems worldwide. Furthermore, MDR-TB and XDR-TB treatments are limited and recommended medicines are often not available revealing an urgent need for new anti-TB alternatives. In the present study, a series of 2-(quinolin-4-yloxy)acetamides were synthesized for further evaluation of minimum inhibitory concentration (MIC) against *Mycobacterium tuberculosis* (Mtb) strains. Moreover, a preliminary structure-activity relationship (SAR) study was also performed. The synthesized compounds were evaluated in a whole-cell assay against *M. tuberculosis* H37Rv and drug-resistant clinical isolate. The most active molecules against *M. tuberculosis* H37Rv (MIC $<1\mu\text{M}$) were selected for cytotoxicity study in Vero cells. The results showed that the molecular volume and hydrophobicity at the *N*-arylamide portion, the effect hydrogen bond donor on the acetamide moiety and an H-bond acceptor at 4-position of the quinoline ring represent three pharmacophoric groups important for antimycobacterial action. Further, the synthesized compounds **6a**, **6h**, **12d-f**, and **12i-n** were active against drug-resistant strains (MICs $\geq 0,001\mu\text{M}$) with devoid of apparent cytotoxicity to Vero (IC₅₀s $\geq 20\mu\text{M}$). Therefore, these data indicate that this class of compounds may furnish candidates for future development, and to provide drug alternatives for tuberculosis treatment.

Keywords: *Mycobacterium tuberculosis*, antitubercular, quinoline, 2-(quinoline-4-yloxy)acetamides, SAR.

1 INTRODUÇÃO

1.1 TUBERCULOSE

A tuberculose (TB) é uma doença infectocontagiosa, que ataca principalmente o pulmão, podendo ser contraída através do contato com o *Mycobacterium tuberculosis* (*M. tuberculosis*), seu principal agente causador. Segundo dados do relatório de 2015 da Organização Mundial da Saúde (OMS), a TB foi responsável pela morte de 1,5 milhões de pessoas em 2014, sendo que desses óbitos, 25% foram entre pacientes HIV positivos. No mesmo ano, foram estimados 9,6 milhões de novos casos de tuberculose, sendo que em 12% dos casos os pacientes eram HIV positivos (WHO, 2015). A TB é a segunda maior causa de morte por doenças infecciosas em todo o mundo, estando somente atrás da síndrome da imunodeficiência humana (SIDA) (WHO, 2015). Esse panorama evidencia as proporções pandêmicas da TB e as razões da doença ser considerada um dos maiores problemas de saúde pública do mundo (WHO, 2015). Todos os países do mundo têm registro de casos de TB e, a cada ano, estima-se o surgimento de milhões de novos casos. O sudoeste asiático e regiões do pacífico oeste contabilizaram 58% dos casos de TB no ano de 2014. A região da África soma a maior incidência de casos e de mortes em relação ao total da população. Em relação ao Brasil, no ano de 2014, a OMS estimou o surgimento de 42 a 56 casos de TB a cada 100.000 habitantes (Figura 1). Dentre as capitais brasileiras, Porto Alegre é a terceira com a maior incidência, registrando 100 novos casos de TB a cada 100.000 habitantes no ano de 2012, ficando atrás somente de Cuiabá e Recife, com registros de 117 e 101 novos casos, respectivamente (Ministério da Saúde, 2012).

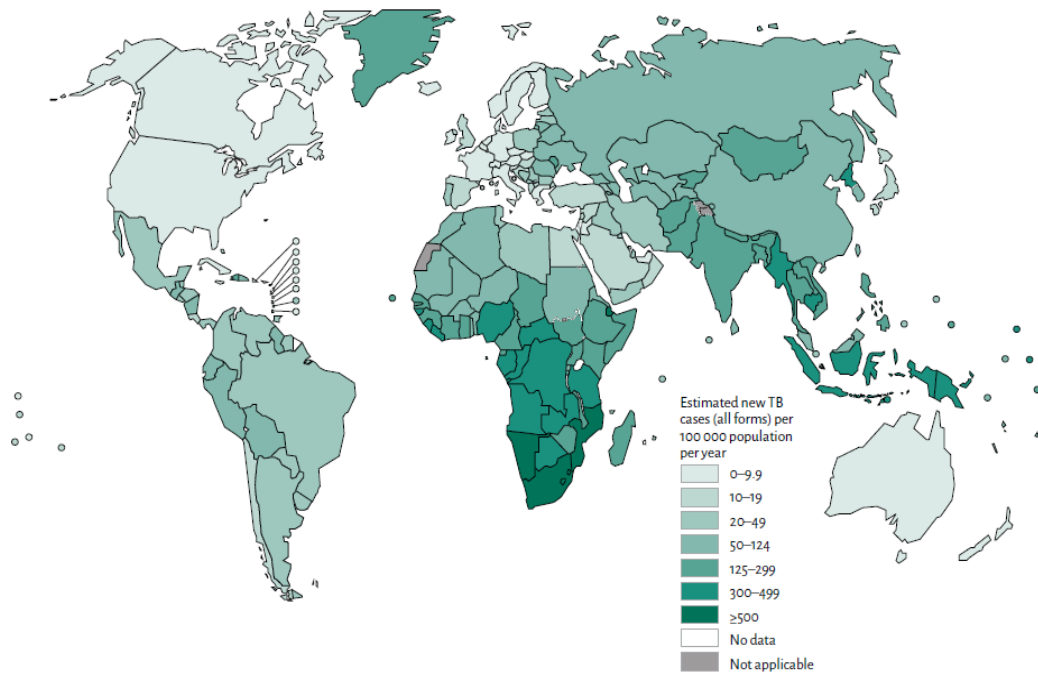


Figura 1. Incidência da Tuberculose (WHO, 2015)

1.2 PATOGÊNESE

Embora o *M. tuberculosis* possa infectar diversos órgãos do hospedeiro (TB extrapulmonar), a TB pulmonar é a manifestação mais comum (Kaufmann SHE, 2001; Flynn JL, Chan J, 2001).

A infecção em humanos é normalmente adquirida pela inalação de aerossóis contendo um pequeno número de bacilos (Kaufmann SHE, 2001; Russell DG, 2007) através de gotículas (*droplets*) expelidas da garganta e dos pulmões de indivíduos que possuem a forma pulmonar ativa da doença (Kaufmann SHE, 2001; Lamichhane G, 2010). Uma vez nos pulmões, os bacilos são internalizados por fagocitose pelos macrófagos alveolares e induzem uma resposta pró-inflamatória localizada, que leva ao recrutamento de outras células do sistema imune do hospedeiro, como neutrófilos, monócitos e células dendríticas (Russell DG, 2007; Ernst JD, 2012; Zahrt TC, 2003). Os macrófagos alveolares ativados por estímulos específicos podem transferir o *M. tuberculosis* fagocitado para os lisossomos, a fim de serem eliminados (Kaufmann SHE, 2001). No entanto, o bacilo tem desenvolvido inúmeras estratégias que evitam a sua eliminação e permitem que o mesmo sobreviva dentro dos macrófagos (Zahrt TC, 2003), uma vez que essas células são

capazes de conter o crescimento, mas não de eliminar o patógeno (Flynn JL, 2001).

O primeiro mecanismo utilizado pelo hospedeiro para conter o crescimento do *M. tuberculosis* durante a infecção persistente, bem como, limitar o crescimento bacilar e a disseminação em sítios adicionais de infecção, é a formação dos granulomas (Zahrt TC, 2003). Granulomas são agregados organizados de células imunes formados em resposta a um estímulo persistente, de natureza infecciosa ou não infecciosa, e representam a principal característica da TB (Ramakrishnan L, 2012). Eles são formados basicamente por macrófagos, linfócitos, neutrófilos, células dendríticas, fibroblastos e células que secretam componentes da matriz extracelular (Figura 2) (Russell DG, 2007; Ramakrishnan L, 2012). Regiões de necrose (caseosas), formadas a partir da morte dos componentes celulares, também são observadas (Ramakrishnan L, 2012). Neste estágio, indivíduos capazes de impedir a proliferação do *M. tuberculosis* desenvolvem uma infecção latente (sem manifestação clínica da doença) e assintomática (Kaufmann SHE, 2005; Lamichhane G, 2010), na qual o microrganismo se encontra em um estado metabólico reduzido (Kaufmann SH, 2005; Koul A *et al.*, 2011).

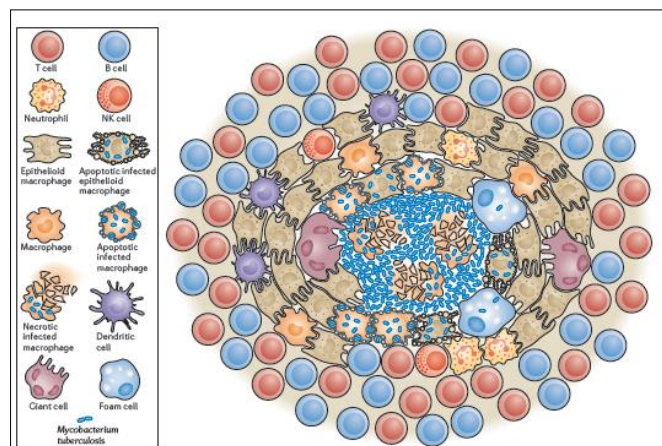


Figura 2. Estrutura e constituintes celulares do granuloma da TB. (Ramakrishnan L, 2012)

Porém, a infecção de um indivíduo imunocomprometido tipicamente resultará no estabelecimento de uma infecção aguda, caracterizada pela

replicação bacilar descontrolada e disseminação do microrganismo. Neste caso, os sintomas da doença aguda incluem fadiga, perda de peso, febre baixa e tosse crônica contagiosa (Zahrt TC, 2003).

Estima-se que um terço da população mundial está infectada com a forma latente do *M. tuberculosis* e calcula-se que o risco de desenvolvimento da doença em pacientes saudáveis é de aproximadamente 10% ao longo da vida (Lamichhane G, 2010). Além disso, acredita-se que 5% destes pacientes saudáveis irão desenvolver a TB ativa em algum estágio da vida (Koul A *et al.*, 2011). No entanto, estudos epidemiológicos mostram que a coinfeção com o HIV aumenta o risco anual de reativação da doença para até 10% (Koul A *et al.*, 2011; Elston JW, Thaker HK, 2008; Parrish NM, Dick JD, Bishai WR, 1998). Além da coinfeção com o HIV, a reativação da doença é frequentemente desencadeada por condições que comprometem o sistema imune do paciente tais como: casos de má nutrição, idade avançada, abuso de drogas, terapia com imunossupressores ou diabetes (Russell DG, 2007; Parrish NM, Dick JD, Bishai WR, 1998). A diminuição da resposta imune desencadeia uma série de eventos que podem levar ao rompimento do granuloma, danos ao tecido pulmonar e espalhamento de milhares de partículas infectadas através das vias aéreas (Russell DG, 2007).

1.3 TRATAMENTO

Apesar de existirem diferentes regimes de tratamento contra a TB, a OMS recomenda aquele conhecido como DOTS (do inglês, *Directly Observed Treatment Short Course*) (Ducati RG *et al.*, 2006). A quimioterapia consiste em uma associação de fármacos de primeira linha – isoniazida (INH), rifampicina (RIF), pirazinamida e etambutol - durante dois meses, seguida por quatro meses com INH e RIF (Koul A *et al.*, 2011; WHO, 2003; Ramaswamy S, Musser JM., 1998), podendo curar até 95% dos casos de TB (Koul A *et al.*, 2011). Além disso, a estratégia do DOTS inclui outros cinco componentes: *i*) estabelecer uma rede de indivíduos treinados a administrar e supervisionar o DOTS; *ii*) criar laboratórios e profissionais habilitados para o diagnóstico da TB; *iii*) implementar um sistema de fornecimento confiável de medicamentos de alta

qualidade (preferencialmente, sem custo aos pacientes); *iv*) compromisso governamental e *v*) sistema de monitoramento dos casos, tratamento e resultados (WHO, 2003; Yew WW, Leung CC, 2008).

Essa estratégia tem prevenido a ocorrência de novas infecções e, principalmente, dificultado o surgimento de casos de TB resistente a múltiplas drogas (TB-MDR) (Ducati RG *et al.*, 2006). No entanto, diversos fatores como o aumento da prevalência de coinfeção com o HIV, especialmente em áreas mais pobres, associado ao surgimento de cepas de *M. tuberculosis* resistentes ao tratamento, levaram ao questionamento da efetividade do DOTS (Lienhardt C *et al.*, 2012).

A falha do tratamento, definida como a presença de culturas positivas após cinco meses de terapia apropriada (WHO, 2010), pode ser resultado da falta de adesão pelo paciente devido à duração e complexidade do tratamento proposto, possíveis custos do tratamento inviabilizando sua continuidade, efeitos adversos ou resistência do bacilo aos fármacos (Elston JW, Thaker HK, 2008; Ramaswamy S, Musser JM., 1998).

1.4 RESISTÊNCIA AOS FÁRMACOS

Uma potencial ameaça ao controle da TB é a emergência de linhagens de *M. tuberculosis* que não podem ser contidas empregando-se as terapias padrões anti-TB (Zager EM, McNerney R, 2008).

As micobactérias possuem uma alta taxa de resistência intrínseca a maioria dos antibióticos e agentes quimioterápicos devido à difícil permeabilidade da sua parede celular. No entanto, tal barreira não tem capacidade suficiente para produzir níveis significativos de resistência, o que requer um mecanismo adicional (Jarlier V, Nikaido H, 1994). No caso da TB, a resistência aos fármacos é devida a mutações genéticas que resultam na perda da susceptibilidade aos antimicrobianos. A resistência aos fármacos anti-TB surge a partir da seleção de cepas mutantes com resistência inata a agentes individuais seguida da exposição a fármacos que não apresentam capacidade esterilizante (Dorman SE, Chaisson RE, 2007). Fármacos de ação lenta, prescrição imprópria, dificuldade de acesso aos medicamentos e sistemas de

saúde ineficientes, têm resultado em tratamento incompleto e relapso, podendo assim gerar a supressão parcial do crescimento micobacteriano e favorecer o surgimento de populações bacterianas resistentes a fármacos (Sacchetti JC, Rubin EJ, Freundlich JS, 2008; Dorman SE, Chaisson RE, 2007).

A TB-MDR é definida como aquela na qual o paciente possui a doença ativa com bacilo resistente a, pelo menos, INH e RIF. A TB-MDR pode ser contraída através de infecção com bacilos já resistentes (resistência primária) ou pode ser desenvolvida no decorrer do tratamento (resistência adquirida) (WHO, 2010). Embora o DOTS seja altamente eficiente no controle da TB susceptível a fármacos (ou resistente somente à INH), ele é comumente insuficiente no controle da TB-MDR (Yew WW, Leung CC, 2008; WHO, 2010). Casos de TB-MDR são mais difíceis de curar e requerem um tratamento com medicamentos de segunda linha (fluoroquinolonas, aminoglicosídeos, tioamidas), os quais são menos efetivos e mais tóxicos, com exceção de algumas fluoroquinolonas, além de ter um custo mais elevado que os regimes baseados em medicamentos de primeira linha (Yew WW, Leung CC, 2008; Zager EM, McNerney R, 2008; Dorman SE, Chaisson RE, 2007; WHO, 2010).

Pacientes coinfectados com TB-MDR e HIV são os que possuem o pior prognóstico, uma vez que tal associação tem provocado altas taxas de mortalidade, especialmente quando diagnosticada tardiamente (Elston JW, Thaker HK, 2008; Yew WW, Leung CC, 2008). Pacientes com TB-MDR que tiveram um período de infecção prolongado e aqueles coinfectados com HIV, morreram nos dois primeiros meses de terapia (55%) (Kawai *et al.*, 2006). Em 2014, estima-se que 12% das 9,6 milhões de pessoas que desenvolveram TB eram HIV-positivas, sendo a região africana responsável pela maioria desses casos (74%) (WHO, 2015).

Portanto, é evidente a necessidade de melhora nas medidas de controle de infecção e tratamento precoce com terapia antirretroviral para pacientes portadores de HIV e TB-MDR. Essas providências são essenciais para que os casos de TB-MDR sejam detectados e tratados adequadamente, reduzindo assim o risco de infecção e mortalidade (Kawai *et al.*, 2006; Jassal M, Bishai WR, 2009).

Nos últimos anos, casos de TB extensivamente resistente a fármacos (TB-XDR) têm sido relatados em diversos países. A definição mais recente

para TB-XDR denota a condição em que os isolados são resistentes à INH e RIF, a alguma fluoroquinolona e a qualquer medicamento injetável de segunda linha (capreomicina, canamicina, amicacina), resultando em limitadas opções de tratamento (WHO, 2010).

Dados indicam que a TB-XDR está difundida em 105 países, com ao menos um caso reportado e, que aproximadamente 9% dos casos de TB-MDR são também XDR (WHO, 2015). Indivíduos infectados com TB-XDR possuem um prognóstico ruim, com altos índices de falha do tratamento e alta mortalidade (Yew WW, Leung CC, 2008). A situação torna-se ainda mais grave em pacientes portadores de HIV. Em um estudo realizado em uma área rural da África do Sul, a maioria dos pacientes (> 90%) coinfectedados com TB-XDR e HIV vieram a falecer, com uma média de sobrevivência de apenas 16 dias a partir do diagnóstico (Gandhi NR *et al.*, 2006).

Velayati AA *et al.* (2009) documentaram o surgimento de novas formas de bacilos encontrados em pacientes diagnosticados com TB-TDR. Esses isolados foram classificados como linhagens totalmente resistentes aos fármacos (TDR), uma vez que apresentaram resistência *in vitro* a todos os fármacos de primeira e segunda linha testados. Durante o estudo, os pacientes infectados não responderam a nenhuma terapia padrão e permaneceram com culturas positivas após 18 meses de tratamento com fármacos de segunda linha (Velayati AA *et al.*, 2009).

Enquanto a TB-MDR e XDR significam uma ameaça à saúde pública e ao controle da TB no mundo, possíveis casos de TB-TDR aumentam a preocupação quanto a uma futura epidemia de TB incurável (Velayati AA *et al.*, 2009).

Diante de tal cenário, há uma urgente necessidade de pesquisa por novos candidatos a fármacos anti-TB, além da aprovação e uso das que estão em desenvolvimento (Lamichhane G, 2010; Yew WW, Leung CC, 2008). Tratamentos futuros requerem medicamentos com menos efeitos adversos a fim de facilitar a adesão à terapia (Jassal M, Bishai WR, 2009). Esses novos agentes devem, idealmente, possuir atividade bactericida contra o *M. tuberculosis*, tanto no estado de multiplicação ativa quanto no estado de dormência e serem efetivos, tanto no combate da TB susceptível a fármacos quanto em casos MDR/XDR (Ducati RG *et al.*, 2006; Balganes TS, Alzari PM,

Cole ST, 2008). Outra característica desejável é a possibilidade de coadministração com fármacos antirretrovirais e medicamentos utilizados para o tratamento de doenças crônicas, como o diabetes (Koul A *et al.*, 2011)

1.5 QUINOLINAS

Os compostos quinolínicos são estruturas heterocíclicas do tipo benzo[*b*]piridina, dessa forma, apresentam um anel benzênico geminado com uma piridina (Figura 3).

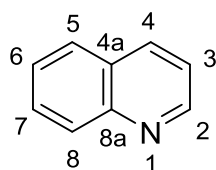


Figura 3: Estrutura geral dos compostos quinolínicos e sua numeração.

Compostos contendo o núcleo quinolínico têm demonstrado um amplo espectro de atividade farmacológica, entre as quais se destacam: atividade antibacteriana (Mahamoud A *et al.*, 2006), anticâncer (Denny WA *et al.*, 2006), antimalárica (Nasveld P, Kitchener S 2005), anti-HIV (Wilson WD *et al.*, 1992; Streckowski L *et al.*, 1991), antituberculose (Lilienkamp A *et al.*, 2009), entre outras.

Com relação à atividade inibitória sobre o *M. tuberculosis*, o núcleo quinolínico tem emergido como privilegiado grupo para o desenvolvimento de compostos anti-TB. Prova disto é sua presença em fármacos anti-TB empregados na clínica como tratamento de segunda escolha como as fluoroquinolonas: levofloxacina, ofloxacina, gatifloxacina e moxifloxacina (Figura 4) (Drlica K, 1999; Kumar R, Madhumathi BS, Nagaraja V, 2014).

Estes compostos inibem a atividade da DNA girase ou da topoisomerase II bacteriana, que regula a topologia do DNA e é essencial à sobrevivência da bactéria (Mathew B, Ross L, Reynolds RC, 2013). A DNA girase torna a molécula de DNA bacteriana compacta e biologicamente ativa. Ao inibir essa enzima, a molécula de DNA deixa de possuir a propriedade de super-helicoidização (do inglês *supercoiling*) para que possa ocupar um pequeno espaço celular para sua expressão, recombinação e replicação (Drlica K &

Zhao X., 1997). As extremidades livres do DNA induzem a síntese descontrolada de RNAm e de proteínas, assim como a produção de exonucleases e a degradação cromossomial. Esses fatores levam à morte celular e também inibem, in vitro, a topoisomerase IV, mas esse fato não contribui para a ação antibacteriana sobre o *M. tuberculosis* uma vez que essa enzima está ausente no bacilo.

Em 2012, a agência regulatória norte-americana FDA (*Food and Drug Administration*) acelerou a aprovação da bedaquilina para o uso combinado em tratamentos de adultos com MDR-TB quando alternativas terapêuticas não estivessem disponíveis (Provisional CDC guidelines). Comercializada sob nome de Sirturo™, esse fármaco da classe quinolínica (Figura 4), age pela inibição da enzima adenosina 5'-trifosfato sintase (ATP sintase) de *M. tuberculosis* (Andries *et al.*, 2005). Apesar da boa eficácia, o medicamento tem apresentado efeitos colaterais potencialmente fatais. Em eletrocardiogramas é possível observar o aumento do intervalo QT (tempo que decorre desde o princípio da despolarização até o fim da repolarização dos ventrículos), o qual tem sido relacionado a arritmias cardíacas graves (Palomino JC, Martin A, 2013). Outros efeitos adversos são relacionados a disfunções hepáticas com mudanças nos níveis de transaminases (Palomino JC, Martin A, 2013).

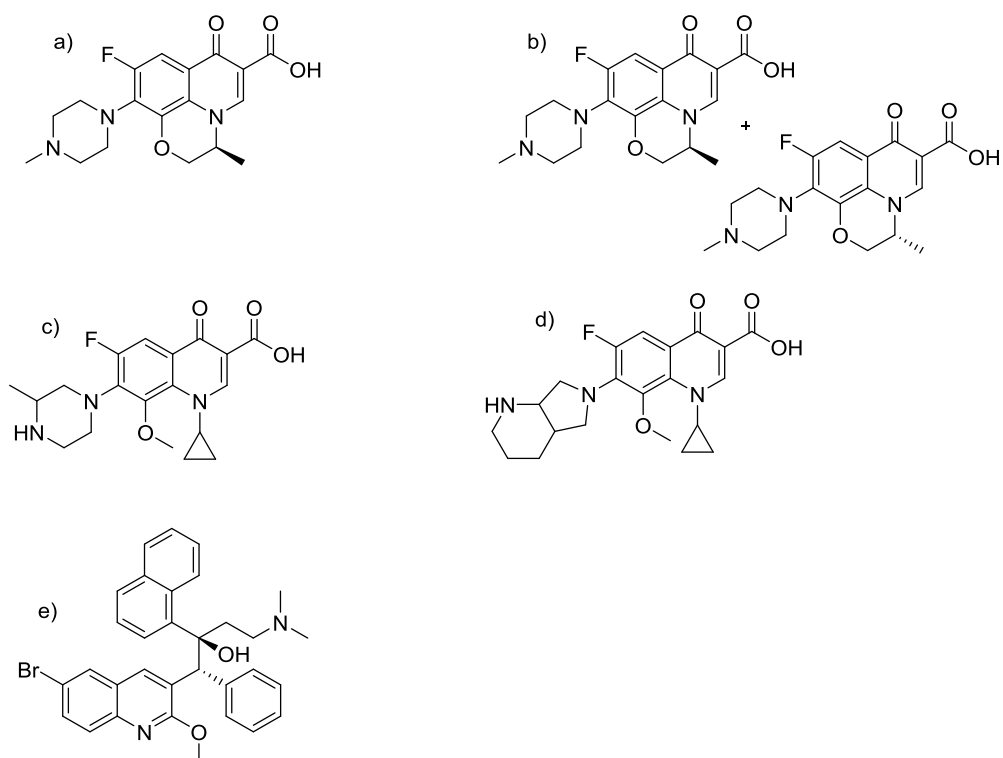


Figura 4. Estruturas químicas de fármacos utilizados para o tratamento da tuberculose contendo o núcleo quinolínico: a) Levofloxacina; b) Ofloxacina; c) Gatifloxacina; d) Moxifloxacina; e) SirturoTM.

O DC159a, outro derivado 8-metoxi fluoroquinolona em fase pré-clínica de estudo, tem demonstrado ser mais ativo do que outras quinolonas com potente atividade *in vitro* e *in vivo* frente às cepas TB-MDR resistentes às fluoroquinolonas com valores de MIC₉₀ na faixa de 0,06 a 0,5 µg/mL (Hoshino K *et al.*, 2008).

Considerando esta classe de compostos presente nos estágios iniciais de desenvolvimento, Lilienkampf e colaboradores (2009) apresentaram uma série de estruturas contendo os anéis quinolínicos hibridizados com o anel isoxazólico como inibidores do *M. tuberculosis* (*in vitro*). Neste trabalho foi demonstrado que o composto líder (MIC 0,9 µM) não apresentou inibição da proteína CYP3A4, o que sugere a possibilidade de coadministração destes compostos com fármacos anti-HIV, um dos complicadores para o tratamento da tuberculose em pacientes coinfectados com vírus HIV (Lilienkampf A *et al.*, 2009).

Na revisão sobre as descobertas e os avanços de novos e promissores quimioterápicos para tratamento da tuberculose, Beena e Rawat (2012) ressaltaram diversos compostos constituídos de um núcleo quinolínico das

classes quinolil hidrazinas, quinolil hidrazonas e 4-amino-7-cloroquinolinas. Muitos destes derivados apresentaram concentração inibitória mínima (MIC) na faixa de 0,78 μM a 66,1 μM (Figura 5). Interessantemente, o padrão de substituição destes compostos revela que a posição do grupo alcoxila no anel quinolínico e a presença do grupamento 2-naftil na porção hidrazônica são relevantes para a atividade anti-TB (Figura 5).

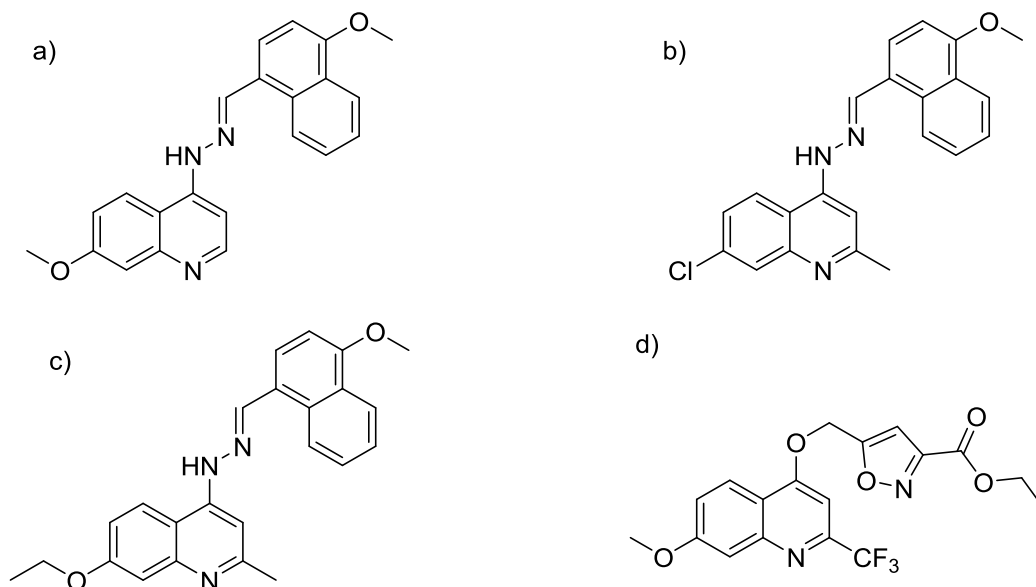


Figura 5. Exemplo de compostos apresentados por Beena, *et al.*, (2012). a) MIC: 0,78 μM ; b) MIC: 0,78 μM ; c) MIC: 0,78 μM ; d) MIC: 66,1 μM .

Outra interessante classe contendo o sistema quinolínico com propriedades anti-TB é a quinoloxiacetamida (QOA), descoberta pelo grupo da GlaxoSmithKline (GSK), utilizando a técnica de triagem fenotípica. Os 2-(quinolin-4-iloxi)acetamidas exibiram considerada atividade inibitória sobre o crescimento do *M. tuberculosis* H37Rv com MIC menor que 1 μM e com baixa citotoxicidade quando testados em células HepG2 ($\text{IC}_{50} > 50 \mu\text{M}$) (Ballell *et al.*, 2013). Dentre os três derivados da classe quinoloxiacetamida reportados, o composto GSK358607A (Figura 6) apresentou melhor atividade frente ao *M. tuberculosis* com concentração mínima inibitória de 0,70 μM e com significativo índice de seletividade (Ballell *et al.*, 2013).

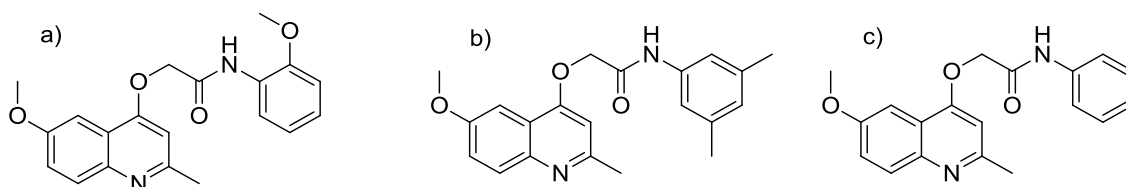


Figura 6. a) Estrutura do GSK358607A(QOA) MIC: 0,70 μ M; b) Estrutura do GSK749336A(QOA), MIC: 0,25 μ M; c) GW857165X (QOA) MIC: 3,3 μ M.

1.6 RELAÇÃO ESTRUTURA QUÍMICA ATIVIDADE BIOLÓGICA (SAR)

O conhecimento da relação existente entre a estrutura química de compostos candidatos a fármacos e suas atividades farmacológicas tem possibilitado aos químicos medicinais promoverem modificações estruturais pontuais visando o aumento da atividade e/ou melhora dos parâmetros farmacocinéticos (Bleicher *et al.*, 2003). Efetivamente, as possibilidades de transformação química a partir de uma estrutura de um composto líder (*lead compound*) são imensas e muitos análogos podem ser previstos. Algumas destas alterações podem compreender a adição de grupamentos doadores/aceptores de ligações de hidrogênio, grupamentos ionizáveis (ex.: ácidos carboxílicos), grupamentos doadores/retiradores de elétrons, grupamentos volumosos (ex.: naftil ou cadeias alifáticas). Outras modificações podem ser relacionadas à distribuição espacial da molécula, mudando parâmetros como planaridade (ex.: troca de anel benzênico por um ciclo hexano), ou alteração de parâmetros de lipossolubilidade pela adição/eliminação de grupos químicos apolares (Barreiro *et al.*, 2008).

Três estratégias estão entre as mais utilizadas para estudar a relação estrutura-atividade de compostos candidatos a fármacos: *i*) simplificação molecular (abordagem disjuntiva); *ii*) introdução de grupos funcionais (abordagem conjuntiva); e *iii*) substituições isostéricas e bioisostéricas (Barreiro *et al.*, 2008). A simplificação molecular reduz a complexidade estrutural, eliminando funções e elementos moleculares que não fazem parte do farmacóforo. Esta estratégia pode levar à preparação de moléculas com acesso sintético facilitado, permitindo assim o aumento de escala dos compostos de interesse visando à realização dos ensaios pré-clínicos subsequentes (Ballel *et al.*, 2013). A abordagem conjuntiva consiste da ligação

de grupos químicos adicionais para as moléculas na tentativa de obter melhores perfis farmacológicos, tais como eficácia, toxicidade e parâmetros farmacocinéticos (DeSimone *et al.*, 2004; González *et al.*, 2012). O grau de complexidade estrutural do candidato a fármaco pode ser mantido, e as modificações propostas envolverem apenas substituições isostéricas e bioisostéricas (Lima e Barreiro, 2005). Assim, com o objetivo de compreender a contribuição de grupos químicos para a atividade e alcançar melhorias, são estabelecidos gradientes eletrônicos, estéricos e lipofílicos entre os grupos químicos propostos para síntese dos análogos estruturais.

Nosso grupo de pesquisa tem desenvolvido estratégias para obtenção de estruturas químicas candidatas a fármacos para o tratamento da tuberculose. Entre as abordagens utilizadas destacam-se o planejamento baseado em alvos moleculares e a otimização estrutural de compostos obtidos a partir de triagens fenotípicas. Nesse contexto, uma de nossas estratégias para o desenvolvimento de novos agentes antituberculose utiliza os compostos líderes GSK358607A identificados por técnicas de HTS (*High Throughput Screening*) (Ballell *et al.*, 2013) e o derivado 5s por triagem fenotípica (Pissinate *et al.*, 2016) (Figura 7).

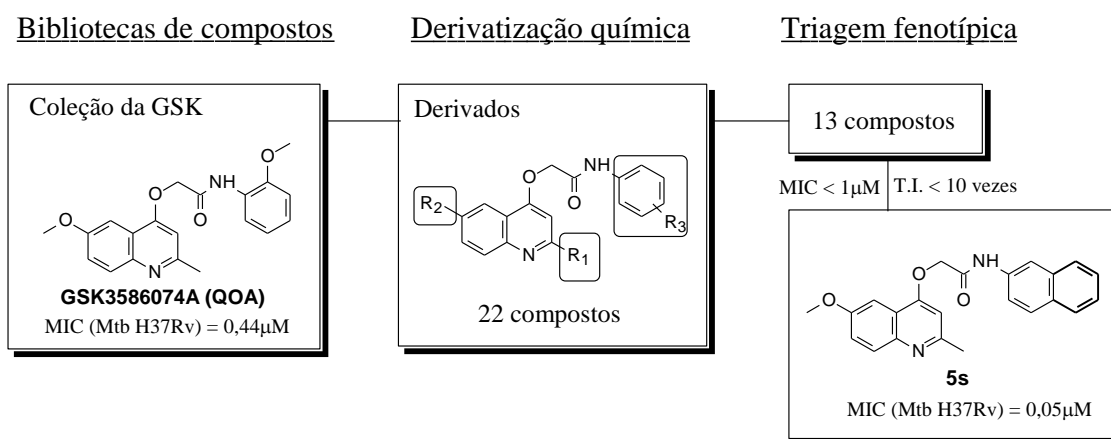


Figura 7. Estratégia geral para a identificação de potenciais compostos antituberculose a partir de composto líder GSK358607A identificado em estudos de triagem fenotípica que culminaram na descoberta do composto 5s.

Pissinate e colaboradores (2016), no intuito de explorar a relação entre a estrutura química com a atividade biológica (SAR), sintetizaram uma série de 22 novos derivados estruturais a fim de identificar grupos funcionais relevantes

para atividade biológica e estabelecer os principais grupos farmacofóricos. A estratégia dos autores foi a derivatização química do composto GSK358607A que resultou na identificação de 13 novos análogos com MICs na faixa de 0,8-0,05 μM . Além disso, os compostos apresentaram ação seletiva ao *M. tuberculosis* H37Rv e potente atividade frente a cepas TB-MDR, com desprovida citotoxicidade às células Vero e HaCat na concentração de 20 μM (Pissinate *et al.*, 2016).

Os autores mostraram que os substituintes nas posições R₂ e R₃ do anel quinolínico e na posição R₃ da porção *N*-arilacetamida são capazes de modular a atividade inibitória sobre o *M. tuberculosis*. Interessantemente, a substituição do grupo 1-metoxifenil na posição R₃ do composto GSK358607A(QOA) por uma 4-bromofenila 5m ou β -naftila 5s contribuiu para o incremento da potência dos compostos. A atividade inibitória em relação ao composto originalmente apresentado pela GSK foi potencializada de 8 a 14 vezes para os análogos contendo grupos de maior volume molecular, sendo o composto 5s apontado o líder da série (MIC = 0,053 μM) (Pissinate *et al.*, 2016).

Neste intuito, torna-se relevante a investigação do aumento do volume molecular e da variação da planaridade na porção acetamida (em R¹ e R²) (trocas bioisostéricas), bem como da contribuição do efeito doador/receptor de H (em R¹ e A) para estabelecimento do perfil farmacológico do composto (Figura 8).

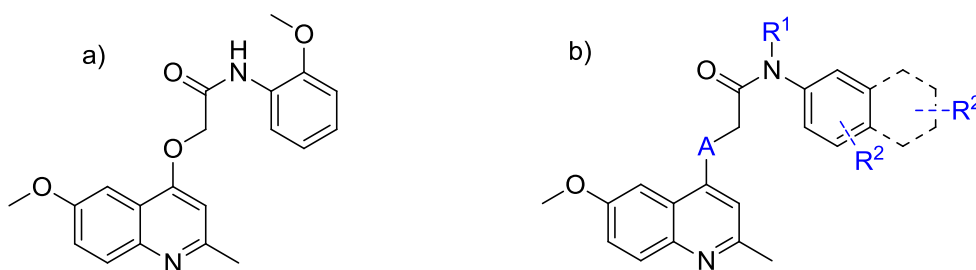


Figura 8. (a) GSK358607A; (b) Modificações de interesse, onde, A = NH ou O; R¹ = H, alquila ou arilas substituídas; R² = Alquila, arila ou naftila substituídas e $n = 1$ ou 2.

2 JUSTIFICATIVA

Regimes de tratamento inapropriados e a não adesão dos pacientes ao tratamento são comumente associados à emergência de cepas de *M. tuberculosis* resistentes a múltiplos fármacos (TB-MDR), cujos isolados são resistentes a pelo menos isoniazida (INH) e rifampicina (RIF), dois dos principais fármacos usados no tratamento padrão da TB, preconizado pela OMS (Basso *et al.*, 1998; Duncan, 2003; Mitchison *et al.*, 2012). Pacientes com TB-MDR devem ser tratados com uma combinação de fármacos de segunda linha que, além de serem significativamente mais caros, possuem mais efeitos tóxicos e são menos efetivos que os fármacos de primeira linha (O'Brien *et al.*, 2001).

Ainda mais preocupante é o surgimento das cepas de *M. tuberculosis* extensivamente resistentes (TB-XDR), definidas como casos de TB cujos isolados são resistentes à INH, RIF e a pelo menos três das seis principais classes de fármacos de segunda linha (aminoglicosídeos, polipetídeos, fluoroquinolonas, tiamidas, ciclosserina e ácido *p*-aminosalicílico) (Dorman *et al.*, 2007; Singh *et al.*, 2007). TB-XDR está sendo relatada em todo o mundo, inclusive nos Estados Unidos, onde a TB estava sendo considerada controlada. Além das cepas TB-MDR e TB-XDR, uma nova linhagem de *M. tuberculosis* foi identificada em 2009 e denominada TB-TDR, ou seja, uma cepa totalmente resistente aos fármacos de primeira e segunda linha, atualmente disponíveis para tratar a TB. Esta forma do bacilo contém a parede celular ainda mais espessa do que o comumente observado e tem sido relatada, com preocupação, em países como Irã e Índia (Loewenberg, 2012; Udwadia *et al.*, 2011). O pouco êxito na terapia e a ocorrência já difundida destas cepas resistentes levam a discussões sobre a drástica situação de casos de TB virtualmente incuráveis (Dorman *et al.*, 2007, Duncan, 2003).

Portanto, a reemergência da TB como um problema de saúde mundial, a proliferação de cepas (MDR, XDR e TDR) e a necessidade de tratamentos mais curtos contra a doença criaram a necessidade urgente do desenvolvimento de terapias anti-TB inovadoras (Koul A *et al.*, 2011). Idealmente, novos fármacos anti-TB deveriam ser efetivos contra as cepas resistentes, diminuir o longo período de tratamento, podendo assim aumentar a

adesão dos pacientes à quimioterapia, diminuir a frequência de doses, possuir mínimas interações medicamentosas (especialmente com os fármacos antirretrovirais) e poucos ou inexistentes efeitos adversos (Koul A et al., 2011).

Nesse contexto, as quinoloxiacetamidas podem representar uma classe atraente de moléculas candidatas a fármacos anti-tuberculose. As determinações das relações existentes entre a estrutura química e as atividades apresentadas são de grande relevância para a compreensão dos grupamentos farmacofóricos e/ou toxicofóricos e a proposição de novas estruturas com atividades farmacológicas otimizadas. A maior expectativa da nossa proposta é desenvolver um novo agente anti-TB eficiente. O presente projeto viabilizará a obtenção de estruturas químicas novas capazes de inibir o crescimento do *M. tuberculosis in vitro* e que apresentam predicados para tornarem-se novas alternativas terapêuticas.

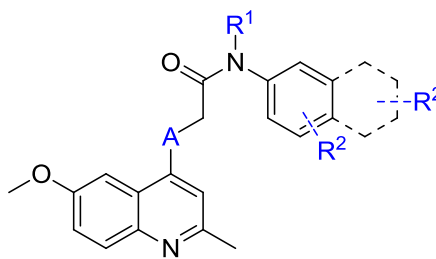
3 OBJETIVOS

3.1 OBJETIVO GERAL

Sintetizar e caracterizar estruturalmente uma série de 2-((quinolin-4-il)oxi)-fenilacetamidas para posterior avaliação *in vitro* da sua capacidade inibitória sobre o crescimento do *M. tuberculosis*.

3.2 OBJETIVOS ESPECÍFICOS

a) Síntese de uma série de 2-((quinolin-4-il)-fenilacetamidas.



Onde, A = NH ou O; R¹ = H, alquila ou arilas substituídas; R² = Alquila, arila ou naftilas substituídas.

- b) Caracterização estrutural dos compostos sintetizados, utilizando técnicas de ressonância magnética nuclear de ¹H e ¹³C (RMN), espectrometria de massas (EM), espectroscopia de infravermelho (FTIR).
- c) Determinação da concentração mínima inibitória (MIC) em relação à cepa de *M. tuberculosis* H37Rv.
- d) Determinação da concentração mínima inibitória (MIC) em relação a cepas de *M. tuberculosis* resistentes à isoniazida obtidas a partir de isolados clínicos.
- e) Avaliação do efeito citotóxico dos compostos sintetizados, através da análise de crescimento de células Vero.
- f) Realização de estudos de estrutura-atividade (SAR) da série de compostos.

4 ARTIGO CIENTÍFICO

2-(Quinolin-4-yloxy)acetamides exhibit nanomolar potency against *Mycobacterium tuberculosis* strains

Bruno Couto Giacobbo^{a,b}, Kenia Pissinate^a, Valnês Rodrigues-Junior^{a,b}, Anne Drumond Villela^{a,c}, Estêvão Silveira Grams^a, Bruno Lopes Abbadi^{a,b}, Rogério Valim Trindade^{a,b}, Maria Martha Campos^{a-c}, Luiz Augusto Basso^{a-c}, Diógenes Santiago Santos^{*,a,b} and Pablo Machado^{*,a,b}

^aInstituto Nacional de Ciência e Tecnologia em Tuberculose, Centro de Pesquisas em Biologia Molecular e Funcional, Pontifícia Universidade Católica do Rio Grande do Sul, 90619-900, Porto Alegre, Rio Grande do Sul, Brazil

^bPrograma de Pós-graduação em Biologia Celular e Molecular, Pontifícia Universidade Católica do Rio Grande do Sul, 90619-900, Porto Alegre, Rio Grande do Sul, Brazil

^cPrograma de Pós-Graduação em Medicina e Ciências da Saúde, Pontifícia Universidade Católica do Rio Grande do Sul, 90619-900, Porto Alegre, Rio Grande do Sul, Brazil

*Corresponding authors. Phone/Fax: +55 51 3320 3629

E-mail addresses: diogenes@pucrs.br (D.S. Santos); pablo.machado@pucrs.br (P. Machado)

Abstract

2-(Quinolin-4-yloxy)acetamides have been described as potent and selective *in vitro* inhibitors of *Mycobacterium tuberculosis* growth. Herein, a new series of compounds yielded highly potent antitubercular agents with minimum inhibitory concentration (MIC) values in nanomolar range against drug-susceptible and drug-resistant *Mycobacterium tuberculosis* strains. Further, the most active compounds were devoid of apparent toxicity to Vero cells ($IC_{50s} \geq 20 \mu M$). Therefore, the data obtained have indicated that 2-(quinolin-4-yloxy)acetamides may furnish candidates for future development of novel alternative therapeutics for tuberculosis treatment.

Treated by the World Health Organization (WHO) as a global public health emergency since early 1990s, the human tuberculosis (TB) has still claimed thousands of lives annually.¹ This infection disease is caused mainly by *Mycobacterium tuberculosis* (Mtb) and has been reported among the top current causes of death triggered by a single pathogen. According to the WHO, 9.6 million new cases of the disease with 1.5 million deaths were reported worldwide in 2014.¹ Multidrug-resistant TB (MDR-TB) and extensively drug-resistant TB (XDR-TB),² HIV coinfection,³ limited effectivity of vaccine *Mycobacterium bovis* bacillus Calmette-Guérin (BCG),⁴ and the massive amount of individuals infected with latent or dormant bacillus⁵ have strongly contributed to the elevated incidence and mortality of TB. Further complicating this scenario, there are an increasing number of cases of infections caused by drug-resistant strains for which treatment options are restricted and suboptimal.^{1,6} Taken together, the points above described highlight the *paramount* need for *novel drugs, if possible, endowed with innovative mechanism of action*. Within this context, quinoline-containing compounds have been used in several drug discovery campaigns aiming novel antimycobacterial compounds.⁷ In addition, this privileged scaffold has been obtained in clinically useful anti-TB drugs such as bedaquiline⁸ and some fluoroquinolones.⁹ In line with research of new antitubercular candidates bearing a quinoline ring, we have recently described the structural optimization of previously reported 2-(quinolin-4-ylloxy)acetamide **1**¹⁰ (**Figure 1**) with some encouraging results.¹¹ Compound **1** was obtained from phenotypic screening together with a set of 177 leading anti-TB compounds.¹⁰ Our optimization efforts produced the lead structure **2** (**Figure 1**) which was 8.8-fold more potent than **1** with minimum inhibitory concentration (MIC) against

M. tuberculosis H37Rv of 0.05 μM .¹¹ In addition, compound **2** exhibited inhibitory activity against drug-resistant Mtb strains.

Therefore, in a sequence of our ongoing project in obtaining improved active compounds against drug-resistant Mtb strains, a crucial attrition point in TB treatment, a new series of 2-(quinolin-4-yloxy)acetamides and some analogue compounds were synthesized. Firstly, all molecules were assayed against *M. tuberculosis* H37Rv and their structural requirements for potency were evaluated. Moreover, most active structures against *M. tuberculosis* H37Rv were tested against a clinically isolated drug-resistant strain. Finally, apparent toxicity of compounds to Vero cells was also evaluated.

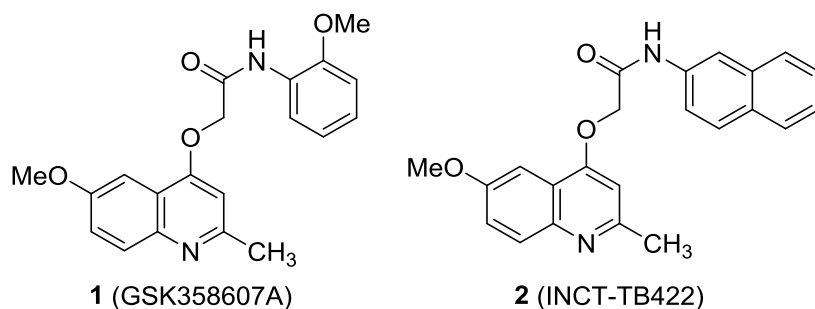
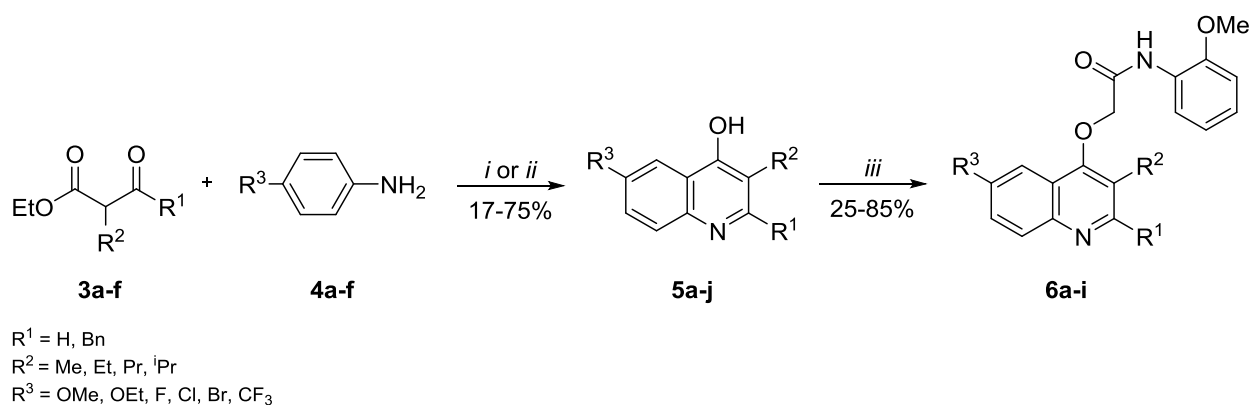


Figure 1. Quinoline-based antimycobacterial compounds.

The synthetic method for obtaining the 2-(quinolin-4-yloxy)acetamides **6a-i** was conducted in three synthetic steps. First, 4-hydroxyquinolines **5a-j** were prepared from classical Conrad-Limpach reaction between β -ketoesters **3a-f** and anilines **4a-f** (Scheme 1) in an one pot procedures.¹² This reaction was performed in presence of magnesium sulfate and acetic acid using refluxing ethanol as solvent for 16 h to furnish the β -anilinoacrylate intermediates which were not isolated or characterized. Thermal cyclization of the intermediates was obtained after heating the crude product using

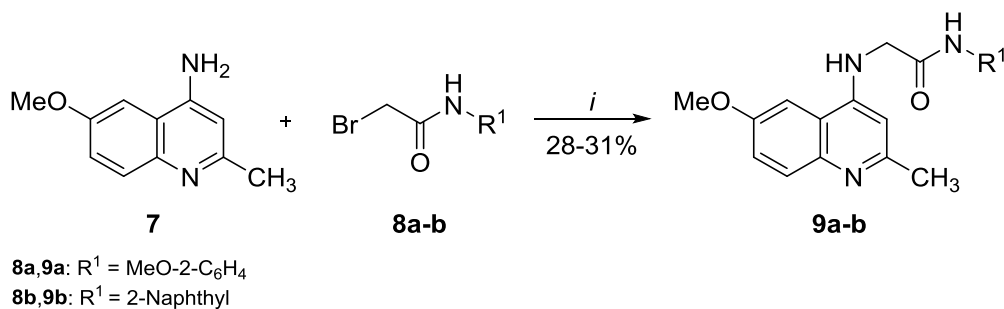
Dowtherm A[®] at 230-250 °C for 15 min to afford 4-hydroxyquinolines **5a-f** with 29-75% yields. By contrast, halogenated 4-hydroxyquinolines **5g-j** were synthesized through cyclocondensation reaction of β -ketoester **3a** and anilines **4c-f** in the presence of polyphosphoric acid (PPA) at 80-120 °C for 6 hours with 17-56% yields (**Scheme 1**). Notably, even after several attempts compounds **5a-f** were not obtained using polyphosphoric acid mediated reactions. Moreover, according to the spectroscopy data, no sign of Knorr products (2-hydroxyquinolines) were observed in both *cyclocondensation* methods. In the second reaction step, 2-bromo-*N*-(2-methoxyphenyl)acetamide was obtained by the acylation reaction of 2-methoxyaniline using bromoacetyl chloride according to a previously reported approach.¹³⁻¹⁴ Finally, *O*-alkylation reaction of 4-hydroxyquinolines **5b-j** with 2-bromo-*N*-(2-methoxyphenyl)acetamide using potassium carbonate and *N,N*-dimethylformamide (DMF) as the solvent afforded 2-(quinolin-4-yloxy)acetamides **6a-i** with 25-85% yields.



Scheme 1. Reactants and conditions: *i*) = (1) MgSO₄, AcOH, EtOH, 90 °C, 16 h; (2) Dowtherm A[®], 230-250 °C, 15 min. *ii*) = PPA, 80-120 °C, 6 h. *iii*) = 2-bromo-*N*-(2-methoxyphenyl)acetamide, K₂CO₃, DMF, 25 °C, 16 h.

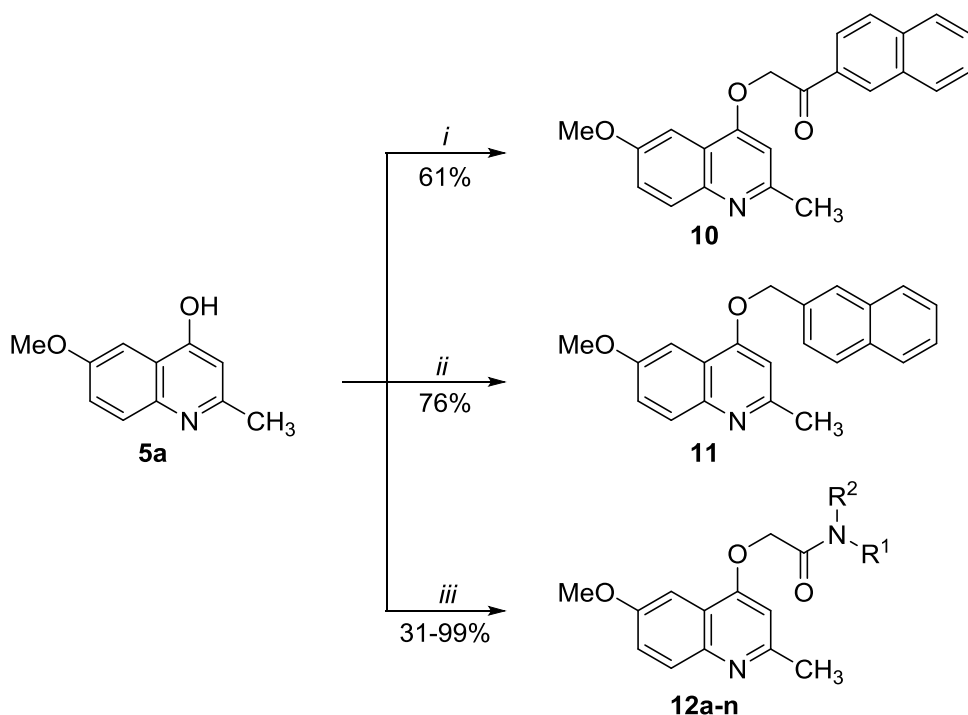
In order to evaluate the exchange of oxygen by a nitrogen at 4-position of quinoline ring, 2-(quinolin-4-ylamino)acetamides **9a-b** were synthesized (**Scheme 2**). The

products were obtained after alkylation reaction of 4-aminoquinoline **7** with 2-bromo-*N*-arylacetamides **8a-b** which were prepared as already described.¹³⁻¹⁴ The reaction was accomplished in the presence of sodium hydride dissolved in dry DMSO under argon atmosphere. The amino derivative compounds **9a-b** were isolated with 28-31% yields.



Scheme 2. Reaction Condition: *i*) NaH, DMSO, 80 °C, 3.5 h.

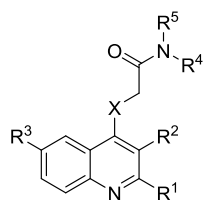
Structural analogues to compound **2** were synthesized using the 4-hydroxyquinoline **5a** (**Scheme 3**). Alkylation reaction of **5a** using 2-bromo-1-(naphthalen-2-yl)ethan-1-one in presence of excess of potassium carbonate and DMF as the solvent afforded the quinoline **10** with 61% yield. In addition, the same reaction utilizing 2-(bromomethyl)naphthalene as alkylating agent furnished the compound **11** with 76% yield. Finally, 2-(quinolin-4-yloxy)acetamides **12a-n** were prepared by *O*-alkylation reaction of 4-hydroxyquinoline **5a** (**Scheme 3**). The synthetic protocol was the same already described employing potassium carbonate as base and DMF as the solvent to offer targeted molecules with 31-99% yields. All synthesized compounds showed the proposed structures based on their analytical data (Supporting Information).



Scheme 3. Reactants and conditions: *i*) = 2-bromo-1-(naphthalen-2-yl)ethan-1-one, K_2CO_3 , DMF, 25 °C, 8 h. *ii*) = 2-(bromomethyl)naphthalene, K_2CO_3 , DMF, 25 °C, 8 h. *iii*) = 2-bromo-*N*-arylacetamides, K_2CO_3 , DMF, 25 °C, 16 h.

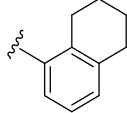
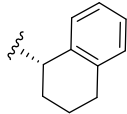
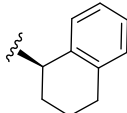
The synthesized quinoline-based compounds were evaluated in a whole-cell assay against *M. tuberculosis* H37Rv using the anti-TB drug isoniazid (INH) as the positive control.^{10,15} In general, alkyl lipophilic substituents directly attached to the *N*-arylacetamide group yielded compounds with potent antimycobacterial action while both improvement of alkyl chain length at the 2-position or change of methoxy group attached at the 6-position of the quinoline ring yielded compounds with decreased activity (**Table 1**). Indeed, the change of methyl group attached at the 2-position of quinoline ring (R^1) by an ethyl group reduced the potency by almost 2-fold.

Table 1. ClogP values and *in vitro* antimycobacterial activity of 2-(quinolin-4-yloxy)acetamides and their analogues against *M. tuberculosis* H37Rv.



6a-i, 9a-b, 10, 11, 12a-n

Entry	ClogP ^a	X	R ¹	R ²	R ³	R ⁴	R ⁵	MIC (μM)
1	3.32	O	Me	H	MeO	H	MeO-2-C ₆ H ₄	0.44 ¹¹
2	5.01	O	Me	H	MeO	H	2-Naphthyl	0.05 ¹¹
6a	3.85	O	Et	H	MeO	H	MeO-2-C ₆ H ₄	0.86
6b	4.38	O	Pr	H	MeO	H	MeO-2-C ₆ H ₄	>26.3
6c	4.25	O	ⁱ Pr	H	MeO	H	MeO-2-C ₆ H ₄	>26.3
6d	5.34	O	Me	Bn	MeO	H	MeO-2-C ₆ H ₄	>22.6
6e	3.85	O	Me	H	OEt	H	MeO-2-C ₆ H ₄	1.75
6f	3.21	O	Me	H	F	H	MeO-2-C ₆ H ₄	14.7
6g	3.78	O	Me	H	Cl	H	MeO-2-C ₆ H ₄	1.75
6h	3.93	O	Me	H	Br	H	MeO-2-C ₆ H ₄	0.78
6i	4.00	O	Me	H	CF ₃	H	MeO-2-C ₆ H ₄	>25.6
9a	3.55	NH	Me	H	MeO	H	MeO-2-C ₆ H ₄	>28.5
9b	5.24	NH	Me	H	MeO	H	2-Naphthyl	6.73
10	5.35	O	Me	H	MeO	-	-	1.75
11	6.16	O	Me	H	MeO	-	-	1.90
12a	3.96	O	Me	H	MeO	Me	MeO-2-C ₆ H ₄	>27.3
12b	3.32	O	Me	H	MeO	-CH ₂ (CH ₂) ₃ CH ₂ -		>31.8
12c	5.01	O	Me	H	MeO	Ph	Ph	>25.1
12d	5.40	O	Me	H	MeO	H		0.05
12e	4.85	O	Me	H	MeO	H		0.05

12f	5.40	O	Me	H	MeO	H		0.83
12g	4.83	O	Me	H	MeO	H		1.66
12h	4.83	O	Me	H	MeO	H		13.28
12i	4.78	O	Me	H	MeO	H	(Me) ₂ -3,4-C ₆ H ₃	0.11
12j	4.33	O	Me	H	MeO	H	Me-4-C ₆ H ₄	0.12
12k	4.86	O	Me	H	MeO	H	Et-4-C ₆ H ₄	0.06
12l	5.39	O	Me	H	MeO	H	Pr-4-C ₆ H ₄	0.05
12m	5.92	O	Me	H	MeO	H	Bu-4-C ₆ H ₄	0.10
12n	6.45	O	Me	H	MeO	H	Pent-4-C ₆ H ₄	0.005
INH	-	-	-	-	-	-	-	1.46

^aClogP calculated by ChemBioDraw Ultra, version 13.0.0.3015. INH, isoniazid.

Whereas inhibitory activity of compound **1** (R¹ = Me) in our experimental conditions was 0.44 μM the 2-(quinolin-4-yloxy)acetamide **6a** (R¹ = Et) exhibited MIC of 0.86 μM. In addition, the improvement of alkyl side chain with a propyl and isopropyl groups at R¹ in the compounds **6b** and **6c**, respectively, greatly reduced the activity leading both molecules to MIC > 26.3 μM. Similarly, the presence of bulky lipophilic benzyl group at the 3-position of quinoline ring (R²) in the structure **6d** was not tolerate to retain the antitubercular potency *in vitro* (MIC > 22.6 μM). 2-(Quinolin-4-yloxy)acetamides **6e-i** were synthesized in order to evaluate whether the increase of alkyl chain length as well as the presence of halogens at 6-position of quinoline ring (R³) could improve the activity. As already reported, the presence of methoxy group at this position has been detrimental for potency as its change by hydrogen reduced significantly the activity.¹¹ Ethoxy substituted compound **6e** showed a MIC value of

1.75 μM which was nearly 4-fold less active than **1** ($\text{R}^3 = \text{MeO}$). Among halogenated compounds, bromo substituted **6h** was the most effective structure with MIC value of 0.78 μM while 2-(quinolin-4-yloxy)acetamides **6f** ($\text{R}^3 = \text{F}$) and **6g** ($\text{R}^3 = \text{Cl}$) exhibited MICs of 14.7 μM and 1.75 μM , respectively. Notably, the order of potency followed the improvement of both lipophilicity (**Table 1**) and atomic radius in the evaluated halogen atoms. Compound **6i** bearing a trifluoromethyl group at R^3 showed also decreased activity with MIC $> 25.6 \mu\text{M}$ denoting, once more, the necessity of methoxy group at the 6-position of heterocycle to high activity.

In the next round of our SAR study, the substituents attached at the 2-, 3-, and 6-positions of quinoline rings of the compounds **1** and **2** were maintained while the oxygen at the 4-position was changed by a nitrogen. This modification produced molecules with increased polarity by presence of NH group which may acts as hydrogen bonding donor-acceptor pair at a putative target. 2-(Quinolin-4-ylamino)acetamides **9a-b** presented MIC values $> 28.5 \mu\text{M}$ and 6.73 μM , respectively, indicating the importance of oxygen at the 4-position for anti-Tb activity of the synthesized compounds.

In order to assess the importance of amide group to antimycobacterial activity, analogues compounds **10** and **11** were synthesized and their inhibitory action to the Mtb growth was determined. Quinoline **10** retaining the ketone group exhibited MIC of 1.75 μM which was 35-fold less active than lead **2**. Similar MIC value of 1.90 μM was observed to molecule **11** which which does not encompass the entire amide group. According to these findings, the nitrogen from amide group appears to be imperative to potency whereas carbonyl group may present only a secondary role. However, further study is needed to clarify this point. Evaluating the importance of hydrogen attached to the amide nitrogen, activity elicited by 2-(quinolin-4-yloxy)acetamides **12a-c** indicated

that secondary amides can be detrimental for the potent anti-Tb activity from this chemical class as all three compounds were devoid of activity in the tested concentrations (MIC > 25.1 μ M).

Focusing our SAR study on the lead compound **2**, structures **12d-h** were proposed and synthesized for further evaluation against *M. tuberculosis* H37Rv strain. First, 2-tetrahydronaphthyl derivative **12d** attached directly at arylamide group was designed to reduce the reactivity of 2-naphthyl group in an attempt to improve the metabolic stability observed for 2-(quinolin-4-yloxy)acetamide **2**.¹¹ Notably, changing the 2-naphthyl group with a 2-tetrahydronaphthyl substituent the potency was maintained as MIC values of both molecules (**2** and **12d**) were 0.05 μ M. This finding denotes that potency showed by lead compound **2** does not appear to be dependent of planarity of 2-naphthyl ring. Reducing the hydrophobicity from structure **12d** by using a 2,3-dihydro-1*H*-inden-5-yl group the activity was also maintained at submicromolar range as MIC for compound **12e** was of 0.05 μ M. By contrast, 1-tetrahydronaphthyl derivative **12f** was almost 17-fold less active than analogue compound **12d** (0.05 μ M) presenting MIC of 0.83 μ M. Chiral substituents attached at the *N*-arylamide group of compounds **12g** and **12h** furnished molecules with reduced activity when compared to the lead **2**. Interestingly, the *S* stereoisomer was 8-fold more potent than *R* against the bacilli with observed MIC of 1.66 μ M for **12g** and a value of 13.28 μ M for compound **12h**.

Structures **12i-n** were proposed aiming the molecular simplification of 2-(quinolin-4-yloxy)acetamide **12d** and in an attempt of mimic the hydrophobic six-membered ring attached at the benzene group. Similar MIC values were obtained for 3,4-dimethyl substituted compound **12i** and 4-methyl derivative **12j**. Compound **12i** presented MIC of 0.11 μ M while 2-(quinolin-4-yloxy)acetamide **12j** inhibited the *Mtb* growth at minimal concentration of 0.12 μ M. Increasing alkyl chain length with 4-ethyl and 4-

propyl attached to the benzene ring of the compounds **12k** and **12l**, respectively, afforded molecules with same potency order obtained for lead compound **2**. Structures **12k** and **12l** exhibited MICs of 0.06 and 0.05 μM , respectively. By contrast, antimycobacterial *in vitro* activity of butyl substituted **12m** was 2-fold less effective than their counterparts (0.10 μM). Notably, when pentyl substituent was attached at the 4-position of benzene ring yielded a highly potent antitubercular structure with MIC value as low as 0.005 μM . Compound **12n** was 10-fold more potent when compared to the lead structure **2** and 292-fold more potent than first line drug INH (**Table 1**). This finding places this molecule in a select group of structures with MIC in the nanomolar range against Mtb.

2-(Quinolin-4-yloxy)acetamides containing MIC values lower than 0.2 μM (**12d-e** and **12i-n**) were selected for both inhibitory activity of clinical isolate (PE-003) and viability studies using Vero cells. The PE-003 strain has been described as a multidrug-resistant clinical isolate with resistance to drugs as isoniazid, rifampin, etambutol, and streptomycin.¹⁶ Targeted sequencing from this strain has revealed mutation in the *inhA* regulatory region C(-15)T.¹⁶ Interestingly, evaluated compounds were even more potent against PE-003 than *M. tuberculosis* H37Rv strain (**Table 2**).

Table 2. *In vitro* antitubercular activity against *M. tuberculosis* H37Rv, drug-resistant clinical isolate, and viability of Vero cells exposed to the synthesized 2-(quinolin-4-yloxy)acetamides **12d-e** and **12i-n**.

Comp.	MIC (nM)		Viability (% \pm SEM) ^a
	H37Rv	PE-003	Vero
12d	53.0	8.0	87.6 \pm 5.7
12e	55.0	5.5	89.3 \pm 12.0
12i	111.0	37	114.4 \pm 6.9
12j	116.0	39	89.8 \pm 9.5
12k	57.0	5.7	85.5 \pm 1.9
12l	54.0	5.5	76.8 \pm 4.2
12m	103.0	7.9	95.5 \pm 5.3
12n	5.1	1.0	79.2 \pm 7.2
INH	1,460	>70,000	-
ETH	Nd	61,181	-
MOX	Nd	99.0	-

^aData are expressed as means of cell viability \pm SEM for each compounds tested at 20 μ M. nd – not determined. INH, isoniazid. ETH, ethambutol. MOX, moxifloxacin.

2-(Quinolin-4-yloxy)acetamide **12n** exhibited surprising MIC value of 1.0 nM which was almost 100-fold more potent than presented by fluoroquinolone-based drug moxifloxacin. Exposing the Vero cell lineages to the 20 μ M of compounds **12d-e** and **12i-n** for 72 hours did not significantly affect the cell viability.¹⁷ Moreover, *in vitro* screening of 2-(Quinolin-4-yloxy)acetamides **12d-e** and **12i-n** against *Escherichia coli* (ATCC 25922), *Pseudomonas aeruginosa* (ATCC 27853), *Staphylococcus aureus* (ATCC 25923) and *Acinetobacter baumannii* (ATCC BAA 747) at the 20 μ M concentration did not show any antimicrobial activity (data not shown). These findings denote the possibility of low toxicity of compounds to the mammalian cells and their likely high degree of selectivity against Mtb.

In summary, herein we showed the synthesis of a new series of 2-(quinolin-4-yloxy)acetamides and their antitubercular activity *in vitro*. The compounds were obtained by well established synthetic protocols using accessible reactants and reagents that afforded the molecules in reasonably yields. In addition, the synthesized compounds showed potent and selective activity against drug-sensitive and drug-resistant Mtb strains with no apparent cytotoxicity to the Vero cells. The nanomolar antitubercular activity elicited by 2-(quinolin-4-yloxy)acetamides reveal that this *class of compounds* may furnish candidates for future development of novel drugs for TB treatment. Studies to identify the target(s) of 2-(quinolin-4-yloxy)acetamides antimycobacterial action are in progress, and these data will be communicated in the future.

ASSOCIATED CONTENT

Supporting Information

The Supporting Information is available free of charge on the website.

Synthetic procedures, analytical data, and bioassay protocols. (PDF)

Funding Sources

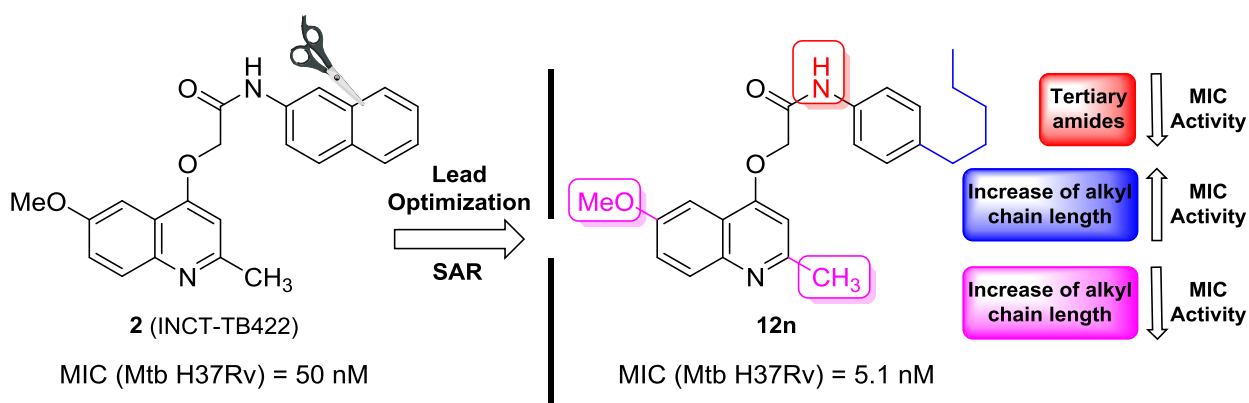
This work was supported by funds from the National Institute of Science and Technology on Tuberculosis (INCT-TB), Decit/SCTIE/MS-MCT-CNPq-FNDCT-CAPES (Brazil) to D. S. Santos and L. A. Basso. M. M. Campos, L. A. Basso, D. S. Santos, and P. Machado are Research Career Awardees of the National Research Council of Brazil (CNPq). The fellowships from CNPq (K. Pissinate, V. Rodrigues-

Junior, and E. S. Grams), CAPES (A. D. Villela and B. L. Abbadi), and FAPERGS (R. V. Trindade) are also acknowledged.

Notes

The authors declare no competing financial interests.

Graphical Abstract



REFERENCES

1. Global tuberculosis report 2015, World Health Organization. Available from: http://www.who.int/tb/publications/global_report/en/, accessed in March 2016.
2. Gandhi, N. R.; Nunn, P.; Dheda, K.; Schaaf, H. S.; Zignol, M.; Soolingen, D. v.; Jensen, P.; Bayona J. Multidrug-resistant and extensively drug-resistant tuberculosis: a threat to global control of tuberculosis. *Lancet* **2010**, *375*, 1830-1843.
3. Pawlowski, A.; Jansson, M.; Skold, M.; Rottenberg, M. E.; Kallenius, G. Tuberculosis and HIV Co-infection. *PLoS Pathogens* **2012**, *8*, 1–7.
4. Fine, P. E. M. Variation in protection by BCG: implications of and for heterologous immunity. *Lancet* **1995**, *346*, 1339-1345.
5. Zhang, Y.; Yew, W. W.; Barer, M. R. Targeting persisters for tuberculosis control. *Antimicrob Agents Chemother.* **2012**, *56*, 2223-2230.

6. Hoffner, S. Unexpected high levels of multidrug-resistant tuberculosis present new challenges for tuberculosis control. *Lancet* **2012**, 380, 1367–1369.
7. Singh, S.; Kaur, G.; Mangla, V.; Gupta, M. K. Quinoline and quinolones: promising scaffolds for future antimycobacterial agents. *J. Enzyme Inhib. Med. Chem.* **2015**, 30, 492-504.
8. Palomino, J. C.; Martin, A. TMC207 becomes bedaquiline, a new anti-TB drug. *Future Microbiol.* **2013**, 8, 1071-1080.
9. Shandil, R. K.; Jayaram, R.; Kaur, P.; Gaonkar, S.; Suresh, B. L.; Mahesh, B. N.; Jayashree, R.; Nandi, V.; Bharath, S.; Balasubramanian, V. Moxifloxacin, ofloxacin, sparfloxacin, and ciprofloxacin against *Mycobacterium tuberculosis*: Evaluation of in vitro and pharmacodynamics indices that best predict in vivo efficacy. *Antimicrob. Agents Chemother.* **2007**, 51, 576–582.
10. Ballell, L.; Bates, R. H.; Young, R. J.; Alvarez-Gomez, D.; Alvarez-Ruiz, E.; Barroso, V.; Blanco, D.; Crespo, B.; Escribano, J.; Gonzalez, R.; Lozano, S.; Huss, S.; Santos-Villarejo, A.; Julio Martin-Plaza, J.; Mendoza, A.; Jose Rebollo-Lopez, M.; Remuinan-Blanco, M.; Luis Lavandera, J.; Perez-Herran, E.; Javier Gamo-Benito, F.; Francisco Garcia-Bustos, J.; Barros, D.; Castro, J. P.; Cammack, N. Fueling Open-Source Drug Discovery: 177 Small-Molecule Leads against Tuberculosis. *ChemMedChem* **2013**, 8, 313–321.
11. Pissinate, K.; Villela, A. D.; Rdrigues-Junior, V.; Giacobbo, B. C.; Grams, E. S.; Abbadi, B. L.; Trindade, R. V.; Nery, L. R.; Bonan, C. D.; Back, D. F.; Campos, M. M.; Basso, L. A.; Santos, D. S.; Machado, P. 2-(Quinolin-4-yloxy)acetamides Are Active against Drug-Susceptible and Drug-Resistant *Mycobacterium tuberculosis* Strains. *ACS Med. Chem. Lett.* **2016**, 7, 35-39.

12. Brouet, J.-C.; Gu, S.; Peet, N. P.; Williams, J. D. A. Survey of Solvents for the Conrad-Limpach Synthesis of 4-Hydroxyquinolones. *Synth. Commun.* **2009**, *39*, 1563-1569.
13. Macpherson, I. S.; Kirubakaran, S.; Gorla, S. K.; Riera, T. V.; D'Aquino, J. A.; Zhang, M.; Cuny, G. D.; Hedstrom, L. The structural basis of cryptosporidium-specific IMP dehydrogenase inhibitor selectivity, *J. Am. Chem. Soc.* **2010**, *132*, 1230-1231.
14. Pissinate, K.; Rostirolla, D. C.; Pinheiro, L. M.; Suryadevara, P.; Yogeeswari, P.; Sriram, D.; Basso, L. A.; Machado, P.; Santos, D. S. Synthesis and evaluation of thiazolyl-1*H*-benzo[*d*]imidazole inhibitors of *Mycobacterium tuberculosis* inosine monophosphate dehydrogenase. *J. Braz. Chem. Soc.* **2015**, *26*, 1357-1366.
15. Palomino, J. C.; Martin, A.; Camacho, M.; Guerra, H.; Swings, J.; Portaels, F. Resazurin microtiter assay plate: Simple and inexpensive method for detection of drug resistance in *Mycobacterium tuberculosis*. *Antimicrob. Agents Chemother.* **2002**, *46*, 2720-2722.
16. Costa, E. R. D.; Ribeiro, M. O.; Silva, M. S. N.; Arnold, L. S.; Rostirolla, D. C.; Cafrune, P. I.; Espinoza, R. C.; Palaci, M.; Telles, M. A.; Ritacco, V.; Suffys, P. N.; Lopes, M. L.; Campelo, C. L.; Miranda, S. S.; Kremer, K.; Silva, P. E. A.; Fonseca, L. S.; Ho, J. L.; Kritski, A. L.; Rossetti, M. L. R. Correlations of mutations in *katG*, *oxyR-ahpC* and *inhA* genes and *in vitro* susceptibility in *Mycobacterium tuberculosis* clinical strains segregated by spoligotype families from tuberculosis prevalent countries in South America. *BMC Microbiol.* **2009**, *9*, 39.
17. Tuberculosis Antimicrobial Acquisition & Coordinating Facility (TAACF) – Description of TAACF Assays.

Supporting Information

2-(Quinolin-4-yloxy)acetamides exhibit nanomolar potency against *Mycobacterium tuberculosis* strains

Bruno Couto Giacobbo, Kenia Pissinate, Valnês Rodrigues-Junior, Anne Drumond Villela, Estêvão Silveira Grams, Bruno Lopes Abbadi, Rogério Valim Trindade, Maria Martha Campos, Luiz Augusto Basso, Diógenes Santiago Santos* and Pablo Machado*

TABLE OF CONTENTS

1. Chemistry section
2. General procedure for the preparation of 4-hydroxyquinolines **5a-j**
3. General procedure for the preparation of 2-bromo-*N*-aryl-acetamides
4. General procedure for the preparation of 2-(quinolin-4-yloxy)acetamides **6a-i** and **12a-n**; physicochemical, spectroscopic, and spectrometric data
5. Procedure for the preparation of 2-(quinolin-4-ylamino)acetamides **9a-b**; physicochemical, spectroscopic, and spectrometric data
6. General procedure for the preparation of 4-hydroxyquinolines **10** and **11**
7. ¹H NMR and ¹³C NMR spectra of synthesized compounds
8. *Mycobacterium tuberculosis* inhibition assay
9. Cytotoxicity investigation

1. Chemistry section

All commercially available solvents and reagents were obtained from commercial suppliers and used without further purification. All reactions involving reactants, reagents or intermediates sensitive to air or moisture were performed under an inert atmosphere of argon. The reactions were monitored by thin layer chromatography (TLC) with Macherey-Nagel ALUGRAM® Xtra SIL G/UV₂₅₄ (0.2 mm) plates. Melting points were measured using a Microquímica MQAPF-302 apparatus. ¹H NMR spectra were acquired on a Varian 400 or *Agilent DD2 spectrometer* (Federal University of Rio Grande do Sul, UFRGS/Brazil) (¹H at 400.13 MHz or 500.13 MHz, respectively) at 25 °C in 5 mm sample tubes. ¹³C NMR spectra were acquired on a Varian 400 or *Agilent DD2 spectrometer* (¹³C at 100.63 MHz or 125.63 MHz, respectively) at 25 °C. Chemical shifts (δ) were expressed in parts per million (ppm) relative to DMSO-*d*₆ (δ 2.49 for ¹H and δ 39.5 for ¹³C), which was used as the solvent, and to TMS, which was used as the internal standard. Splitting patterns were designated as follows: s, singlet; d, doublet; dd, doublet of doublets; m, multiplet. High-resolution mass spectra (HRMS) were obtained for all compounds on an LTQ Orbitrap Discovery mass spectrometer (Thermo Fisher Scientific, Bremen, Germany). This hybrid system combined an LTQ XL linear ion trap mass spectrometer and an Orbitrap mass analyzer. The experiments were performed via direct infusion of the sample in MeOH:H₂O (1:1) with 0.1% formic acid (flow rate 10 μ L/min) in positive-ion mode using electrospray ionization (ESI). Elemental composition calculations were executed using the specific tool included in the Qual Browser module of the Xcalibur (Thermo Fisher Scientific, release 2.0.7) software. Compound purity was determined by HPLC using an Äkta HPLC system (GE Healthcare® Life Sciences) equipped with a binary pump, manual injector, and UV detector. The Unicorn 5.31 software was used for data acquisition and processing. HPLC analysis conditions were as follows: RP column 5 μ m Nucleodur C-18 (250 \times 4.6 mm); flow rate 1.5 mL/min; UV detection at 270 nm; 100% water (0.1% acetic acid) was maintained from 0 to 7 min followed by a linear gradient from 100% water (0.1% acetic acid) to 90% acetonitrile/methanol (1:1, v/v) from 7 to 15 min; the last partition was maintained for an additional 15 min (15 to 30 min) and subsequently returned to 100% water (0.1% acetic acid) in 5 min (30 to 35 min) and was maintained for an additional 10 min (35 to 45 min). All evaluated compounds were \geq 90% pure.

1.1 General procedure for the preparation of 4-hydroxyquinolines 5a-j

4-Hydroxyquinolines **5a-j** were prepared from classical Conrad-Limpach reaction between β -ketoesters **3a-f** and anilines **4a-f**. The method was slight modified by using magnesium sulfate instead of Dean-Stark.¹

Method A

To a solution containing the aniline **4** (8.12 mmol) and anhydrous MgSO₄ (10 mmol) in ethanol (10 mL) was added acetic acid (6,3 mmol) and β -ketoester **3** (16.24 mmol). The mixture was heated at 90 °C for 16 hours. After removal of the drying agent (MgSO₄) by

filtration the residue was dried under vacuum. Then, 15 mL of Dowtherm A[®] was added forming a solution which was heated at 230-250 °C for 15 min. The reaction mixture was cooled to room temperature; the product was filtered and washed with hexane, diethyl ether and ethyl acetate. Finally, the product was dried under vacuum.

Method B

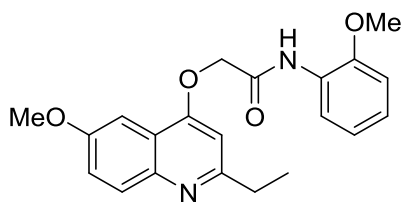
In a flask was added 6.5 g of polyphosphoric acid and aniline **4** (8.12 mmol) and heated to 80 °C for 15 min. After, β -ketoester **3** (16.24 mmol) was added dropwise. The resulting solution was heated at 120 °C for 6 hours. After cooling to the room temperature, the reaction mixture was neutralized with aqueous 3M NH₄OH solution. The precipitate was washed with water (3 x 100 mL) and dried under vacuum.

1.2 General procedure for the preparation of 2-bromo-*N*-aryl-acetamides.

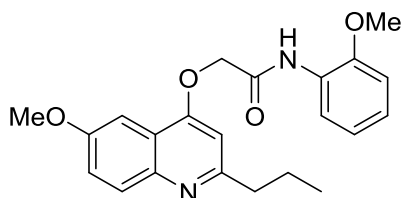
Bromoacetyl chloride (0.425 mL, 5.1 mmol) in dry dichloromethane (5 mL) was added dropwise to a solution containing the respective amine (4.1 mmol) and a catalytic amount of dimethylaminopyridine (DMAP) (0.150 g, 30 mmol %) in dry dichloromethane (20 mL) maintained in an ice bath under an argon atmosphere. The resulting solution was stirred at 0 °C for 30 min, and the temperature was then increased to 25 °C. After stirring for an additional 4 hours, the reaction mixture was diluted with diethyl ether (50 mL). All of the stirring time was accomplished under an argon atmosphere. The organic layers were washed sequentially with a solution of 1 N HCl (2 x 50 mL), water (1 x 100 mL), saturated aqueous NaHCO₃ (3 x 50 mL), and brine (5% w/v, 1 x 50 mL). Finally, the organic solution was dried over anhydrous MgSO₄ and evaporated under vacuum, and the residue was purified by flash chromatography on silica gel and eluted with chloroform-methanol (40:1).

1.3 General procedure for the preparation of the 2-(quinolin-4-yloxy)acetamides **6a-i and **12a-n**.**

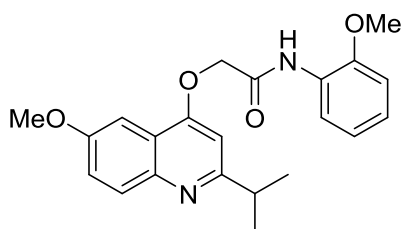
4-Hydroxyquinolines **5** (1.1 mmol) were added to a stirred solution containing 2-bromo-*N*-aryl-acetamide (1.0 mmol) and K₂CO₃ (3.12 mmol) in 6 mL of *N,N*-dimethylformamide (DMF) under an argon atmosphere. After stirring for 16 h, the reaction mixture was dissolved in 200 mL of distilled water. The precipitated product was filtered, washed with water and dried under vacuum. Purification of the compounds were performed by flash chromatography on silica gel (Macherey-Nagel, 35-70 mesh) using hexane: ethyl acetate (1:1) as eluent.



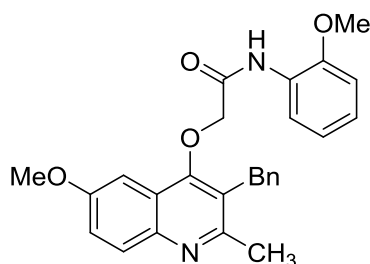
2-((2-Ethyl-6-methoxyquinolin-4-yl)oxy)-*N*-(2-methoxyphenyl)acetamide (**6a**): Yield 25%; m.p.: 157-158 °C; ¹H NMR (500 MHz, DMSO-*d*₆) δ ppm 1.3 (t, *J*=6.8 Hz, 3 H), 2.8 (m, 2 H), 3.8 (s, 3 H), 3.9 (s, 3 H), 5.1 (s, 2 H), 6.9 (s, 2 H), 7.1 (m, 2 H), 7.4 (d, *J*=8.8 Hz, 1 H), 7.5 (s, 1 H), 7.8 (d, *J*=8.8 Hz, 1 H), 8.1 (d, *J*=6.8 Hz, 1 H), 9.4 (s, 1 H); ¹³C NMR (126 MHz, DMSO-*d*₆) δ ppm 13.5, 31.6, 55.4, 55.8, 67.0, 100.1, 101.4, 111.2, 119.8, 120.4, 120.9, 121.2, 124.7, 126.4, 129.8, 144.1, 149.1, 156.4, 158.9, 161.8, 165.5; FTMS (ESI) *m/z* 367.1644 [M + H]⁺; calcd for C₂₁H₂₂N₂O₄: 367.1652.



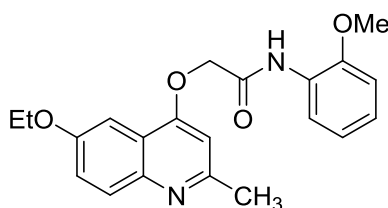
2-((6-Methoxy-2-propylquinolin-4-yl)oxy)-*N*-(2-methoxyphenyl)acetamide (**6b**): Yield 51%, m.p.: 155-156 °C; ¹H NMR (500 MHz, DMSO-*d*₆) δ ppm 0.9 (s, 3 H), 1.7 (s, 2 H), 2.8 (s, 2 H), 3.8 (s, 3 H), 3.9 (s, 3 H), 5.1 (s, 2 H), 6.9 (s, 2 H), 7.1 (s, 2 H), 7.4 (d, *J*=8.3 Hz, 1 H), 7.5 (s, 1 H), 7.8 (d, *J*=8.3 Hz, 1 H), 8.1 (s, 1 H), 9.4 (s, 1 H); ¹³C NMR (126 MHz, DMSO-*d*₆) δ ppm 13.8, 22.3, 40.5, 55.4, 55.8, 67.0, 100.1, 101.9, 111.2, 119.8, 120.4, 120.9, 121.2, 124.7, 126.4, 129.8, 144.2, 149.2, 156.4, 158.9, 160.7, 165.5; FTMS (ESI) *m/z* 381.1802 [M + H]⁺; calcd for C₂₂H₂₄N₂O₄: 381.1809.



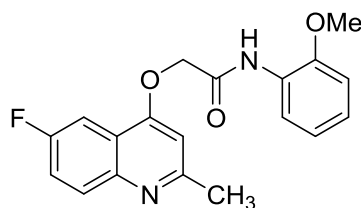
2-((2-Isopropyl-6-methoxyquinolin-4-yl)oxy)-*N*-(2-methoxyphenyl)acetamide (**6c**): Yield 47%; m.p.: 145-146 °C; ¹H NMR (500 MHz, DMSO-*d*₆) δ ppm 1.3 (s, 3 H), 1.2 (s, 3 H), 3.1 (m, 1 H), 3.8 (s, 3 H), 3.9 (s, 3 H), 5.08 (s, 2 H), 6.9 (m, 1 H), 6.95 (s, 1H), 7.1 (m, 2 H), 7.4 (dd, *J*=9.0, 2.7 Hz, 1 H), 7.5 (d, *J*=2.4 Hz, 1 H), 7.8 (d, *J*=9.3 Hz, 1 H), 8.1 (d, *J*=7.8 Hz, 1 H), 9.4 (s, 1 H); ¹³C NMR (126 MHz, DMSO-*d*₆) δ ppm 22.3, 36.6, 55.4, 55.8, 67.1, 100.1, 100.3, 111.2, 120.0, 120.5, 121.0, 121.2, 124.8, 126.4, 130.0, 144.0, 149.2, 156.4, 159.0, 165.6, 165.6; FTMS (ESI) *m/z* 381.1802 [M + H]⁺; calcd for C₂₂H₂₄N₂O₄: 381.1809.



2-((3-Benzyl-6-methoxy-2-methylquinolin-4-yl)oxy)-*N*-(2-methoxyphenyl)acetamide (**6d**): Yield 75%; m.p.: 162-163 °C; ^1H NMR (500 MHz, $\text{DMSO-}d_6$) δ ppm 2.47 (s, 3 H), 3.73 (s, 3 H), 3.90 (s, 3 H), 4.29 (s, 2 H), 4.77 (s, 2 H), 7.0 (t, $J=7.6$ Hz, 1 H), 7.1 (d, $J=7.8$ Hz, 1 H), 7.1 (d, $J=8.3$ Hz, 1 H), 7.2 (m, 3 H), 7.3 (t, $J=7.6$ Hz, 2 H), 7.4 (dd, $J=9.0, 2.7$ Hz, 1 H), 7.5 (d, $J=2.4$ Hz, 1 H), 7.9 (d, $J=9.3$ Hz, 1 H), 8.1 (d, $J=7.8$ Hz, 1 H), 9.4 (s, 1 H); ^{13}C NMR (126 MHz, $\text{DMSO-}d_6$) δ ppm 23.2, 31.3, 55.4, 55.6, 72.7, 100.1, 111.0, 120.3, 120.7, 121.3, 122.4, 124.2, 124.6, 126.0, 126.3, 127.9, 128.4, 130.1, 139.2, 143.7, 149.0, 157.0, 157.3, 158.0, 162.4, 165.8; FTMS (ESI) m/z 443.1960 $[\text{M} + \text{H}]^+$; calcd for $\text{C}_{27}\text{H}_{28}\text{N}_2\text{O}_4$: 443.1965.

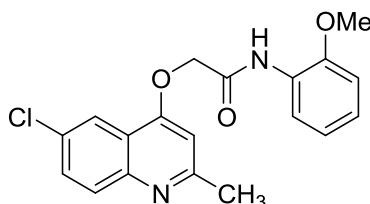


2-((6-Ethoxy-2-methylquinolin-4-yl)oxy)-*N*-(2-methoxyphenyl)acetamide (**6e**): Yield 58%; m.p.: 196-197 °C; ^1H NMR (500 MHz, $\text{DMSO-}d_6$) δ ppm 1.4 (s, 3 H), 2.5 (s, 3 H), 3.9 (s, 3 H), 4.2 (q, $J=5.9$ Hz, 2 H), 5.0 (s, 2 H), 6.9 (m, 2 H), 7.1 (s, 2 H), 7.4 (d, $J=8.3$ Hz, 1 H), 7.5 (s, 1 H), 7.8 (d, $J=8.8$ Hz, 1 H), 8.1 (d, $J=6.4$ Hz, 1 H), 9.4 (s, 1 H); ^{13}C NMR (126 MHz, $\text{DMSO-}d_6$) δ ppm 14.6, 25.0, 55.8, 63.5, 67.0, 101.0, 102.4, 111.2, 119.6, 120.5, 120.7, 121.3, 124.7, 126.4, 129.6, 144.1, 149.0, 155.6, 156.9, 158.7, 165.4; FTMS (ESI) m/z 367.1642 $[\text{M} + \text{H}]^+$; calcd for $\text{C}_{21}\text{H}_{22}\text{N}_2\text{O}_4$: 367.1652.

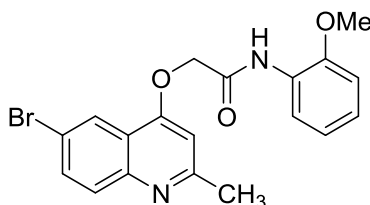


2-((6-Fluoro-2-methylquinolin-4-yl)oxy)-*N*-(2-methoxyphenyl)acetamide (**6f**): Yield 85%; m.p.: 188-189 °C; ^1H NMR (500 MHz, $\text{DMSO-}d_6$) δ ppm 2.6 (s, 3 H), 3.9 (s, 3 H), 5.0 (s, 2 H), 7.0 (t, $J=7.3$ Hz, 1 H), 7.0 (s, 1 H), 7.1 (m, 2 H), 7.6 (td, $J=8.8, 2.9$ Hz, 1

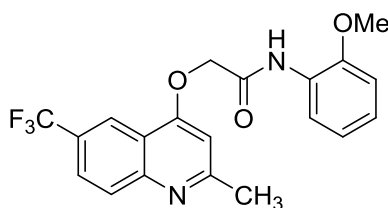
H), 7.9 (dd, $J=9.5, 1.7$ Hz, 1 H), 8.0 (dd, $J=9.3, 5.4$ Hz, 1 H), 8.1 (d, $J=7.3$ Hz, 1 H), 9.4 (s, 1 H); ^{13}C NMR (126 MHz, $\text{DMSO-}d_6$) δ ppm 25.1, 55.7, 67.1, 103.0, 104.8, 105.0, 109.5, 111.1, 119.3, 119.4, 119.4, 119.5, 120.5, 120.7, 124.7, 126.3, 130.8, 130.9, 145.4, 149.0, 158.1, 159.0, 159.0, 159.3, 159.4, 160.0, 165.0; FTMS (ESI) m/z 341.1290 $[\text{M} + \text{H}]^+$; calcd for $\text{C}_{19}\text{H}_{17}\text{FN}_2\text{O}_3$: 341.1296.



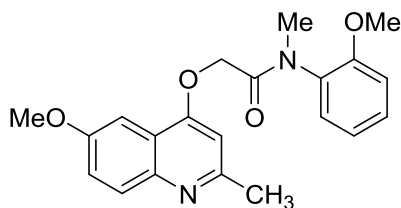
2-((6-Chloro-2-methylquinolin-4-yl)oxy)-*N*-(2-methoxyphenyl)acetamide (**6g**): Yield 70%; m.p.: 201-202 °C; ^1H NMR (500 MHz, $\text{DMSO-}d_6$) δ ppm 2.60 (s, 3 H), 3.91 (s, 3 H), 5.00 (s, 2 H), 6.95 (s, 1 H), 7.04-7.11 (m, 2 H), 7.73 (s, 1 H), 7.89 (s, 1 H), 8.09 (s, 1 H), 8.18 (s, 1 H), 8.3 (s, 1 H), 9.3 (s, 1 H); ^{13}C NMR (126 MHz, $\text{DMSO-}d_6$) δ ppm 25.1, 55.8, 67.2, 103.1, 109.3, 111.1, 119.7, 120.0, 120.4, 120.5, 124.6, 126.3, 129.4, 130.0, 130.1, 146.7, 158.5, 160.4, 164.8; FTMS (ESI) m/z 357.0994 $[\text{M} + \text{H}]^+$; calcd for $\text{C}_{19}\text{H}_{17}\text{ClN}_2\text{O}_3$: 357.1000.



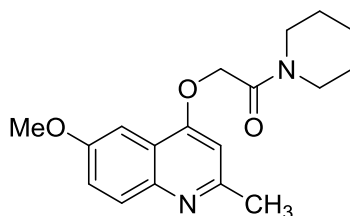
2-((6-Bromo-2-methylquinolin-4-yl)oxy)-*N*-(2-methoxyphenyl)acetamide (**6h**): Yield 32%; m.p.: 196-197 °C; ^1H NMR (400 MHz, $\text{DMSO-}d_6$) δ ppm 2.6 (s, 3 H), 3.9 (s, 3 H), 5.0 (s, 2 H), 7.0 (m, 1 H), 7.0 (s, 1 H), 7.1 (m, 2 H), 7.8 (m, 2 H), 8.1 (d, $J=8.2$ Hz, 1 H), 8.3 (d, $J=1.2$ Hz, 1 H), 9.4 (s, 1 H); ^{13}C NMR (101 MHz, $\text{DMSO-}d_6$) δ ppm 25.4; 56.0; 67.2; 103.3; 111.2; 118.0; 120.3; 120.5; 120.8; 123.4; 124.8; 126.4; 130.4; 132.9; 146.9; 149.1; 158.6; 160.8; 165.1; FTMS (ESI) m/z 401.0490 $[\text{M} + \text{H}]^+$; calcd for $\text{C}_{19}\text{H}_{17}\text{BrN}_2\text{O}_3$: 401.0495.



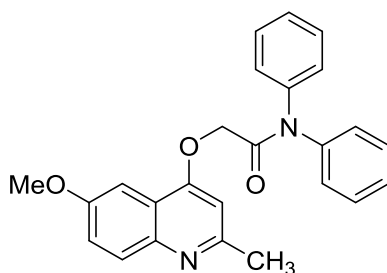
N-(2-Methoxyphenyl)-2-((2-methyl-6-(trifluoromethyl)quinolin-4-yl)oxy)acetamide (**6i**): Yield 56%; m.p.: 203-204 °C; ¹H NMR (500 MHz, DMSO-*d*₆) δ ppm 2.6 (s, 3 H), 3.8 (s, 3 H), 5.1 (s, 2 H), 6.9 (t, *J*=7.1 Hz, 1 H), 7.1 (m, 3 H), 8.0 (d, *J*=8.8 Hz, 1 H), 8.1 (d, *J*=7.8 Hz, 2 H), 8.5 (s, 1 H), 9.3 (s, 1 H); ¹³C NMR (126 MHz, DMSO-*d*₆) δ ppm 25.3, 55.6, 67.3, 103.5, 111.2, 118.2, 119.2, 119.3, 120.3, 120.9, 123.0, 124.6, 124.9, 125.0, 125.2, 126.3, 129.5, 149.2, 149.2, 149.4, 160.0, 162.9, 164.8; FTMS (ESI) *m/z* 391.1251 [M + H]⁺; calcd for C₂₀H₁₇F₃N₂O₃: 391.1264.



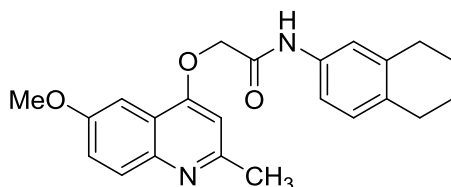
2-((6-Methoxy-2-methylquinolin-4-yl)oxy)-*N*-(2-methoxyphenyl)-*N*-methylacetamide (**12a**): Yield 72%; m.p.: 171-172 °C; ¹H NMR (500 MHz, DMSO-*d*₆) δ ppm 2.5 (s, 3 H), 3.1 (s, 3 H), 3.9 (d, *J*=19.6 Hz, 6 H), 4.5 (d, *J*=15.7 Hz, 1 H), 4.7 (d, *J*=15.2 Hz, 1 H), 6.5 (s, 1 H), 7.0 (t, *J*=6.8 Hz, 1 H), 7.2 (d, *J*=8.3 Hz, 1 H), 7.3 (s, 1 H), 7.3 (d, *J*=8.8 Hz, 1 H), 7.4 (m, 2 H), 7.7 (d, *J*=8.8 Hz, 1 H); ¹³C NMR (126 MHz, DMSO-*d*₆) δ ppm 25.1, 35.9, 55.3, 55.8, 65.5, 99.6, 101.6, 112.8, 119.6, 121.2, 121.5, 129.1, 129.4, 129.6, 130.1, 144.1, 154.6, 156.1, 156.5, 159.4, 166.2; FTMS (ESI) *m/z* 367.1643 [M + H]⁺; calcd for C₂₁H₂₂N₂O₄: 367.1652.



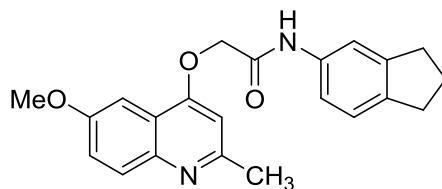
2-((6-Methoxy-2-methylquinolin-4-yl)oxy)-1-(piperidin-1-yl)ethan-1-one (**12b**): Yield 90%; m.p.: 105-105 °C; ¹H NMR (500 MHz, DMSO-*d*₆) δ ppm 1.5 (s, 3 H), 1.6 (s, 4 H), 2.5 (s, 2 H), 3.4 (s, 4 H), 3.9 (s, 3 H), 5.1 (s, 2 H), 6.8 (s, 1 H), 7.3 (d, *J*=9.3 Hz, 1 H), 7.4 (s, 1 H), 7.8 (d, *J*=9.3 Hz, 1 H); ¹³C NMR (126 MHz, DMSO-*d*₆) δ ppm 23.9, 25.1, 25.3, 26.0, 42.2, 45.1, 55.3, 59.8, 66.0, 99.7, 102.3, 119.8, 121.4, 129.5, 144.1, 156.2, 156.8, 159.5, 164.5; FTMS (ESI) *m/z* 315.1694 [M + H]⁺; calcd for C₁₈H₂₂N₂O₃: 315.1703.



2-((6-Methoxy-2-methylquinolin-4-yl)oxy)-*N,N*-diphenylacetamide (**12c**): Yield 31%; m.p.: 173-174 °C; ¹H NMR (500 MHz, DMSO-*d*₆) δ ppm 2.6 (s, 3 H), 3.4 (s, 2 H), 3.8 (s, 3 H), 4.9 (s, 2 H), 6.7 (s, 1 H), 7.3 (m, 11 H), 7.7 (d, *J*=9.3 Hz, 1 H); ¹³C NMR (126 MHz, DMSO-*d*₆) δ ppm 25.0, 55.2, 66.0, 99.5, 101.8, 119.6, 121.5, 129.4, 144.0, 156.0, 156.7, 159.2, 166.0; FTMS (ESI) *m/z* 399.1698 [M + H]⁺; calcd for C₂₅H₂₂N₂O₃: 399.1703.

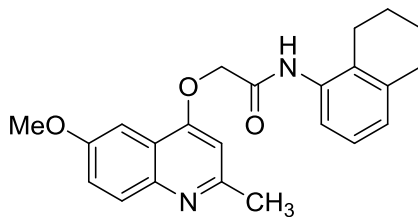


2-((6-Methoxy-2-methylquinolin-4-yl)oxy)-*N*-(5,6,7,8-tetrahydronaphthalen-2-yl)acetamide (**12d**): Yield 99%; m.p.: 163-164 °C; ¹H NMR (500 MHz, DMSO-*d*₆) δ ppm 1.7 (m, 4 H), 2.5 (s, 3 H), 2.7 (m, 4 H), 3.9 (s, 3 H), 5.0 (s, 2 H), 6.8 (s, 1 H), 7.0 (d, *J*=8.3 Hz, 1 H), 7.3 (d, *J*=7.8 Hz, 1 H), 7.4 (m, 2 H), 7.5 (s, 1 H), 7.8 (d, *J*=8.8 Hz, 1 H), 10.1 (s, 1 H); ¹³C NMR (126 MHz, DMSO-*d*₆) δ ppm 22.6, 22.7, 25.0, 28.2, 28.9, 55.3, 67.0, 100.0, 102.1, 117.2, 119.7, 119.9, 121.5, 129.0, 129.4, 132.0, 135.6, 136.7, 144.1, 156.1, 156.7, 159.4, 165.2; FTMS (ESI) *m/z* 377.1850 [M + H]⁺; calcd for C₂₃H₂₄N₂O₃: 377.1860.

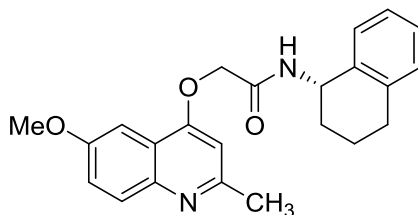


N-(2,3-Dihydro-1*H*-inden-5-yl)-2-((6-methoxy-2-methylquinolin-4-yl)oxy)acetamide (**12e**): Yield 73%; m.p.: 192-193 °C; ¹H NMR (500 MHz, DMSO-*d*₆) δ ppm 2.0 (q, *J*=7.3 Hz, 2 H), 2.5 (s, 3 H), 2.8 (m, 4 H), 3.9 (s, 3 H), 5.0 (s, 2 H), 6.8 (s, 1 H), 7.2 (d, *J*=7.8 Hz, 1 H), 7.3 (m, 2 H), 7.5 (d, *J*=2.9 Hz, 1 H), 7.6 (s, 1 H), 7.8 (d, *J*=9.3 Hz, 1 H), 10.1 (s, 1 H); ¹³C NMR (126 MHz, DMSO-*d*₆) δ ppm 25.0, 25.1, 31.8, 32.5, 55.4, 67.1, 100.1, 102.2, 115.9, 117.8, 119.7, 121.5, 124.2, 129.5, 136.5, 139.0, 144.1, 144.2,

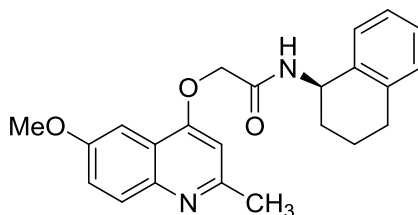
156.2, 156.8, 159.4, 165.3; FTMS (ESI) m/z 363.1695 $[M + H]^+$; calcd for $C_{22}H_{22}N_2O_3$: 363.1703.



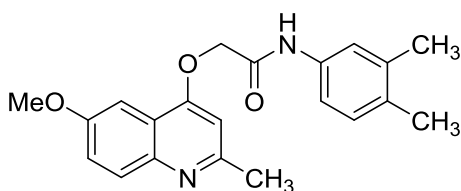
2-((6-Methoxy-2-methylquinolin-4-yl)oxy)-*N*-(5,6,7,8-tetrahydronaphthalen-1-yl)acetamide (**12f**): Yield 66%; m.p.: 218-219 °C; 1H NMR (500 MHz, $DMSO-d_6$) δ ppm 1.7 (m, 4 H), 2.6 (s, 3 H), 2.6 (m, 2 H), 2.7 (m, 2 H), 3.9 (s, 3 H), 5.0 (s, 2 H), 6.9 (s, 1 H), 6.9 (d, $J=7.3$ Hz, 1 H), 7.1 (t, $J=7.6$ Hz, 1 H), 7.3 (d, $J=7.8$ Hz, 1 H), 7.3 (dd, $J=9.0, 2.7$ Hz, 1 H), 7.6 (s, 1 H), 7.8 (d, $J=8.8$ Hz, 1 H), 9.4 (s, 1 H); ^{13}C NMR (126 MHz, $DMSO-d_6$) δ ppm 22.2, 22.3, 24.1, 25.0, 29.1, 55.4, 67.3, 100.3, 102.3, 119.7, 121.4, 122.6, 125.1, 126.4, 129.4, 135.1, 137.5, 144.2, 156.3, 156.7, 159.2, 165.6; FTMS (ESI) m/z 377.1847 $[M + H]^+$; calcd for $C_{23}H_{24}N_2O_3$: 377.1860.



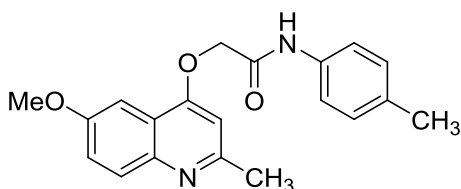
(*S*)-2-((6-Methoxy-2-methylquinolin-4-yl)oxy)-*N*-(1,2,3,4-tetrahydronaphthalen-1-yl)acetamide (**12g**): Yield 52%; m.p.: 190-191°C; 1H NMR (500 MHz, $DMSO-d_6$) δ ppm 1.8 (m, 2 H), 1.9 (m, 2 H), 2.5 (s, 3 H), 2.7 (m, 2 H), 3.8 (s, 3 H), 4.8 (s, 2 H), 5.1 (m, 1 H), 6.8 (s, 1 H), 7.1 (m, 4 H), 7.3 (dd, $J=9.0, 2.7$ Hz, 1 H), 7.4 (d, $J=2.4$ Hz, 1 H), 7.8 (d, $J=8.8$ Hz, 1 H), 8.6 (d, $J=8.8$ Hz, 1 H); ^{13}C NMR (126 MHz, $DMSO-d_6$) δ ppm 20.1, 25.0, 28.7, 29.6, 46.4, 55.3, 67.1, 100.2, 102.1, 119.7, 121.5, 125.7, 126.8, 127.9, 128.8, 129.4, 137.1, 137.1, 144.1, 156.1, 156.7, 159.4, 166.3; FTMS (ESI) m/z 377.1848 $[M + H]^+$; calcd for $C_{23}H_{24}N_2O_3$: 377.1860.



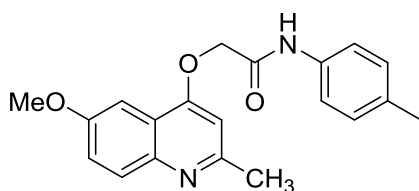
(*R*)-2-((6-Methoxy-2-methylquinolin-4-yl)oxy)-*N*-(1,2,3,4-tetrahydronaphthalen-1-yl)acetamide (**12h**): Yield 79%; m.p.: 190-191 °C; ¹H NMR (500 MHz, DMSO-*d*₆) δ ppm 1.8 (s, 2 H), 1.9 (s, 2 H), 2.5 (s, 3 H), 2.7 (m, 2 H), 3.8 (s, 3 H), 4.9 (s, 2 H), 5.1 (s, 1 H), 6.8 (s, 1 H), 7.1 (m, 3 H), 7.3 (d, *J*=9.3 Hz, 1 H), 7.4 (s, 1 H), 7.8 (d, *J*=8.8 Hz, 1 H), 8.6 (d, *J*=8.3 Hz, 1 H); ¹³C NMR (126 MHz, DMSO-*d*₆) δ ppm 20.1, 25.0, 28.7, 29.6, 46.4, 55.3, 67.1, 100.2, 102.1, 119.7, 121.5, 125.7, 126.8, 127.9, 128.7, 129.4, 137.1, 137.1, 144.1, 156.1, 156.7, 159.4, 166.3; FTMS (ESI) *m/z* 377.1860 [M + H]⁺; calcd for C₂₃H₂₄N₂O₃: 377.1860.



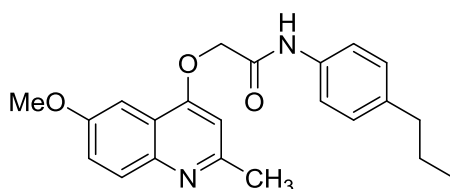
N-(3,4-Dimethylphenyl)-2-((6-methoxy-2-methylquinolin-4-yl)oxy)acetamide (**12i**): Yield 88%; m.p.: 169-170 °C; ¹H NMR (500 MHz, DMSO-*d*₆) δ ppm 2.1 (s, 3 H), 2.2 (s, 3 H), 2.5 (s, 3 H), 3.9 (s, 3 H), 5.0 (s, 2 H), 6.8 (s, 1 H), 7.1 (d, *J*=8.3 Hz, 1 H), 7.4 (m, 2 H), 7.4 (s, 1 H), 7.5 (d, *J*=2.4 Hz, 1 H), 7.8 (d, *J*=8.8 Hz, 1 H), 8.3 (s, 1 H), 10.1 (s, 1 H); ¹³C NMR (126 MHz, DMSO-*d*₆) δ ppm 18.8, 19.6, 25.1, 55.4, 67.1, 79.2, 100.1, 102.2, 117.2, 119.7, 120.8, 121.6, 129.5, 129.6, 131.5, 136.1, 136.4, 144.2, 156.2, 156.8, 159.5, 165.3; FTMS (ESI) *m/z* 351.1696 [M + H]⁺; calcd for C₂₁H₂₂N₂O₃: 351.1703.



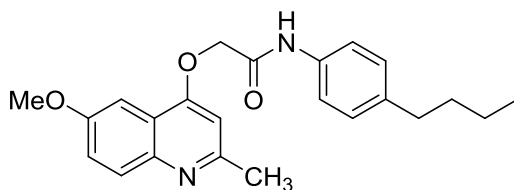
2-((6-Methoxy-2-methylquinolin-4-yl)oxy)-*N*-(*p*-tolyl)acetamide (**12j**): Yield 56%; m.p.: 188-189 °C; ¹H NMR (500 MHz, DMSO-*d*₆) δ ppm 2.2 (s, 3 H) 2.5 (s, 3 H) 3.9 (s, 3 H) 5.0 (s, 2 H) 6.8 (s, 1 H) 7.1 (d, *J*=7.8 Hz, 2 H) 7.3 (d, *J*=9.3 Hz, 1 H) 7.5 (m, 3 H) 7.8 (d, *J*=8.8 Hz, 1 H) 10.2 (s, 1 H); ¹³C NMR (126 MHz, DMSO-*d*₆) δ ppm 20.4, 25.1, 55.4, 67.1, 100.1, 102.2, 119.7, 119.7, 121.5, 129.1, 129.5, 132.7, 135.8, 144.2, 156.2, 156.8, 159.4, 165.4; FTMS (ESI) *m/z* 337.1540 [M + H]⁺; calcd for C₂₀H₂₀N₂O₃: 337.1547.



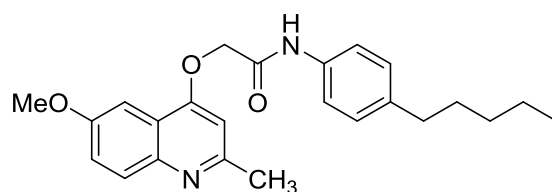
N-(4-Ethylphenyl)-2-((6-methoxy-2-methylquinolin-4-yl)oxy)acetamide (**12k**): Yield 68%; m.p.: 198-199 °C; ¹H NMR (500 MHz, DMSO-*d*₆) δ ppm 1.1 (s, 3 H), 2.5 (s, 5 H), 3.9 (s, 3 H), 5.0 (s, 2 H), 6.8 (s, 1 H), 7.2 (d, *J*=4.4 Hz, 2 H), 7.3 (d, *J*=5.9 Hz, 1 H), 7.5 (d, *J*=12.7 Hz, 3 H), 7.8 (s, 1 H), 10.2 (s, 1 H); ¹³C NMR (126 MHz, DMSO-*d*₆) δ ppm 15.6, 25.0, 27.5, 55.3, 67.1, 100.1, 102.1, 119.7, 121.5, 127.9, 129.4, 136.0, 139.1, 144.1, 156.2, 156.8, 159.4, 165.3; FTMS (ESI) *m/z* 351.1696 [M + H]⁺; calcd for C₂₁H₂₂N₂O₃: 351.1703.



2-((6-Methoxy-2-methylquinolin-4-yl)oxy)-*N*-(4-propylphenyl)acetamide (**12l**): Yield 83%; m.p.: 194-195 °C; ¹H NMR (500 MHz, DMSO-*d*₆) δ ppm 0.9 (t, *J*=7.3 Hz, 3 H), 1.6 (s, *J*=7.4 Hz, 2 H), 2.5 (m, 2 H), 2.5 (s, 3 H), 3.9 (s, 3 H), 5.0 (s, 2 H), 6.9 (s, 1 H), 7.1 (d, *J*=8.8 Hz, 2 H), 7.4 (dd, *J*=8.8, 2.9 Hz, 1 H), 7.5 (d, *J*=2.4 Hz, 1 H), 7.5 (d, *J*=8.8 Hz, 2 H), 7.8 (d, *J*=9.3 Hz, 1 H), 10.2 (s, 1 H); ¹³C NMR (126 MHz, DMSO-*d*₆) δ ppm 13.6, 24.1, 25.1, 36.7, 55.4, 67.1, 100.1, 102.2, 119.7, 121.6, 128.6, 129.5, 136.1, 137.5, 144.2, 156.2, 156.9, 159.5, 165.4; FTMS (ESI) *m/z* 365.1851 [M + H]⁺; calcd for C₂₂H₂₄N₂O₃: 365.1860.



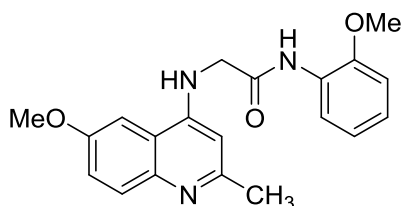
N-(4-Butylphenyl)-2-((6-methoxy-2-methylquinolin-4-yl)oxy)acetamide (**12m**): Yield 84%; m.p.: 143-174 °C; ¹H NMR (500 MHz, DMSO-*d*₆) δ ppm 0.9 (t, *J*=7.3 Hz, 3 H), 1.3 (s, *J*=7.3 Hz, 2 H), 1.5 (q, *J*=7.5 Hz, 2 H), 2.5 (m, 2 H), 2.5 (s, 3 H), 3.9 (s, 3 H), 5.0 (s, 2 H), 6.9 (s, 1 H), 7.1 (d, *J*=8.3 Hz, 2 H), 7.4 (dd, *J*=9.0, 2.7 Hz, 1 H), 7.5 (d, *J*=2.9 Hz, 1 H), 7.5 (d, *J*=8.3 Hz, 2 H), 7.8 (d, *J*=9.3 Hz, 1 H); ¹³C NMR (126 MHz, DMSO-*d*₆) δ ppm 13.7, 21.6, 25.0, 33.1, 34.1, 55.3, 67.0, 100.0, 102.1, 119.6, 121.5, 128.4, 129.4, 136.0, 137.6, 144.1, 156.1, 156.7, 159.4, 165.3; FTMS (ESI) *m/z* 379.2023 [M + H]⁺; calcd for C₂₃H₂₆N₂O₃: 379.2016.



2-((6-Methoxy-2-methylquinolin-4-yl)oxy)-*N*-(4-pentylphenyl)acetamide (**12n**): Yield 95%; m.p.: 118-119 °C; ¹H NMR (400 MHz, DMSO-*d*₆) δ ppm 2.6 (s, 3 H), 3.9 (s, 3 H), 5.0 (s, 2 H), 7.0 (m, 1 H), 7.0 (s, 1 H), 7.1 (m, 2 H), 7.8 (m, 2 H), 8.1 (d, *J*=8.2 Hz, 1 H), 8.3 (d, *J*=1.2 Hz, 1 H), 9.4 (s, 1 H); ¹³C NMR (101 MHz, DMSO-*d*₆) δ ppm 25.4; 56.0; 67.2; 103.3; 111.2; 118.0; 120.3; 120.5; 120.8; 123.4; 124.8; 126.4; 130.4; 132.9; 146.9; 149.1; 158.6; 160.8; 165.1; FTMS (ESI) *m/z* 393.2147 [M + H]⁺; calcd for C₂₄H₂₈N₂O₃: 393.2173.

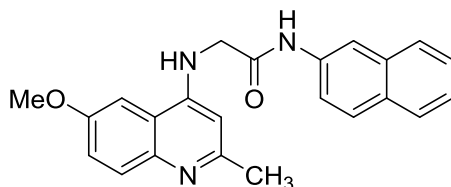
1.4 General procedure for the preparation of the 2-(quinolin-4-ylamino)acetamides **9a-b**.

Under argon atmosphere, sodium hydride (25 mg) dispersed in oil was washed with dry hexane and then stirred in dry DMSO (4 mL) at 45 °C for 20 min. The solution containing the 2-methyl-6-methoxy-4-aminoquinoline **7** (0.5 mmol) dissolved in 4 mL of dry DMSO was added dropwise to the mixture which was stirred for 20 min at 75 °C. 2-Bromo-*N*-acetamides **8a** and **8b** (0.5 mmol) in DMSO (2 mL) was kept under argon atmosphere and added to the reaction mixture with subsequent stirring for 3 h at 80 °C. After completion of the reaction (evaluated by TLC), the reaction mixture was allowed to cool, poured into crushed ice, and then extracted with ethyl acetate (3 x 50 mL). The organic layer was washed with water and dried using magnesium sulfate before to be evaporated and dried under vacuum.² Purification of the compound was accomplished by flash chromatography on silica gel (Macherey-Nagel, 35-70 mesh) eluting with hexane and ethyl acetate (7:3, 1:1, 3:7, 0:1) and ethyl acetate and methanol (9:1).



2-((6-Methoxy-2-methylquinolin-4-yl)amino)-*N*-(2-methoxyphenyl)acetamide (**9a**): Yield 31% (0.113 g), m.p.: 174-175 °C. ¹H NMR (500 MHz, DMSO-*d*₆) δ ppm 2.4 (s, 3 H), 3.7 (s, 3 H), 3.9 (s, 3 H), 4.2 (s, 2 H), 6.4 (s, 1 H), 6.9 (t, *J*=7.1 Hz, 1 H), 7.0 (d,

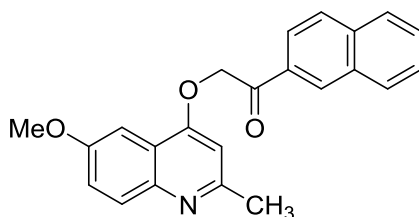
$J=7.8$ Hz, 1 H), 7.0 (d, $J=7.3$ Hz, 1 H), 7.3 (d, $J=8.8$ Hz, 1 H), 7.6 (s, 1 H), 7.7 (m, 2 H), 8.0 (d, $J=7.3$ Hz, 1 H), 9.3 (s, 1 H). ^{13}C NMR (126 MHz, $\text{DMSO-}d_6$) δ ppm 24.3, 46.4, 55.6, 55.7, 99.0, 100.9, 111.2, 117.8, 120.4, 120.8, 120.9, 124.4, 126.9, 128.7, 149.1, 149.8, 155.4, 155.8, 168.0. FTMS (ESI) m/z 352.1669 $[\text{M} + \text{H}]^+$; calcd for $\text{C}_{20}\text{H}_{21}\text{N}_3\text{O}_3$: 352.1656.



2-((6-Methoxy-2-methylquinolin-4-yl)amino)-*N*-(naphthalen-2-yl)acetamide (**9b**): Yield 28% (0.107 g), m.p.: 243-244 °C. ^1H NMR (500 MHz, $\text{DMSO-}d_6$) δ ppm 2.39 (s, 3H), 3.89 (s, 3H), 4.19 (s, 2H), 6.28 (s, 1H), 7.23 (d, $J=9.3$ Hz, 1H), 7.3 (m, 2 H), 7.4 (m, 1 H), 7.5 (s, 1 H), 7.6 (d, $J=7.8$ Hz, 2H), 7.7-7.8 (m, 3 H), 8.29 (s, 1H), 10.3 (s, 1H). ^{13}C NMR (126 MHz, $\text{DMSO-}d_6$) δ ppm 24.99, 46.36, 55.52, 98.72, 100.87, 115.44, 117.93, 120.02, 120.22, 124.63, 126.41, 127.23, 127.42, 128.38, 129.78, 133.35, 136.37, 143.56, 149.42, 155.46, 155.91, 168.58. FTMS (ESI) m/z 372.1707 $[\text{M} + \text{H}]^+$; calcd for $\text{C}_{23}\text{H}_{21}\text{N}_3\text{O}_2$: 372.1707.

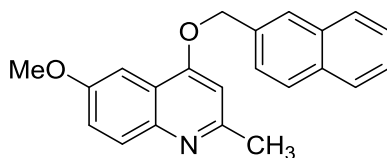
1.5 General procedure for the preparation of the 4-hydroxyquinolines 10 and 11.

The solution containing 4-hydroxyquinoline **5a** (1.1 mmol) and excess of K_2CO_3 (3.12 mmol) dissolved in 6 mL of dimethylformamide (DMF) was added 2-bromo-1-(naphthalen-2-yl)ethan-1-one or 2-(2-bromoethyl)naphthalene (1 mmol). The resulting solution was kept under argon atmosphere and stirred for 8 h at 25 °C. After this time, the reaction mixture was dissolved in 200 mL of distilled water. The precipitated product was filtered off, washed with water and dried under vacuum. Purification of the compounds was performed by flash chromatography on silica gel (Macherey-Nagel, 35-70 mesh) using hexane: ethyl acetate (1:1) as eluent.



2-((6-Methoxy-2-methylquinolin-4-yl)oxy)-1-(naphthalen-2-yl)ethan-1-one (**10**): Yield 61% (0.113 g); m.p.: 176-177 °C; ^1H NMR (500 MHz, $\text{DMSO-}d_6$) δ ppm 2.5 (s, 3 H),

3.9 (s, 3 H), 6.0 (s, 2 H), 7.0 (s, 1 H), 7.3 (d, $J=9.3$ Hz, 1 H), 7.5 (s, 1 H), 7.7 (m, 2 H), 7.8 (dd, $J=9.3, 2.0$ Hz, 1 H), 8.0 (d, $J=8.8$ Hz, 2 H), 8.1 (m, 1 H), 8.2 (d, $J=8.3$ Hz, 1 H), 8.8 (s, 1 H); ^{13}C NMR (126 MHz, $\text{DMSO-}d_6$) δ ppm 25.0, 55.3, 70.5, 99.7, 102.5, 119.8, 121.5, 123.3, 127.1, 127.8, 128.5, 128.9, 129.5, 129.6, 130.0, 131.5, 132.1, 135.3, 144.2, 156.3, 156.9, 159.4, 193.4; FTMS (ESI) m/z 358.1432 $[\text{M} + \text{H}]^+$; calcd for $\text{C}_{23}\text{H}_{19}\text{NO}_3$: 358.1438.



6-Methoxy-2-methyl-4-(naphthalen-2-ylmethoxy)quinoline (**11**): Yield 76% (0.245 g), m.p.: 158-159 °C. ^1H NMR (500 MHz, $\text{DMSO-}d_6$) δ ppm 2.5 (s, 3 H), 3.8 (s, 3 H), 5.5 (s, 2 H), 7.0 (s, 1 H), 7.3 (d, $J=8.8$ Hz, 1 H), 7.4 (s, 1 H), 7.5 (s, 2 H), 7.7 (d, $J=7.8$ Hz, 1 H), 7.8 (d, $J=9.3$ Hz, 1 H), 8.0 (m, 3 H), 8.1 (s, 1 H). ^{13}C NMR (126 MHz, $\text{DMSO-}d_6$) δ ppm 25.1, 55.3, 69.7, 99.7, 102.5, 119.9, 121.3, 125.5, 126.3, 126.3, 126.4, 127.6, 127.9, 128.3, 129.6, 132.6, 132.8, 133.9, 144.1, 156.3, 157.0, 159.6. FTMS (ESI) m/z 323.1396 $[\text{M} + \text{H}]^+$; calcd for $\text{C}_{20}\text{H}_{20}\text{N}_2\text{O}_4$: 323.1390.

7. ^1H NMR and ^{13}C NMR spectra of synthesized compounds

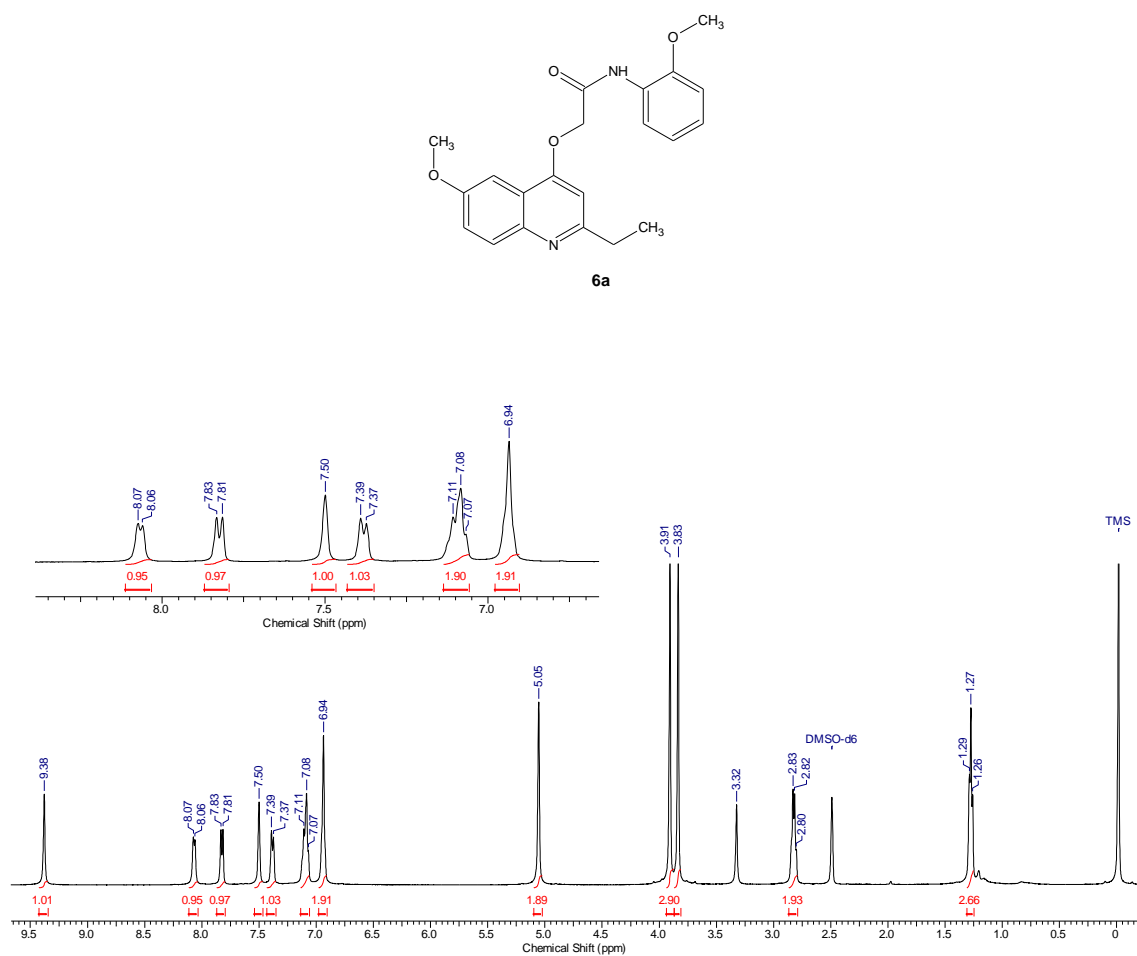


Figure S1. ^1H RMN spectrum of 2-[(6-methoxy-2-ethylquinolin-4-yl)oxy]-N-(2-methoxyphenyl)acetamide (**6a**) in $\text{DMSO-}d_6$.

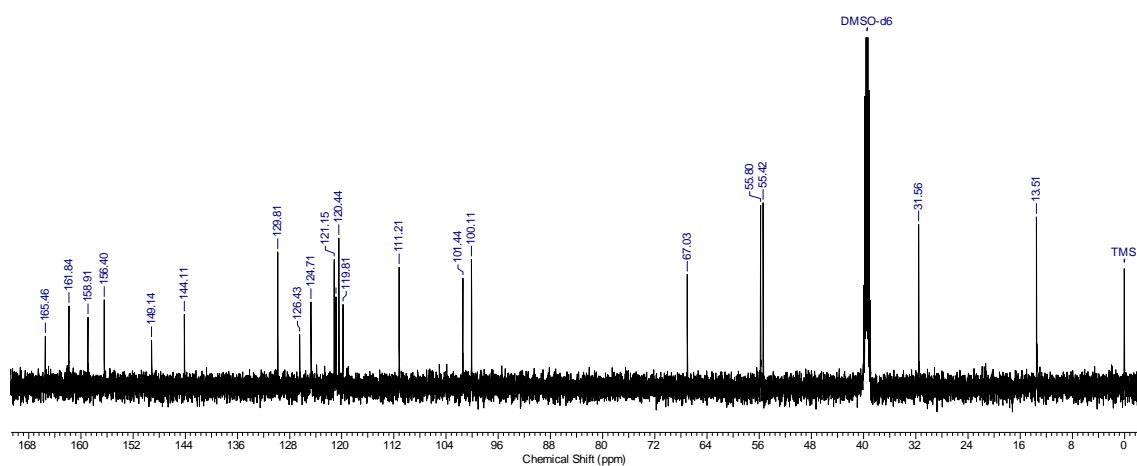


Figure S2. ^{13}C RMN spectrum of 2-[(6-methoxy-2-ethylquinolin-4-yl)oxy]-N-(2-methoxyphenyl)acetamide (**6a**) in $\text{DMSO-}d_6$.

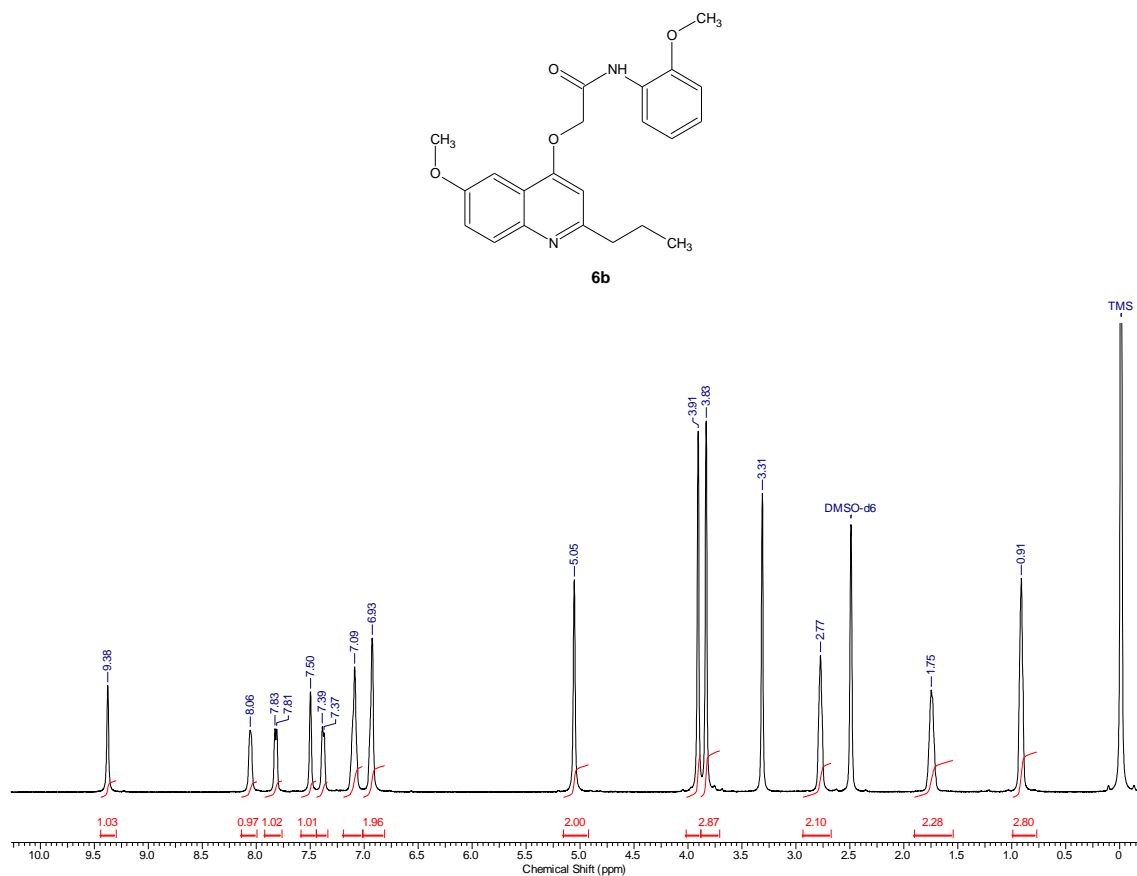


Figure S3. ¹H RMN spectrum of 2-[(6-methoxy-2-propylquinolin-4-yl)oxy]-N-(2-methoxyphenyl)acetamide (**6b**) in DMSO-*d*₆.

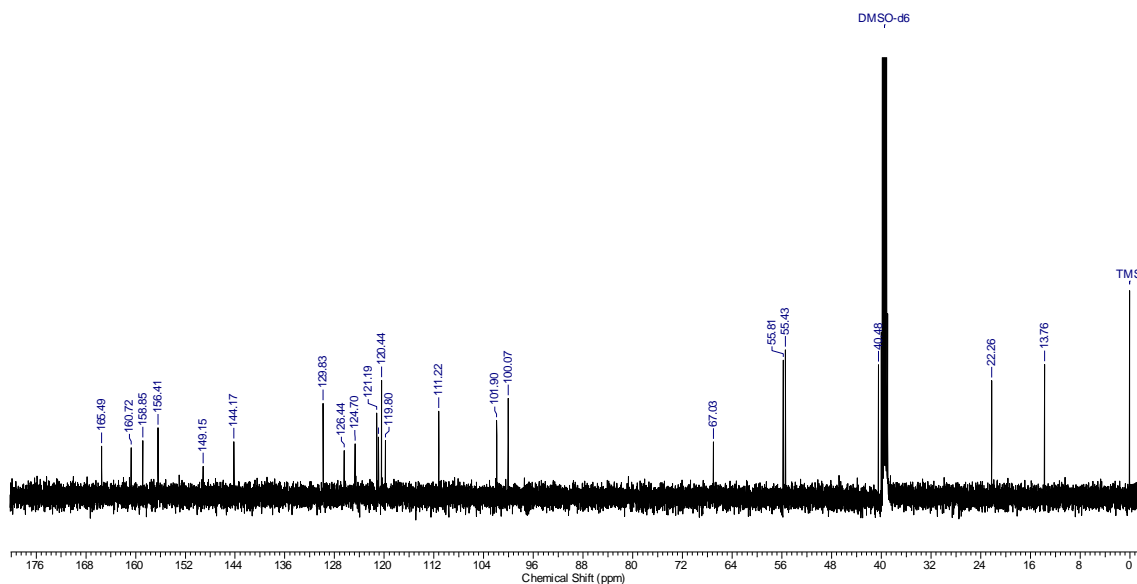


Figure S4. ¹³C RMN spectrum of 2-[(6-methoxy-2-propylquinolin-4-yl)oxy]-N-(2-methoxyphenyl)acetamide (**6b**) in DMSO-*d*₆.

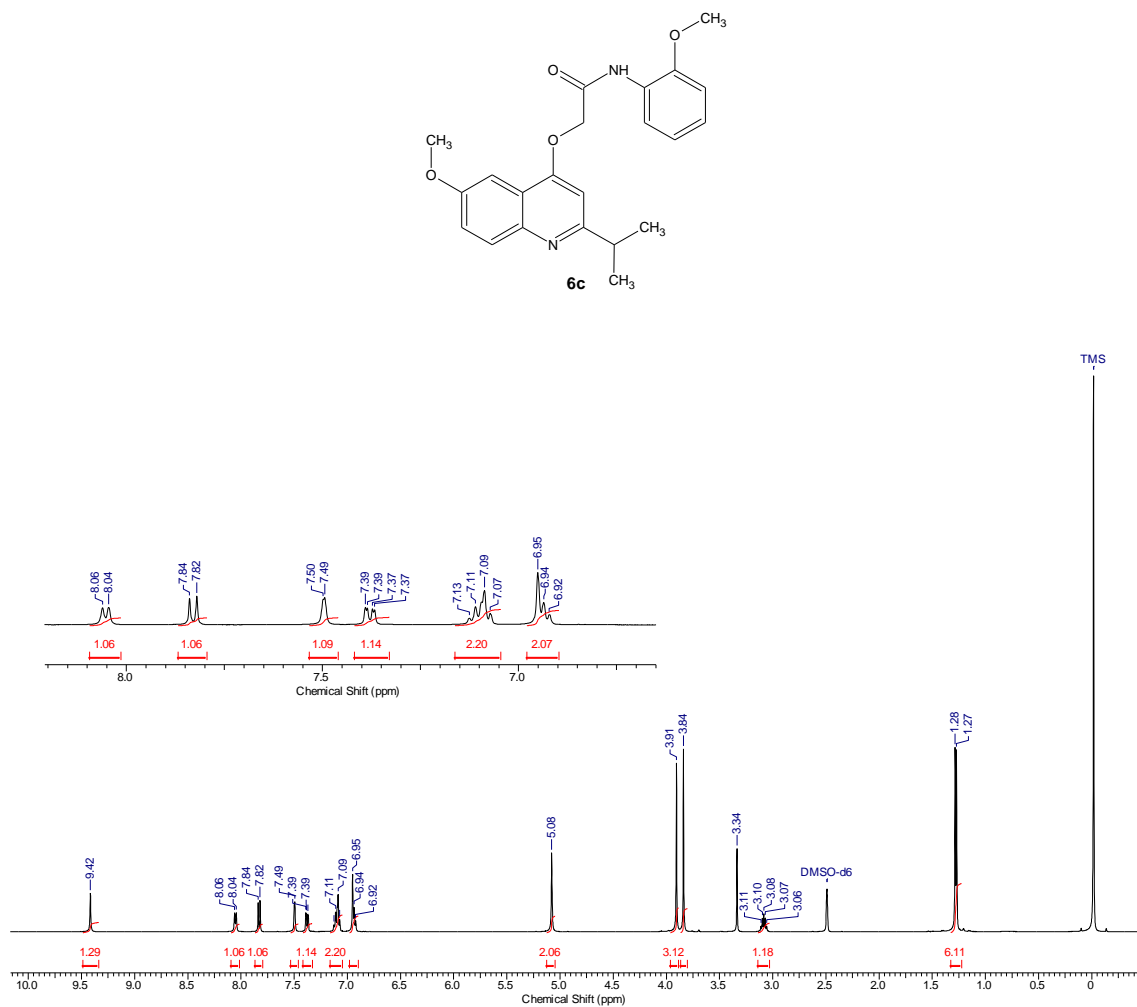


Figure S5. ¹H RMN spectrum of 2-[(6-methoxy-2-isopropylquinolin-4-yl)oxy]-N-(2-methoxyphenyl)acetamide (**6c**) in DMSO-*d*₆.

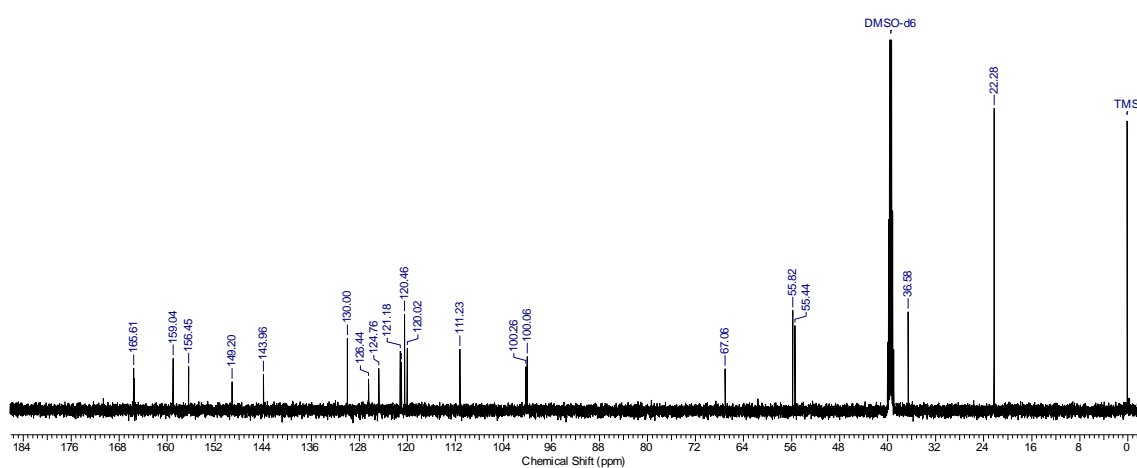


Figure S6. ¹³C RMN spectrum of 2-[(6-methoxy-2-isopropylquinolin-4-yl)oxy]-N-(2-methoxyphenyl)acetamide (**6c**) in DMSO-*d*₆.

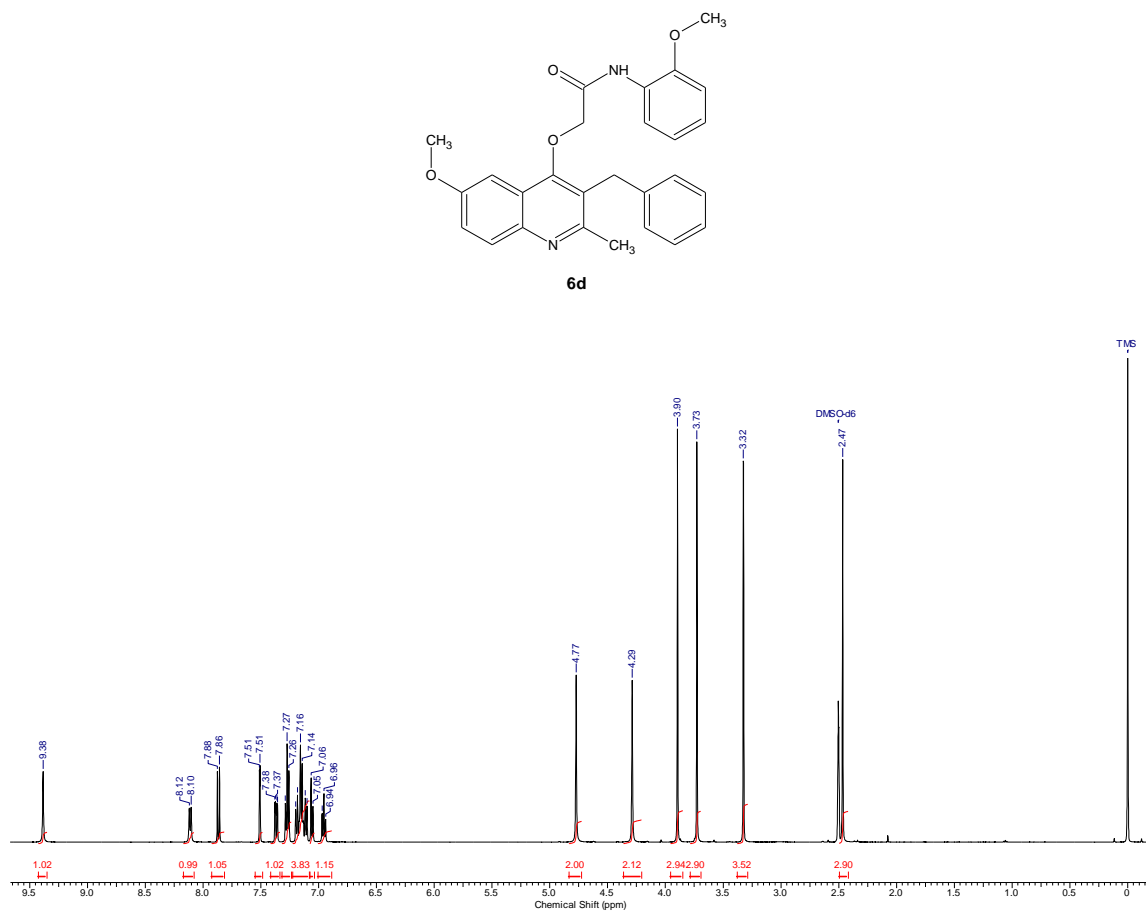


Figure S7. ¹H RMN spectrum of 2-[(3-benzyl-6-methoxy-2-methylquinolin-4-yl)oxy]-*N*-(2-methoxyphenyl)acetamide (**6d**) in DMSO-*d*₆.

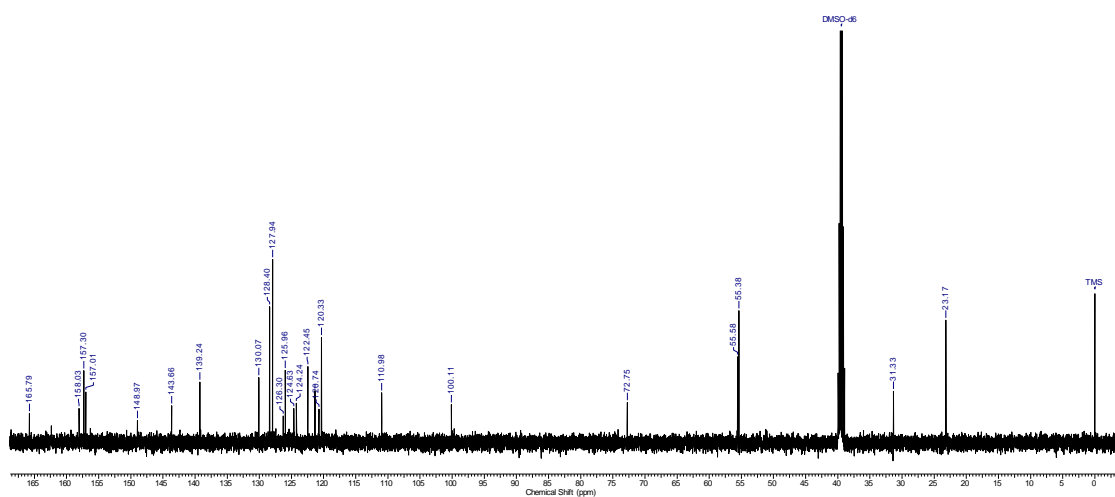


Figure S8. ¹³C RMN spectrum of 2-[(3-benzyl-6-methoxy-2-methylquinolin-4-yl)oxy]-*N*-(2-methoxyphenyl)acetamide (**6d**) in DMSO-*d*₆.

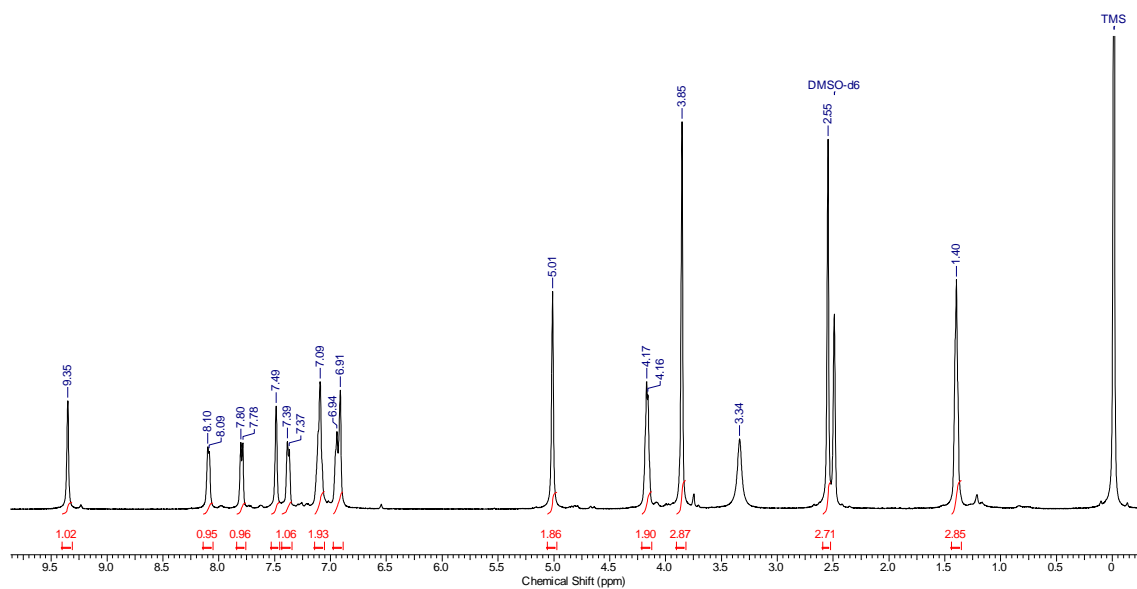
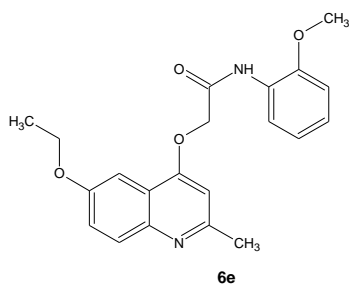


Figure S9. ^1H RMN spectrum of 2-[(6-ethoxy-2-methylquinolin-4-yl)oxy]-*N*-(2-methoxyphenyl)acetamide (**6e**) in $\text{DMSO-}d_6$.

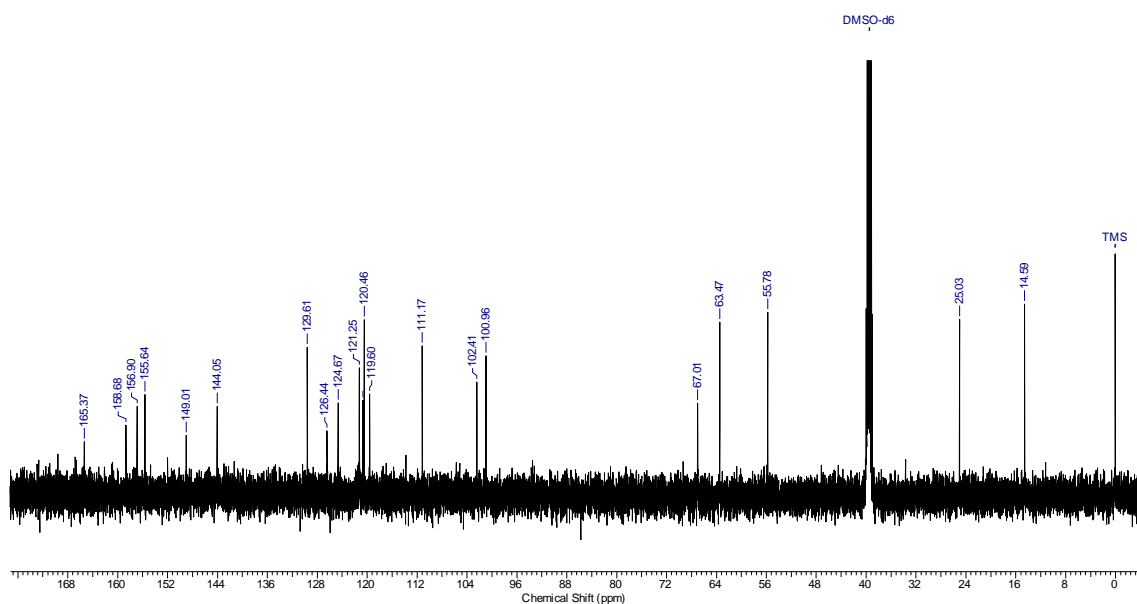


Figure S10. ^{13}C RMN spectrum of 2-[(6-ethoxy-2-methylquinolin-4-yl)oxy]-*N*-(2-methoxyphenyl)acetamide (**6e**) in $\text{DMSO-}d_6$.

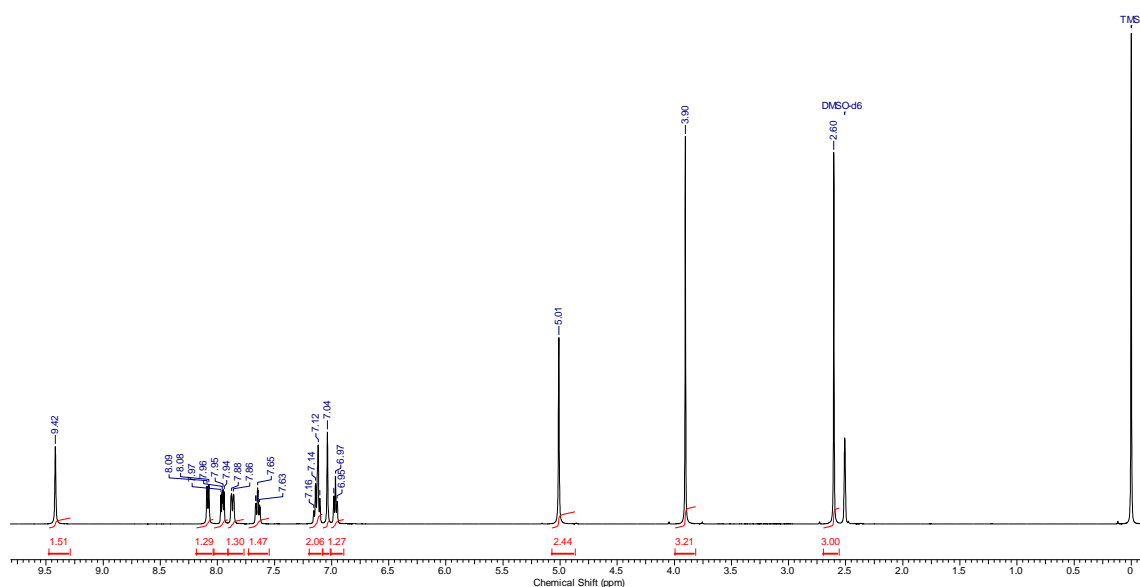
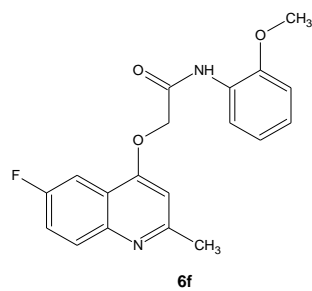


Figure S11. ^1H RMN spectrum of 2-[(6-fluoro-2-methylquinolin-4-yl)oxy]-*N*-(2-methoxyphenyl)acetamide (**6f**) in $\text{DMSO-}d_6$.

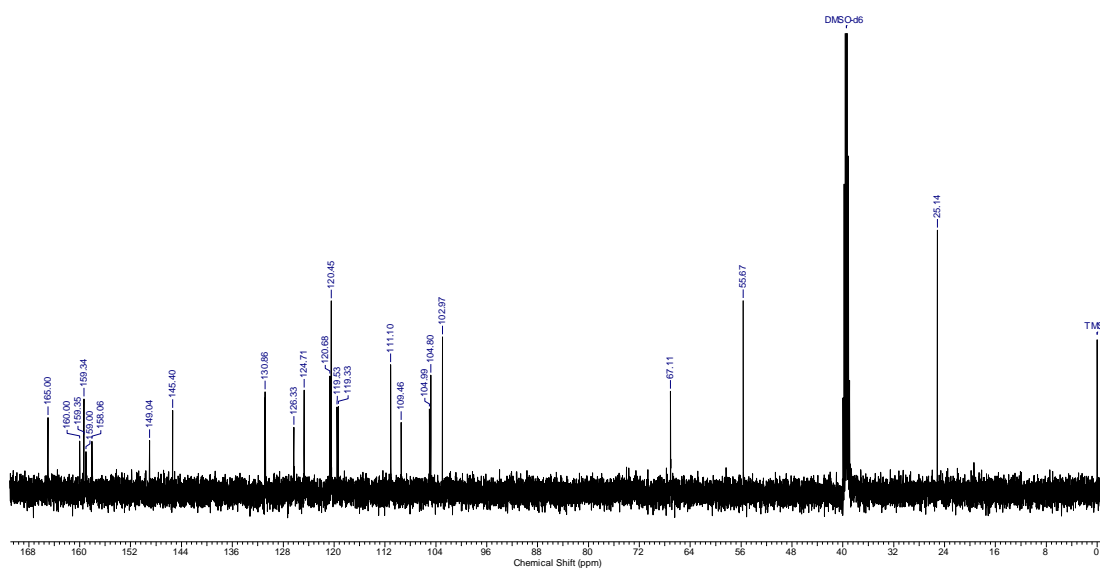


Figure S12. ^{13}C RMN spectrum of 2-[(6-fluoro-2-methylquinolin-4-yl)oxy]-*N*-(2-methoxyphenyl)acetamide (**6f**) in $\text{DMSO-}d_6$.

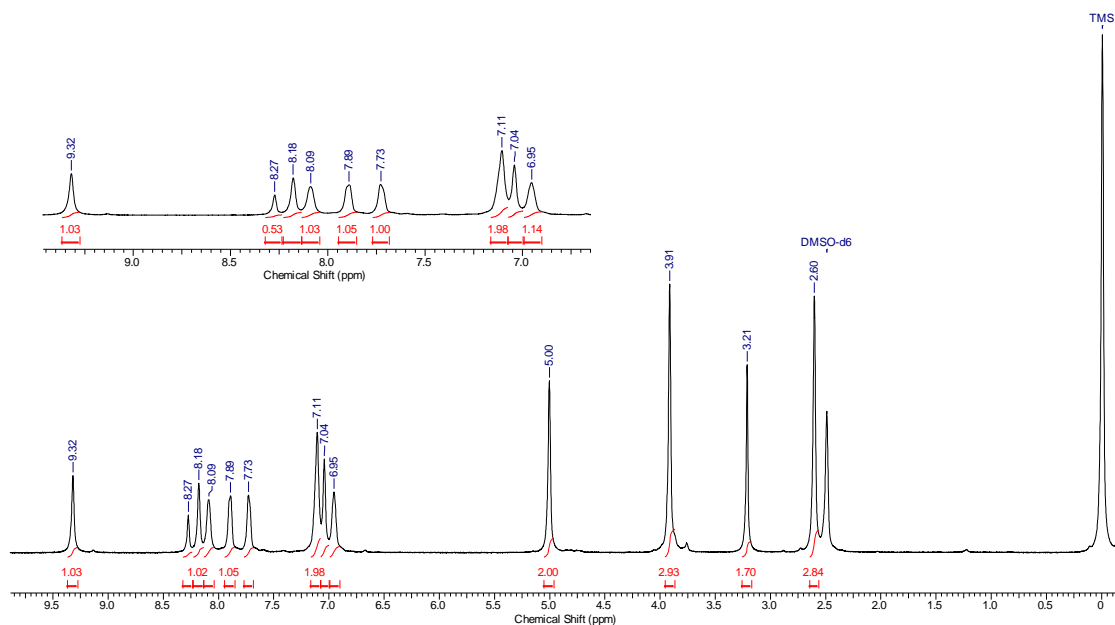
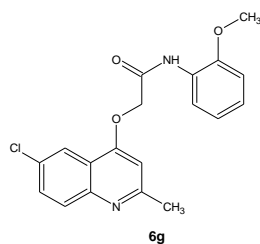


Figure S13. ^1H RMN spectrum of 2-[(6-chloro-2-methylquinolin-4-yl)oxy]-*N*-(2-methoxyphenyl)acetamide (**6g**) in $\text{DMSO-}d_6$.

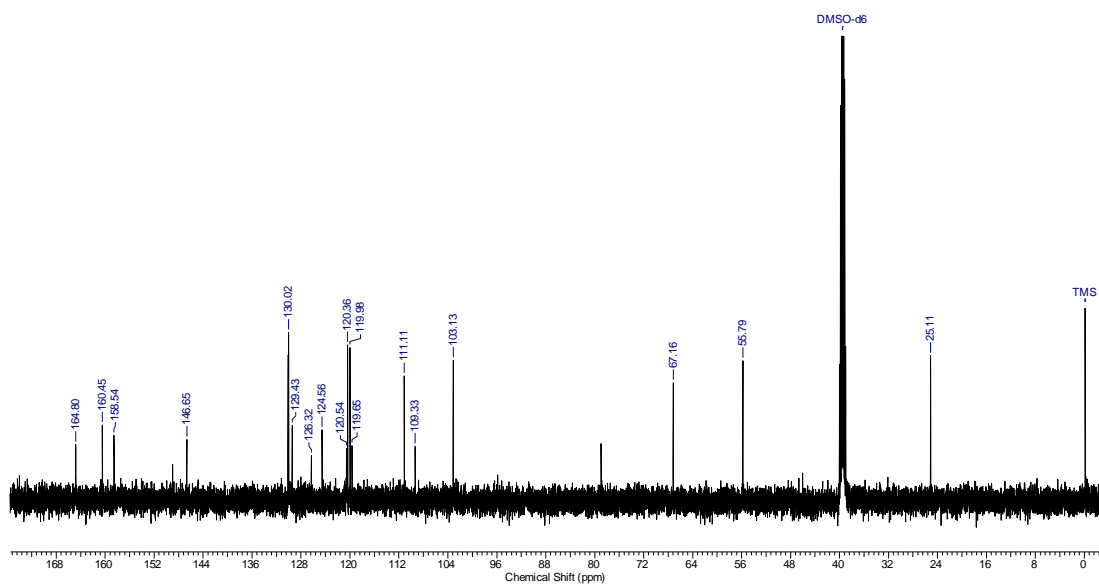


Figure S14. ^{13}C RMN spectrum of 2-[(6-chloro-2-methylquinolin-4-yl)oxy]-*N*-(2-methoxyphenyl)acetamide (**6g**) in $\text{DMSO-}d_6$.

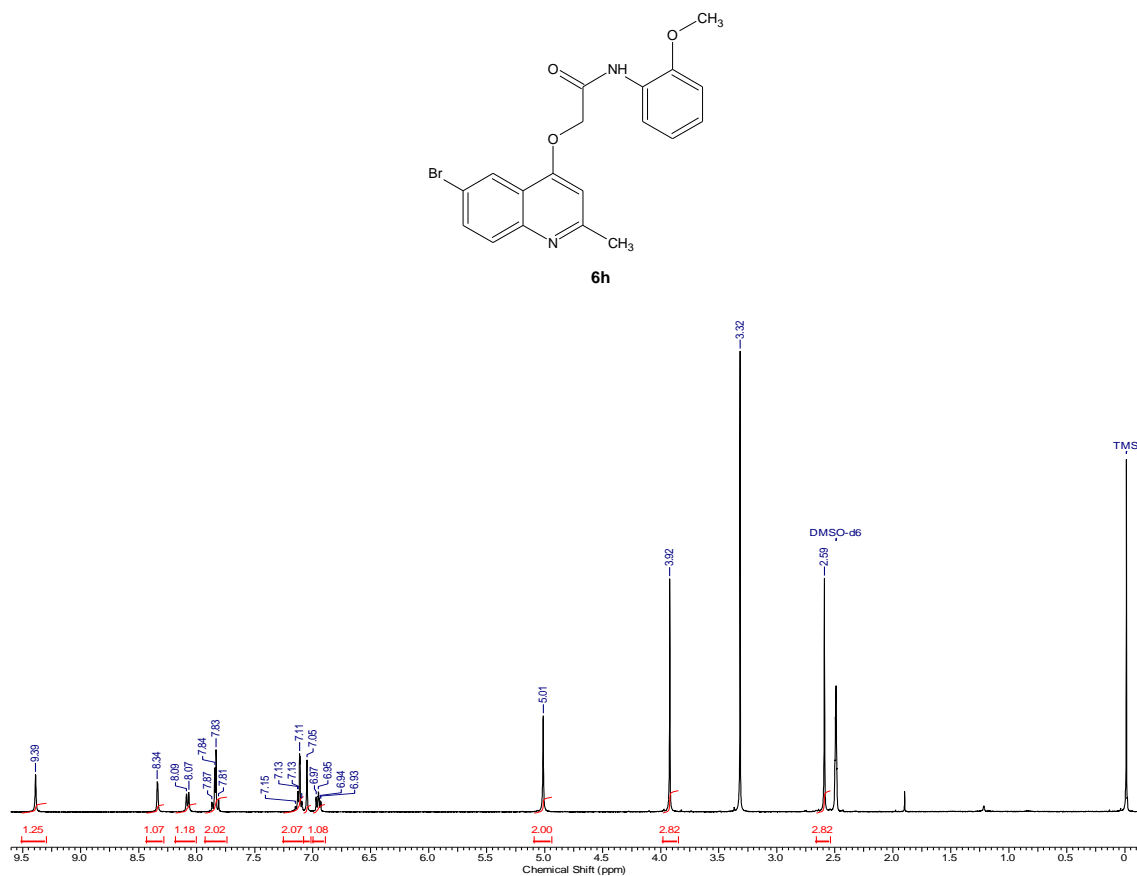


Figure S15. ^1H RMN spectrum of 2-[(6-bromo-2-methylquinolin-4-yl)oxy]-*N*-(2-methoxyphenyl)acetamide (**6h**) in $\text{DMSO-}d_6$.

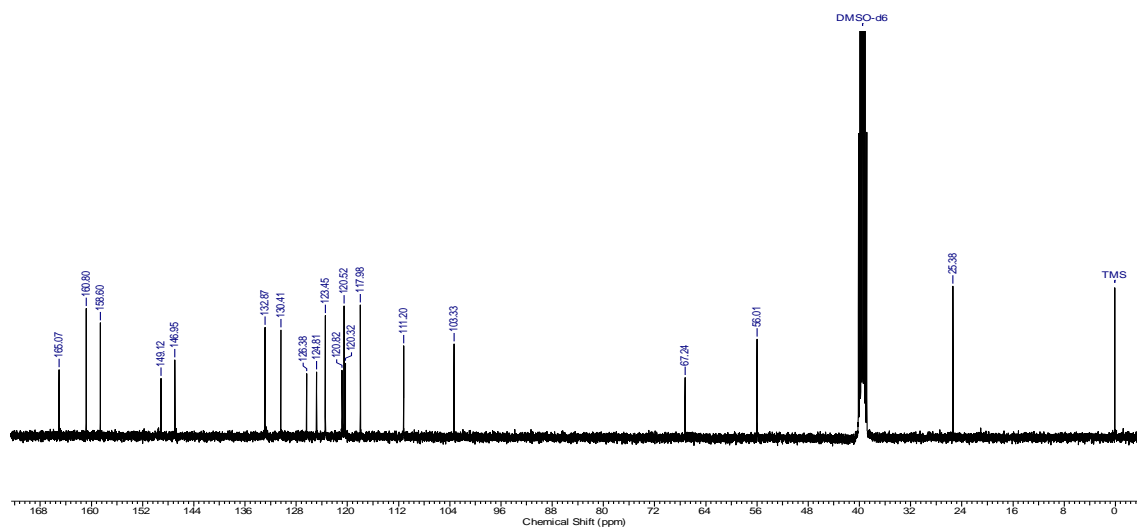


Figure S16. ^{13}C RMN spectrum of 2-[(6-bromo-2-methylquinolin-4-yl)oxy]-*N*-(2-methoxyphenyl)acetamide (**6h**) in $\text{DMSO-}d_6$.

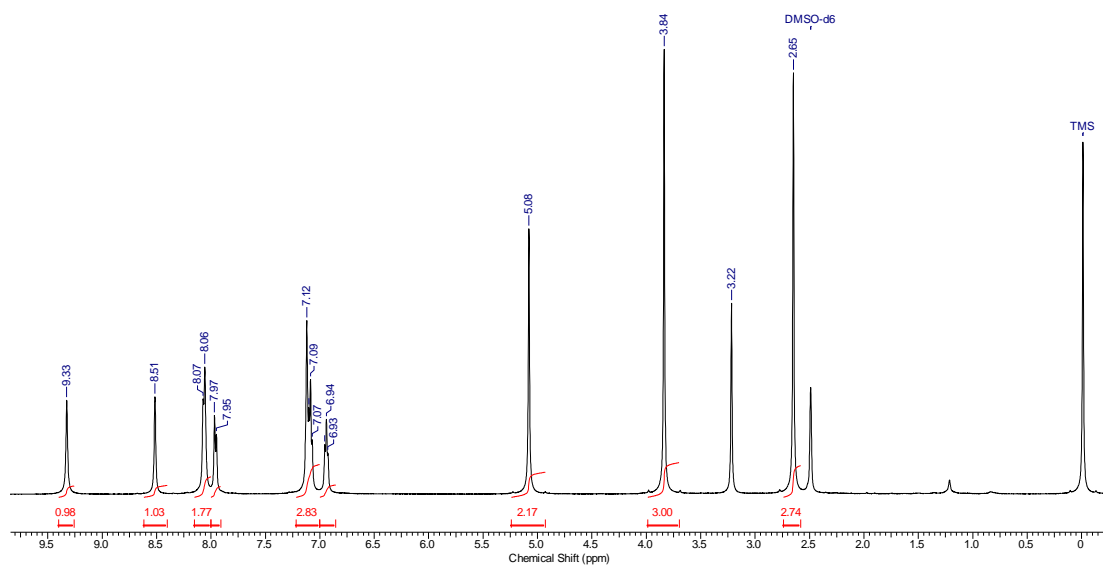
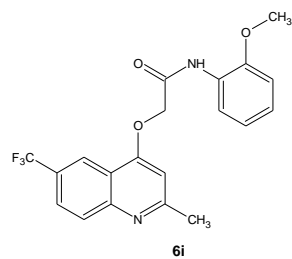


Figure S17. ^1H RMN spectrum of 2-[(6-trifluoromethyl-2-methylquinolin-4-yl)oxy]-*N*-(2-methoxyphenyl)acetamide (**6i**) in $\text{DMSO-}d_6$.

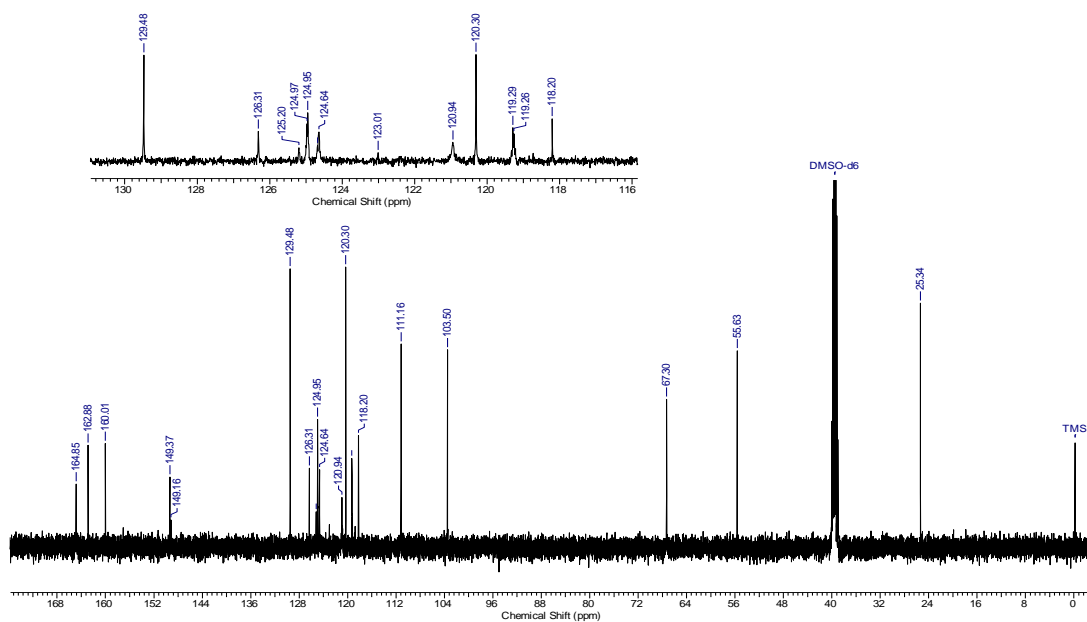


Figure S18. ^{13}C RMN spectrum of 2-[(6-trifluoromethyl-2-methylquinolin-4-yl)oxy]-*N*-(2-methoxyphenyl)acetamide (**6i**) in $\text{DMSO-}d_6$.

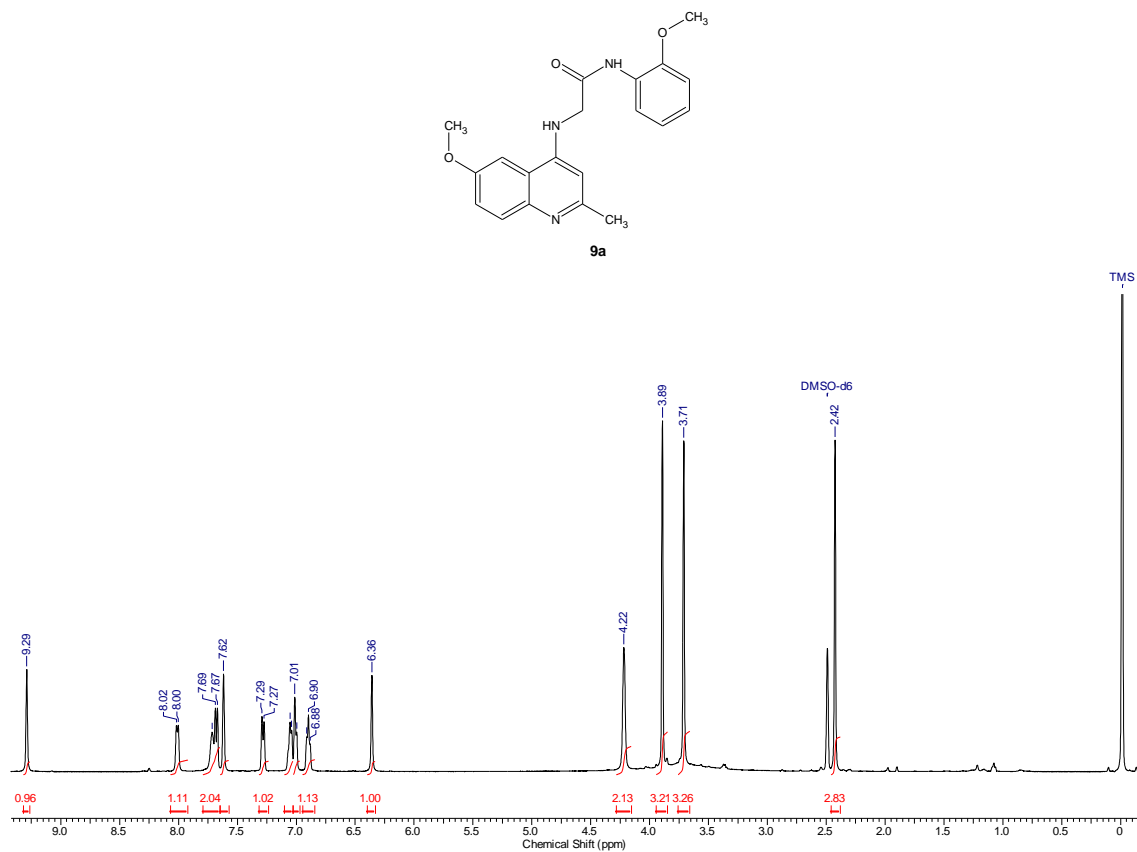


Figure S19. ^1H RMN spectrum of N^2 -[(6-methoxy-2-methylquinolin-4-yl)- N^1 -(2-methoxyphenyl)glycinamide (**9a**) in DMSO- d_6 .

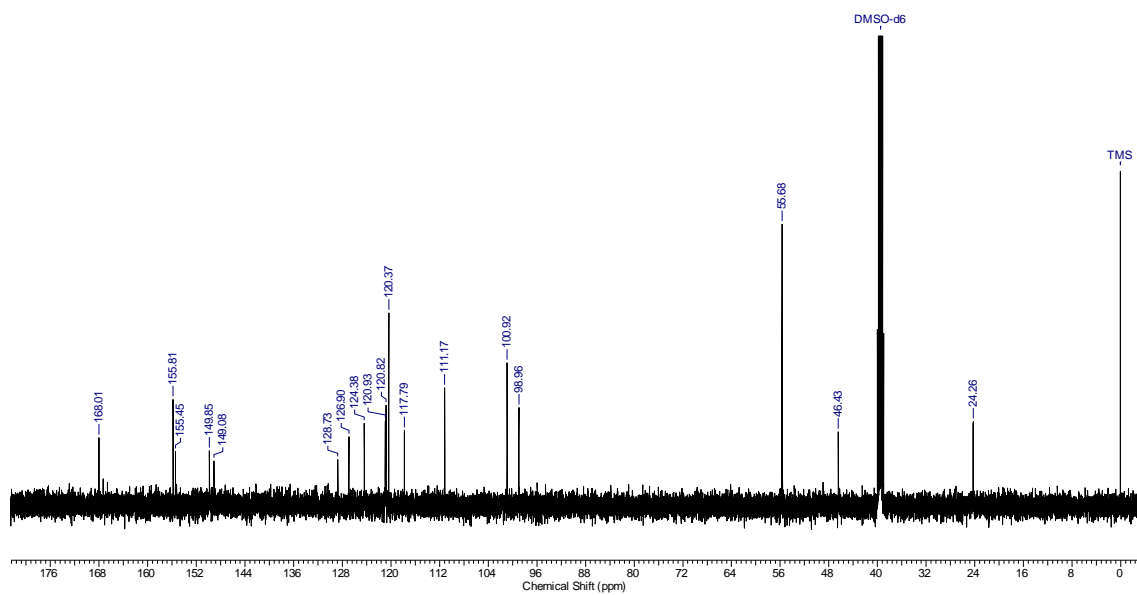


Figure S20. ^{13}C RMN spectrum of N^2 -[(6-methoxy-2-methylquinolin-4-yl)- N^1 -(2-methoxyphenyl)glycinamide (**9a**) in DMSO- d_6 .

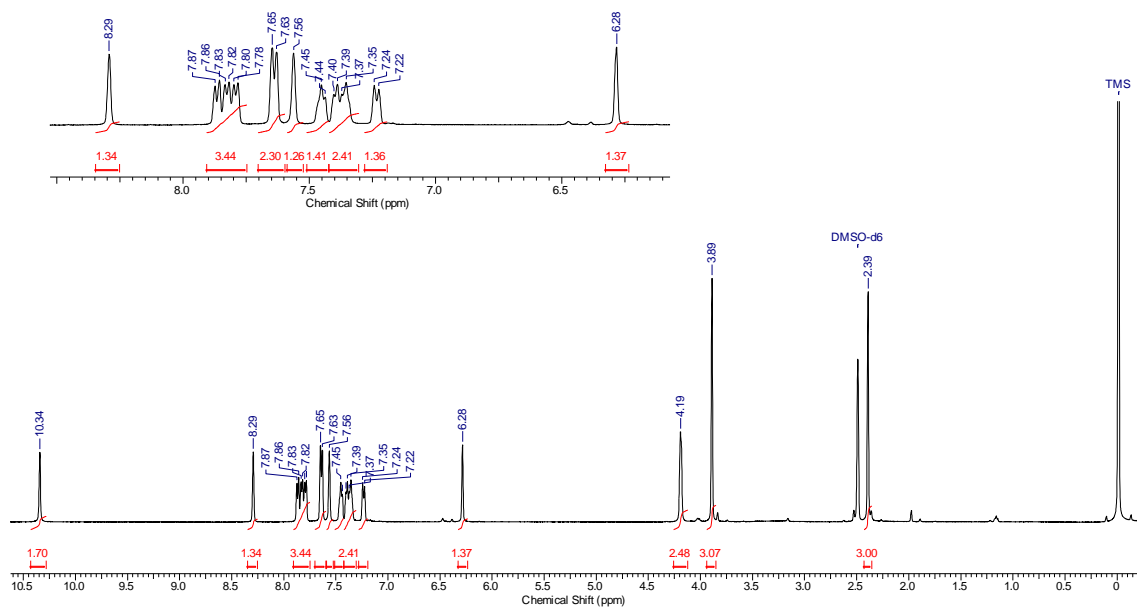
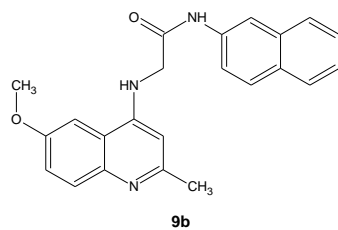


Figure S21. ^1H RMN spectrum of N^2 -[(6-methoxy-2-methylquinolin-4-yl)- N^1 -(2-naphthyl)glycinamide (**9b**) in $\text{DMSO-}d_6$.

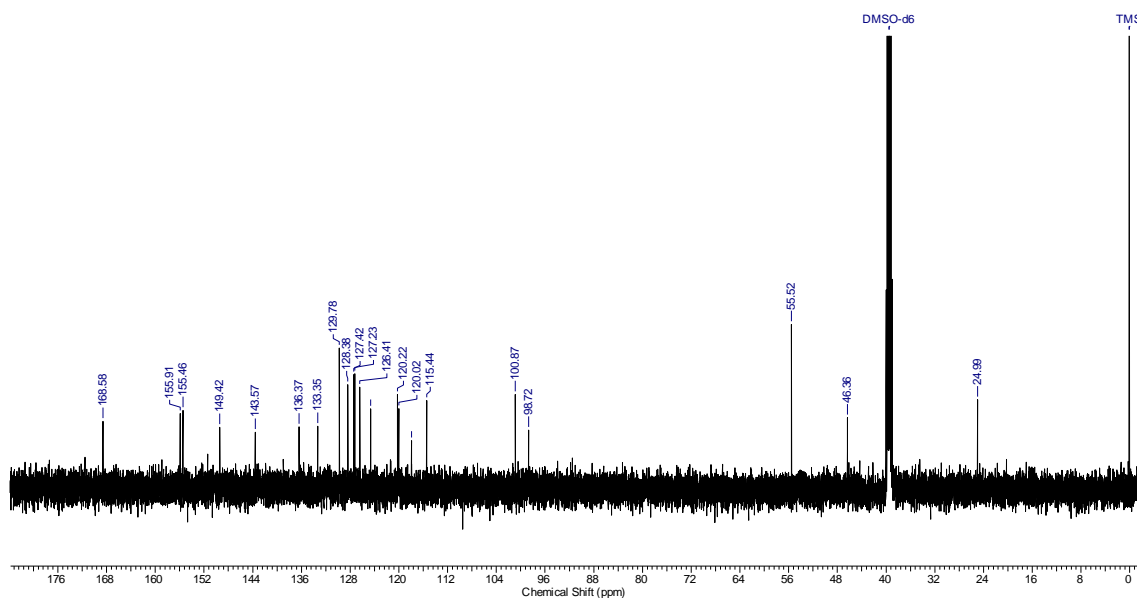


Figure S22. ^{13}C RMN spectrum of N^2 -[(6-methoxy-2-methylquinolin-4-yl)- N^1 -(2-naphthyl)glycinamide (**9b**) in $\text{DMSO-}d_6$.

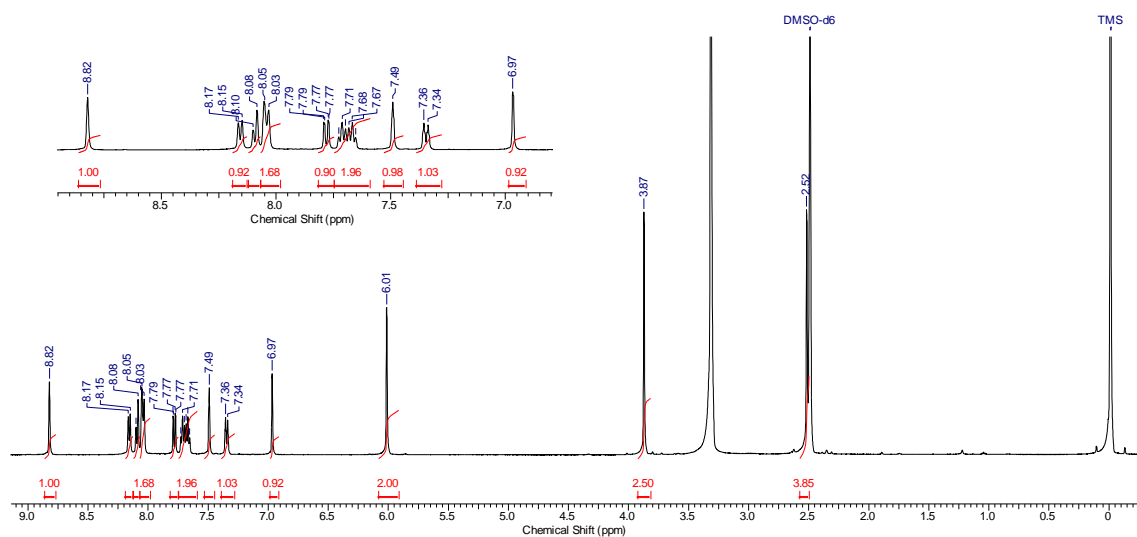
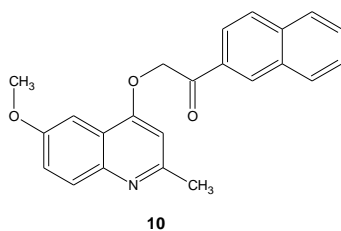


Figure S23. ^1H RMN spectrum of 2-[(6-methoxy-2-methylquinolin-4-yl)oxy]-1-(2-naphthyl)ethanone (**10**) in $\text{DMSO-}d_6$.

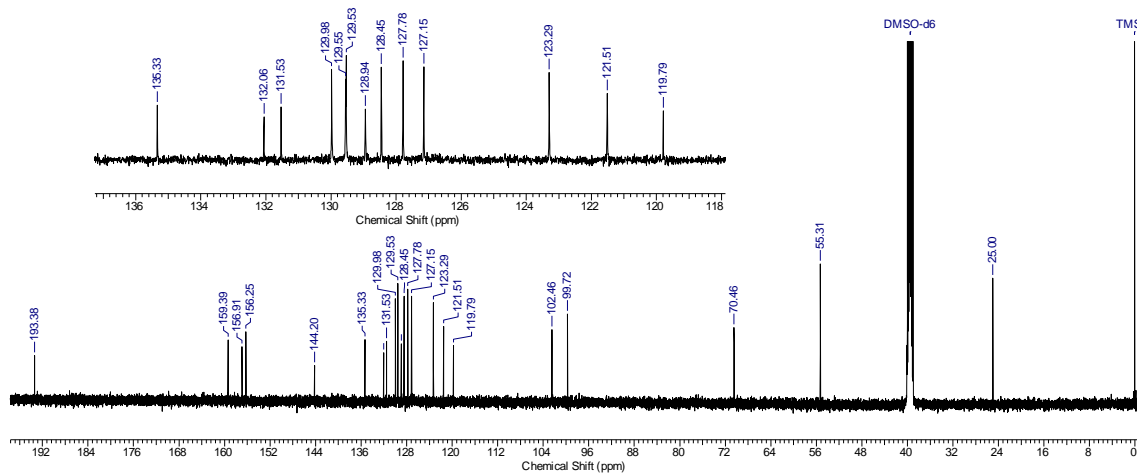


Figure S24. ^{13}C RMN spectrum of 2-[(6-methoxy-2-methylquinolin-4-yl)oxy]-1-(2-naphthyl)ethanone (**10**) in $\text{DMSO-}d_6$.

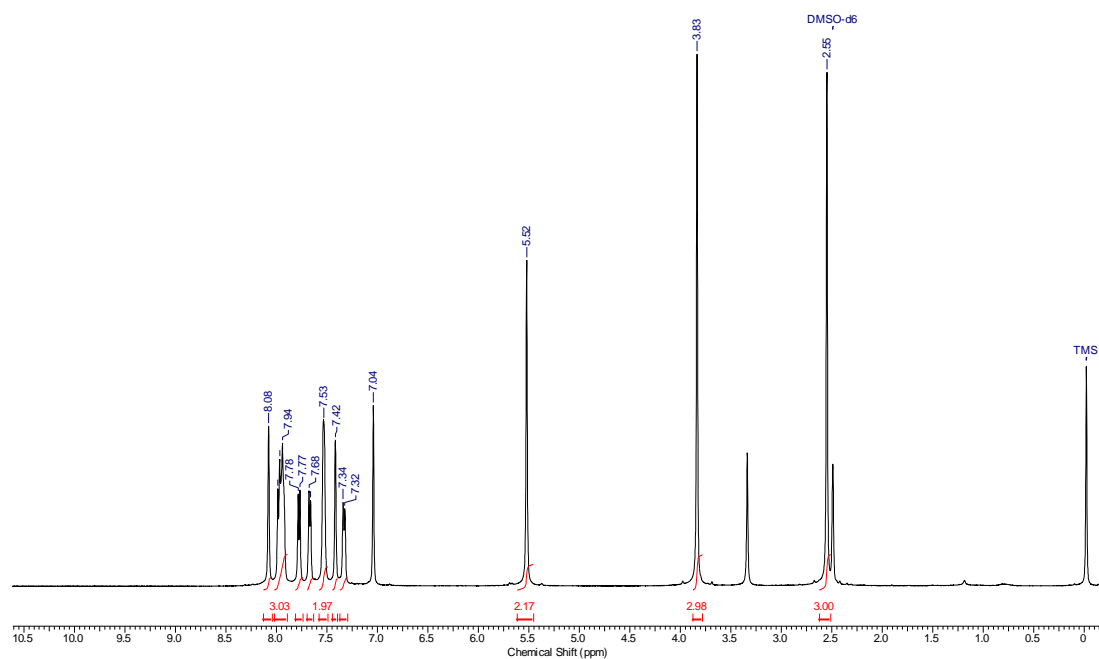
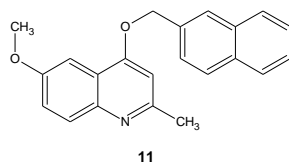


Figure S25. ^1H RMN spectrum of 6-methoxy-2-methyl-4-(2-naphthylmethoxy)quinoline (**11**) in $\text{DMSO-}d_6$.

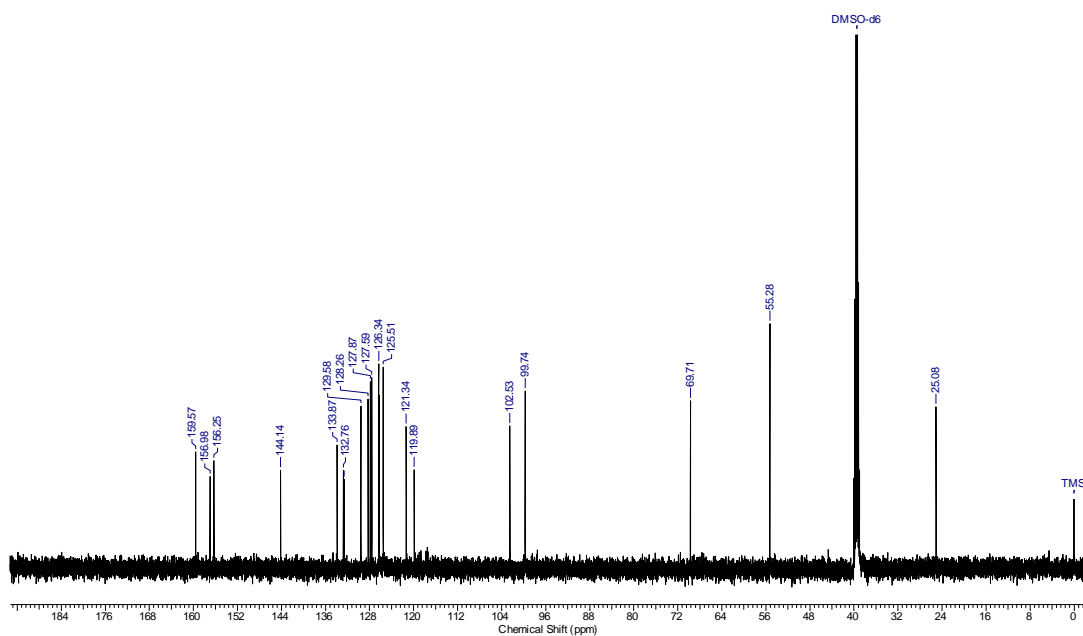
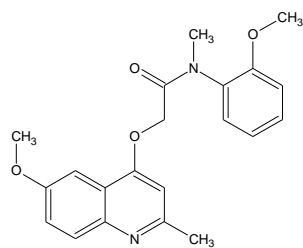


Figure S26. ^{13}C RMN spectrum of 6-methoxy-2-methyl-4-(2-naphthylmethoxy)quinoline (**11**) in $\text{DMSO-}d_6$.



12a

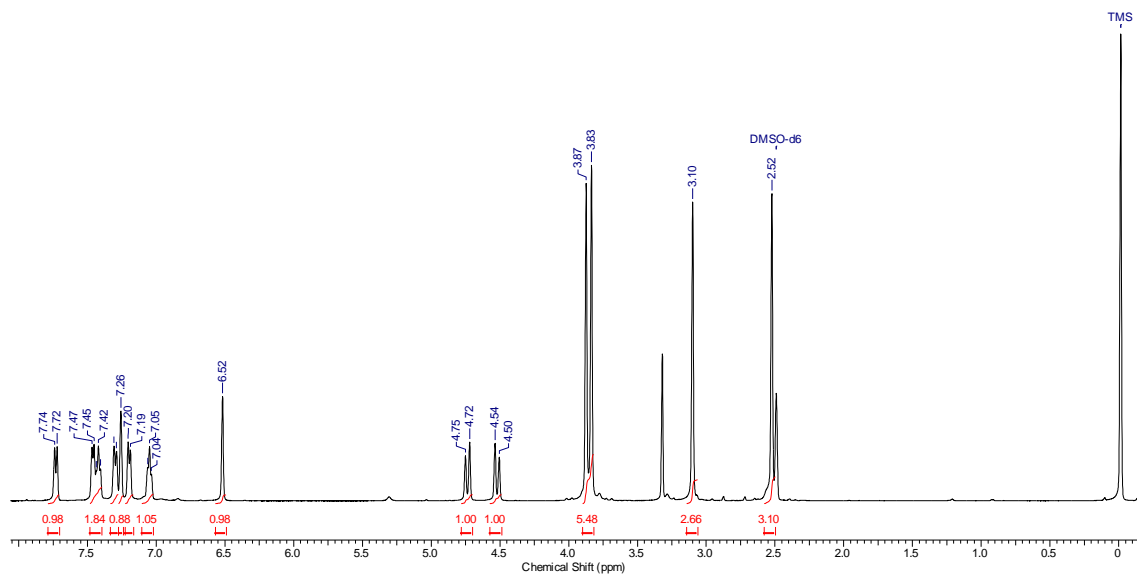


Figure S27. ^1H RMN spectrum of 2-[(6-methoxy-2-methylquinolin-4-yl)oxy]-*N*-(2-methoxyphenyl)-*N*-methylacetamide (**12a**) in $\text{DMSO-}d_6$.

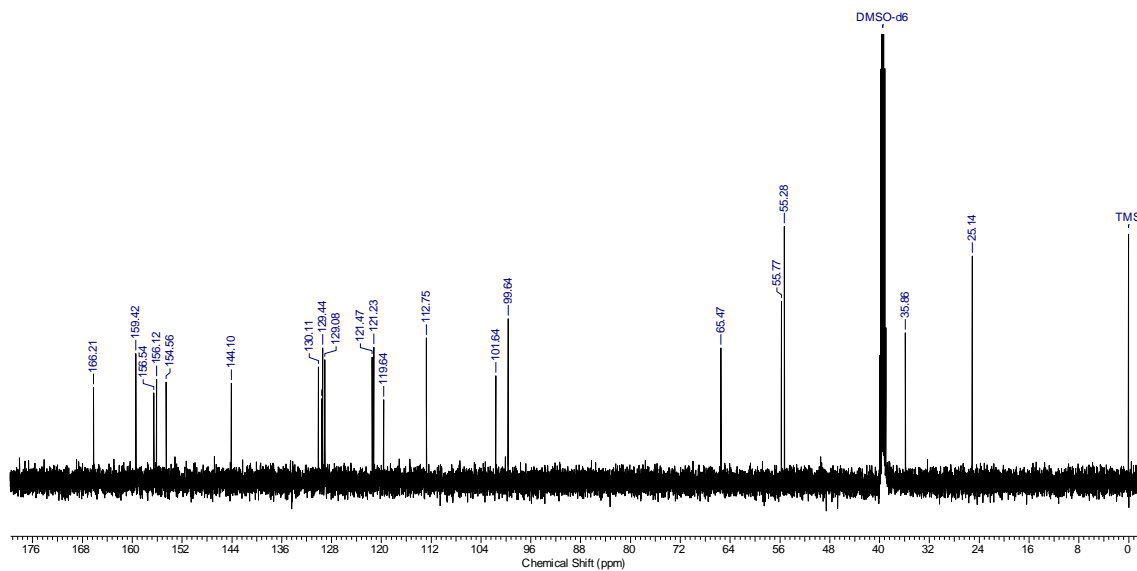


Figure S28. ^{13}C RMN spectrum of 2-[(6-methoxy-2-methylquinolin-4-yl)oxy]-*N*-(2-methoxyphenyl)-*N*-methylacetamide (**12a**) in $\text{DMSO-}d_6$.

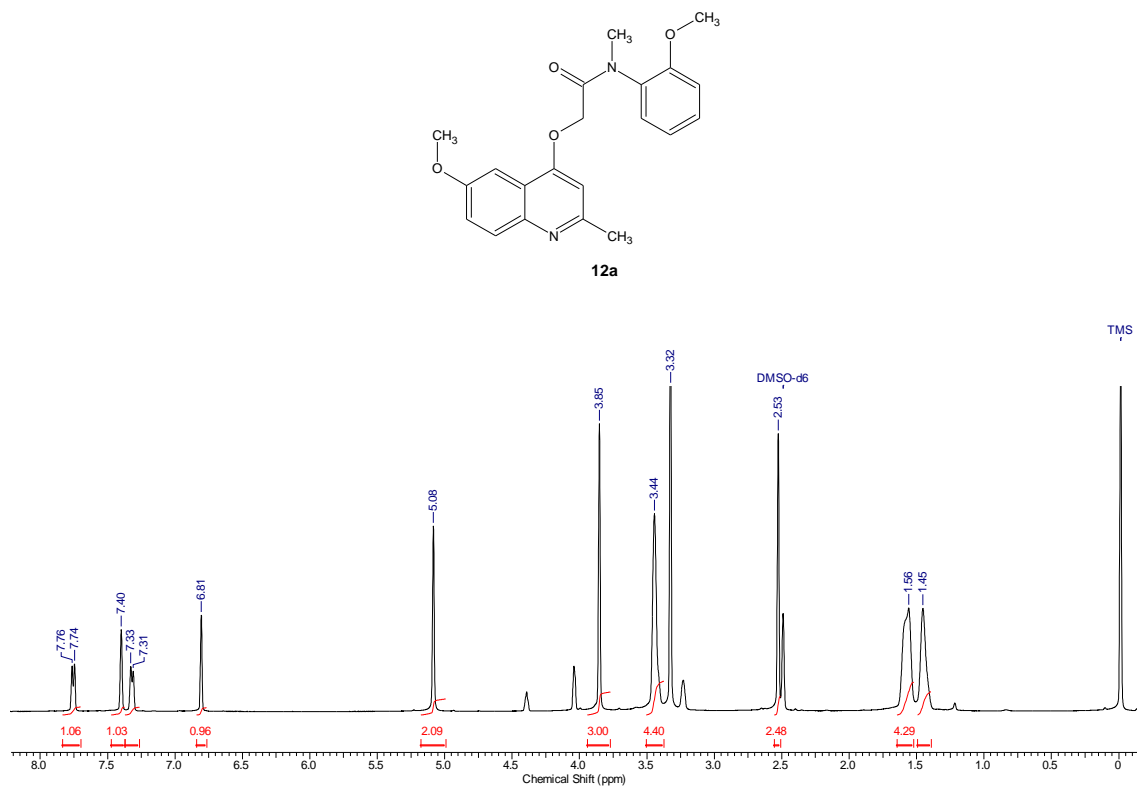


Figure S29. ¹H RMN spectrum of 6-methoxy-2-methyl-4-(2-oxo-piperidin-1-ylethoxy)quinoline (**12b**) in DMSO-*d*₆.

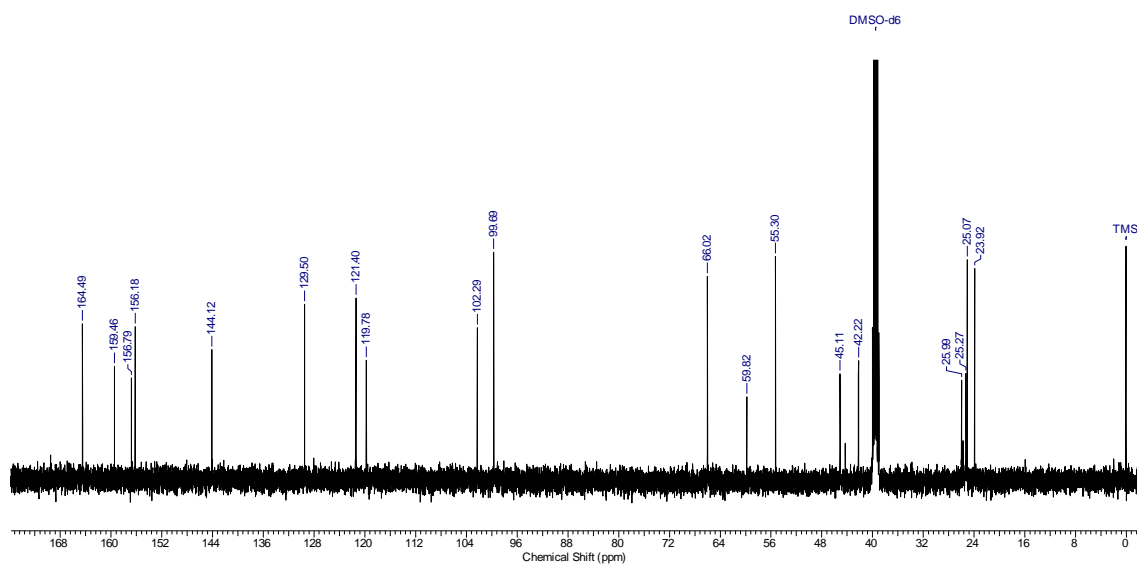


Figure S30. ¹³C RMN spectrum of 6-methoxy-2-methyl-4-(2-oxo-piperidin-1-ylethoxy)quinoline (**12b**) in DMSO-*d*₆.

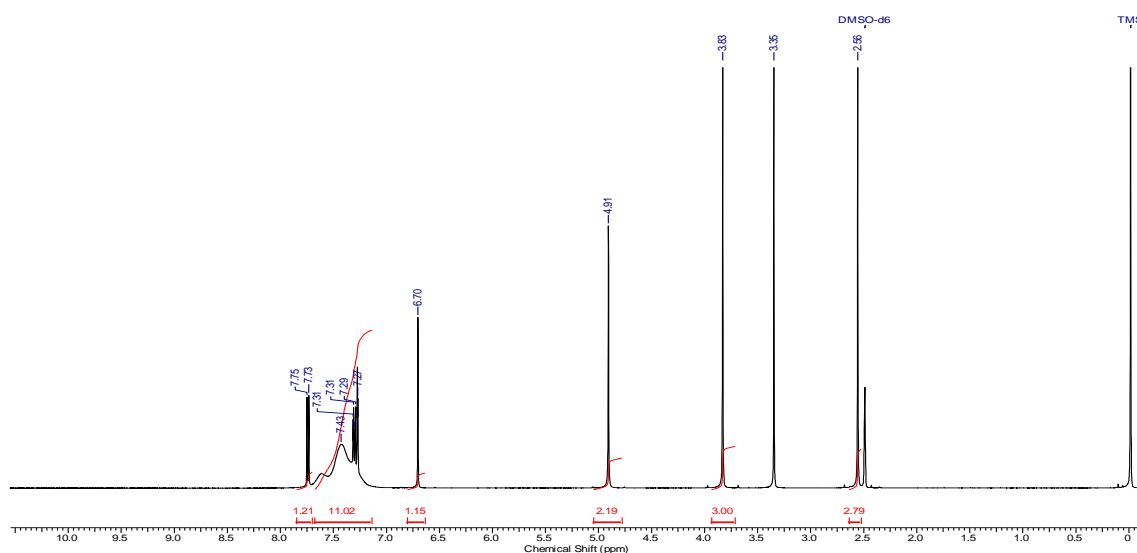
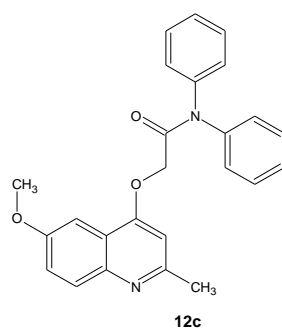


Figure S31. ^1H RMN spectrum of 2-[(6-methoxy-2-methylquinolin-4-yl)oxy]-*N,N*-diphenylacetamide (**12c**) in $\text{DMSO-}d_6$.

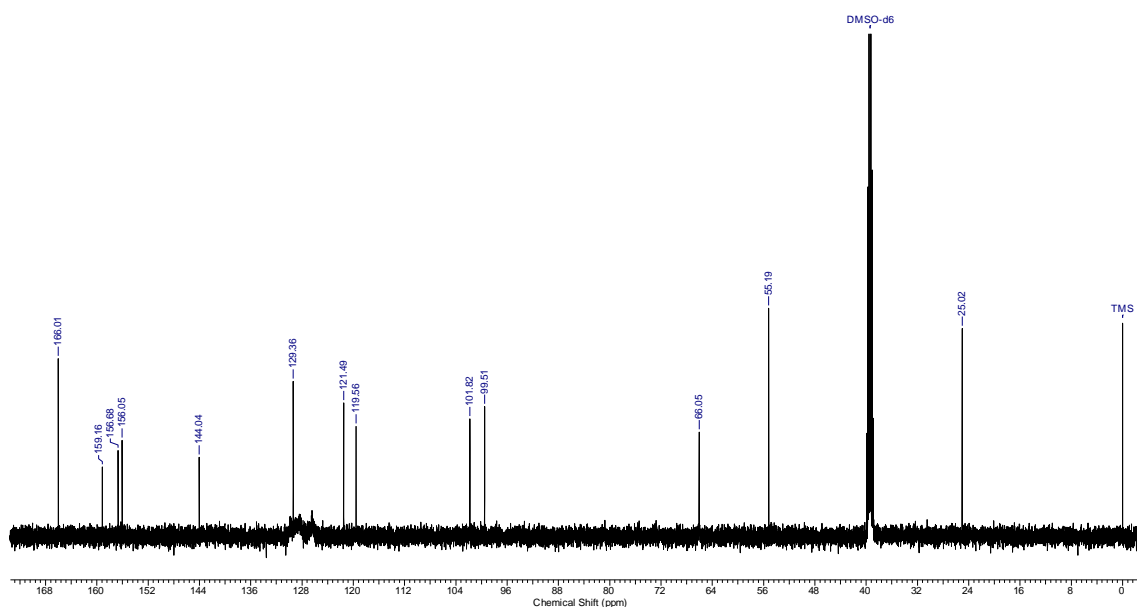


Figure S32. ^{13}C RMN spectrum of 2-[(6-methoxy-2-methylquinolin-4-yl)oxy]-*N,N*-diphenylacetamide (**12c**) in $\text{DMSO-}d_6$.

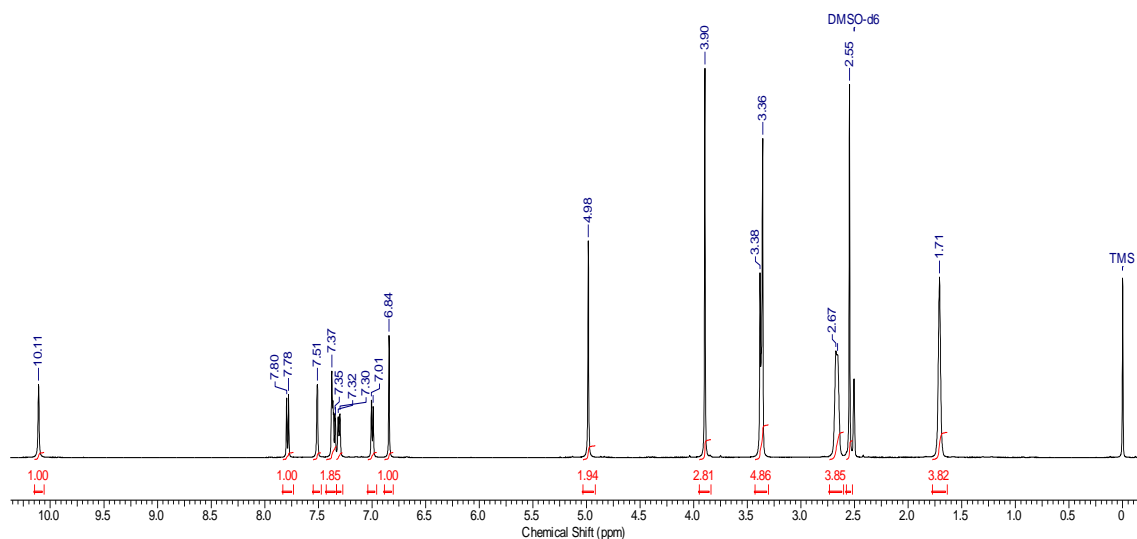
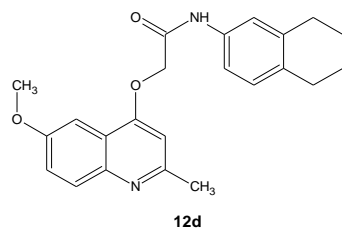


Figure S33. ^1H RMN spectrum of 2-[(6-methoxy-2-methylquinolin-4-yl)oxy]-*N*-(5,6,7,8-tetrahydronaphthalen-2-yl)phenyl)acetamide (**12d**) in $\text{DMSO-}d_6$.

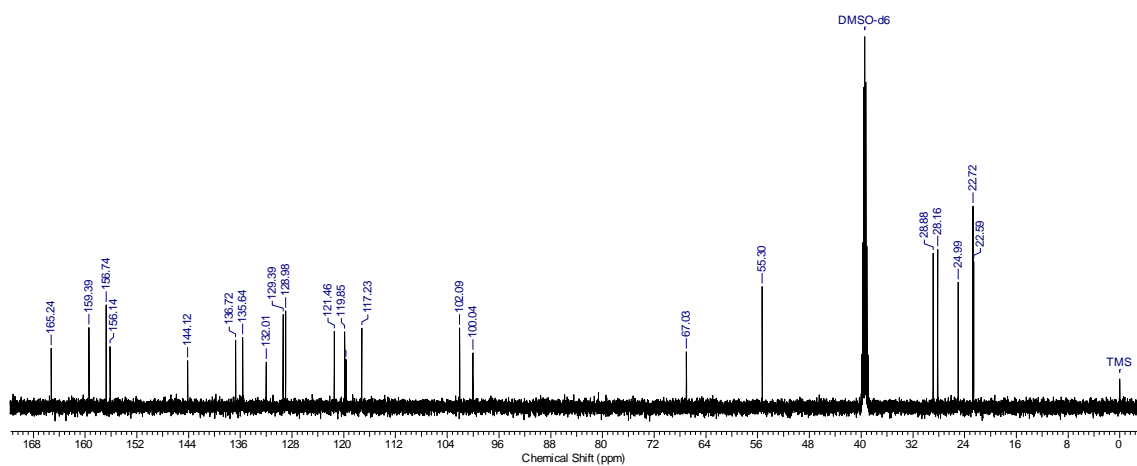
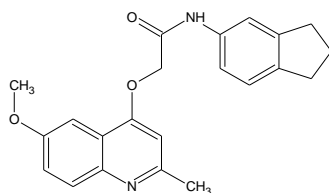


Figure S34. ^{13}C RMN spectrum of 2-[(6-methoxy-2-methylquinolin-4-yl)oxy]-*N*-(5,6,7,8-tetrahydronaphthalen-2-yl)phenyl)acetamide (**12d**) in $\text{DMSO-}d_6$.



12e

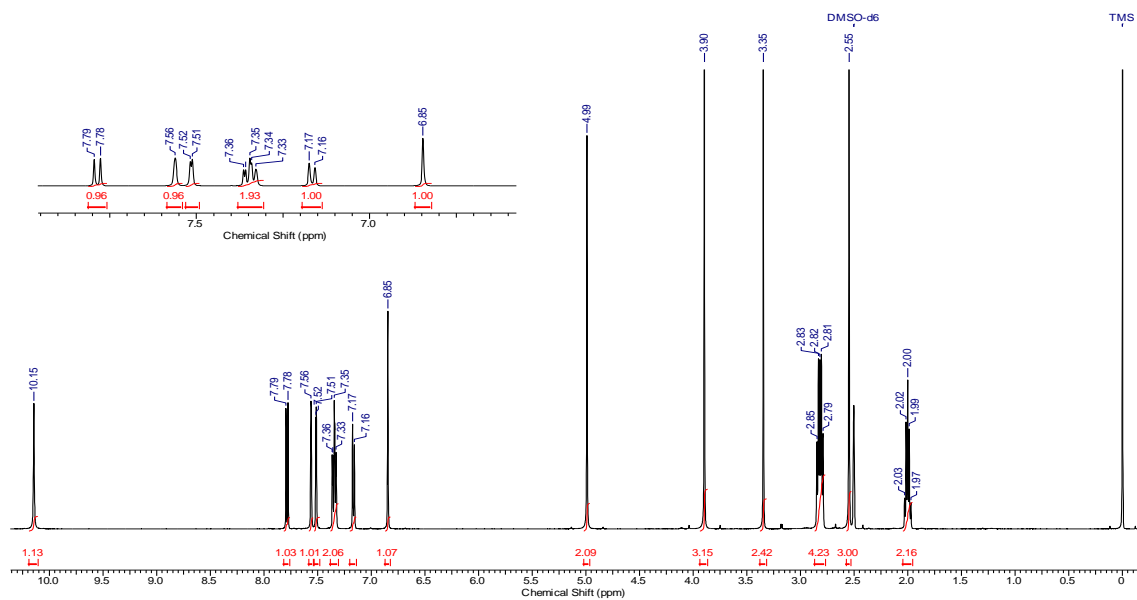


Figure S35. ^1H RMN spectrum of 2-[(6-methoxy-2-methylquinolin-4-yl)oxy]-*N*-(2,3-dihydro-1*H*-inden-5-yl)phenylacetamide (**12e**) in $\text{DMSO-}d_6$.

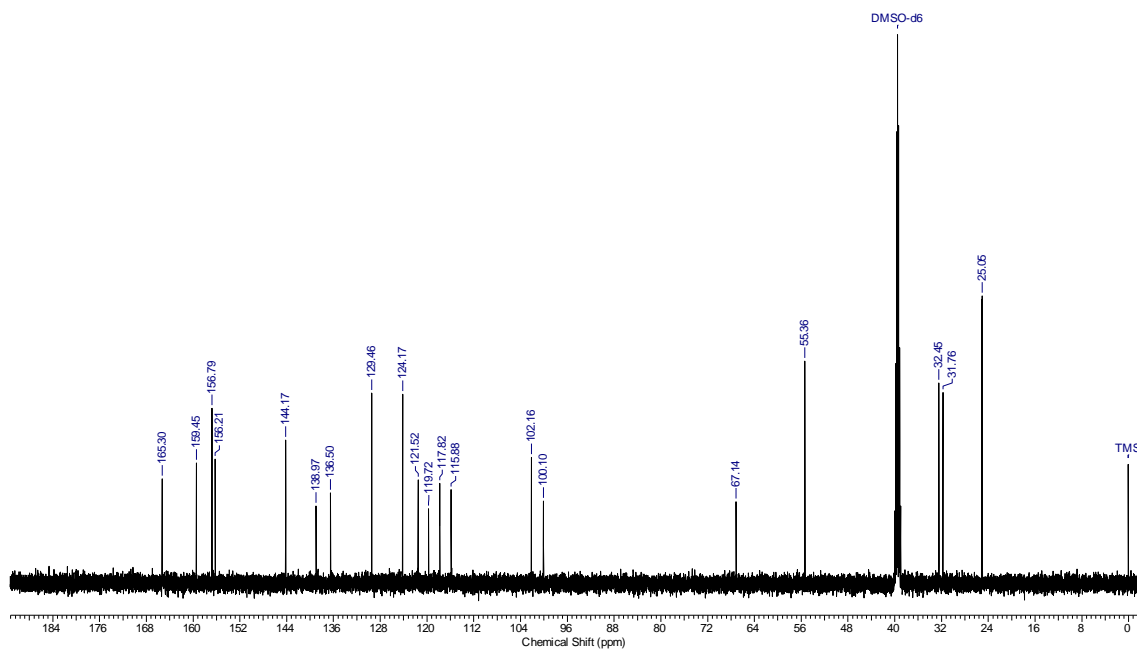


Figure S36. ^{13}C RMN spectrum of 2-[(6-methoxy-2-methylquinolin-4-yl)oxy]-*N*-(2,3-dihydro-1*H*-inden-5-yl)phenylacetamide (**12e**) in $\text{DMSO-}d_6$.

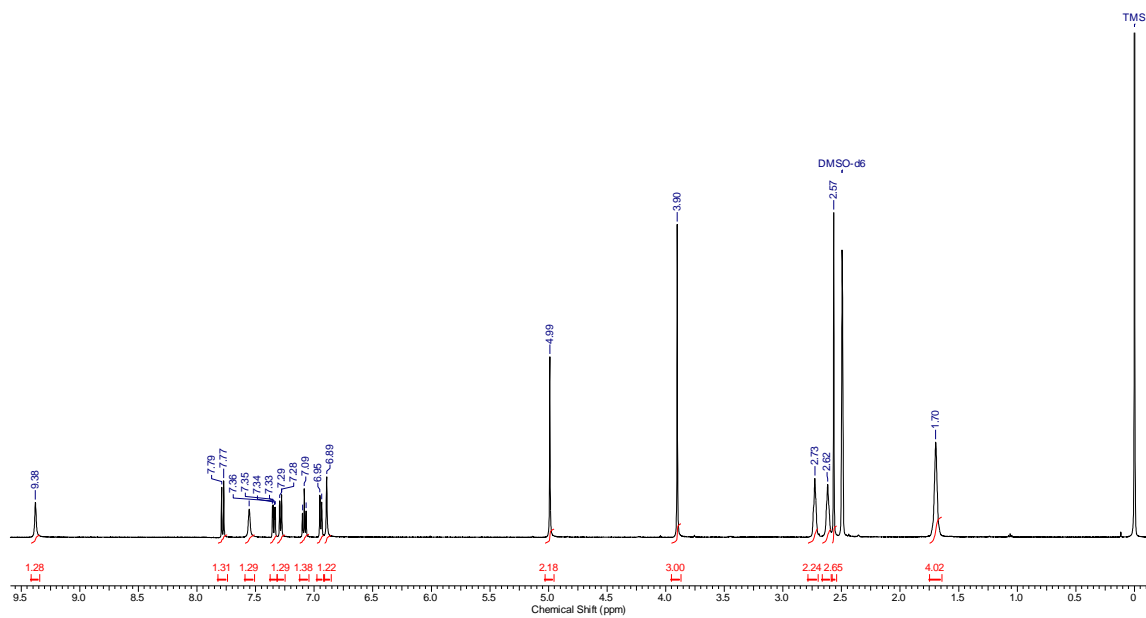
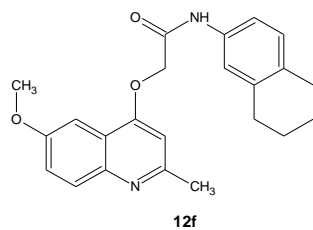


Figure S37. ^1H RMN spectrum of 2-[(6-methoxy-2-methylquinolin-4-yl)oxy]-*N*-(5,6,7,8-tetrahydronaphthalen-1-yl)acetamide (**12f**) in $\text{DMSO-}d_6$.

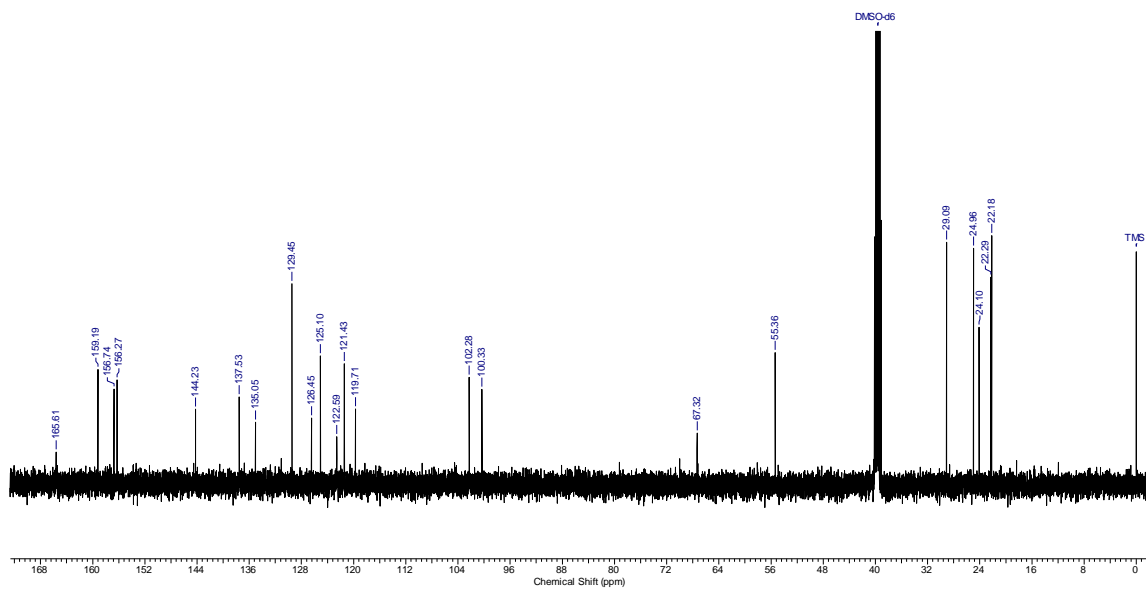


Figure S38. ^{13}C RMN spectrum of 2-[(6-methoxy-2-methylquinolin-4-yl)oxy]-*N*-(5,6,7,8-tetrahydronaphthalen-1-yl)acetamide (**12f**) in $\text{DMSO-}d_6$.

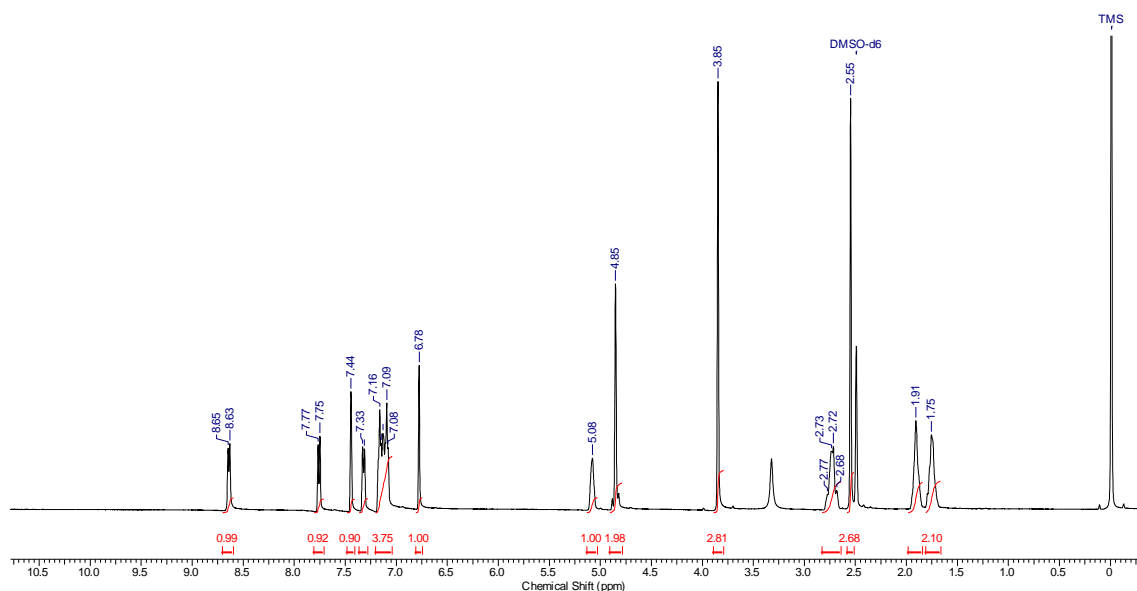
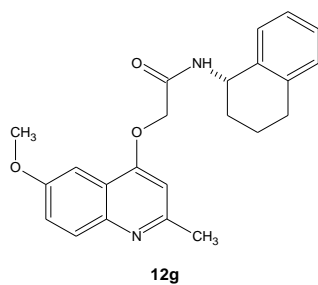


Figure S39. ^1H RMN spectrum of 2-[(6-methoxy-2-methylquinolin-4-yl)oxy]-*N*-[(1*S*)-1,2,3,4-tetrahydronaphthalen-1-yl]acetamide (**12g**) in $\text{DMSO-}d_6$.

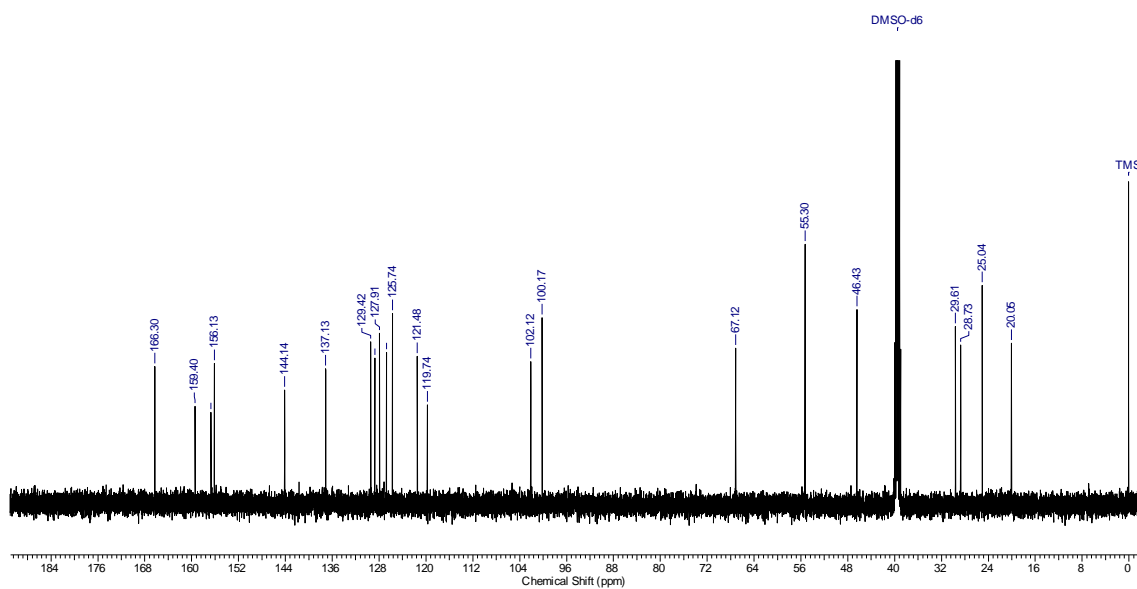


Figure S40. ^{13}C RMN spectrum of 2-[(6-methoxy-2-methylquinolin-4-yl)oxy]-*N*-[(1*S*)-1,2,3,4-tetrahydronaphthalen-1-yl]acetamide (**12g**) in $\text{DMSO-}d_6$.

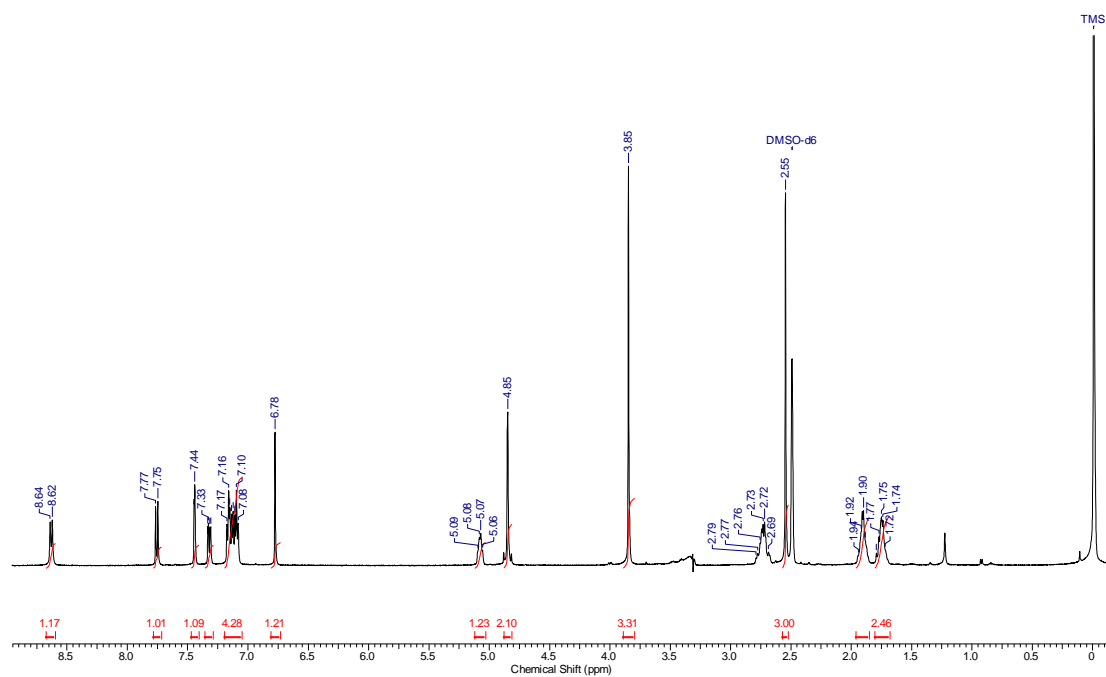
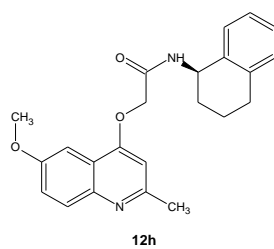


Figure S41. ^1H RMN spectrum of 2-[(6-methoxy-2-methylquinolin-4-yl)oxy]-*N*-[(1*R*)-1,2,3,4-tetrahydronaphthalen-1-yl]acetamide (**12h**) in $\text{DMSO-}d_6$.

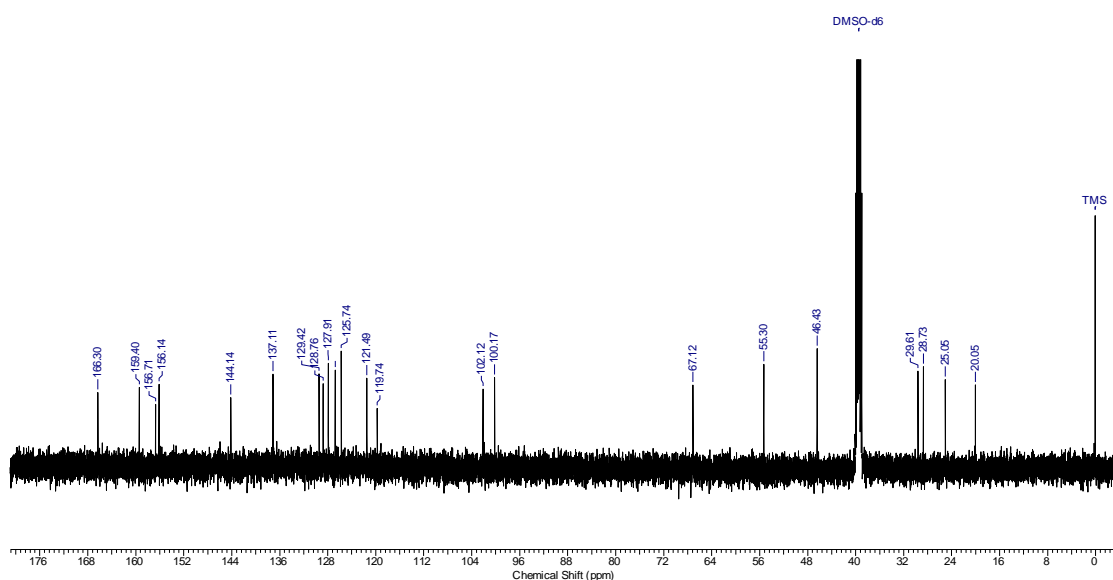


Figure S42. ^{13}C RMN spectrum of 2-[(6-methoxy-2-methylquinolin-4-yl)oxy]-*N*-[(1*R*)-1,2,3,4-tetrahydronaphthalen-1-yl]acetamide (**12h**) in $\text{DMSO-}d_6$.

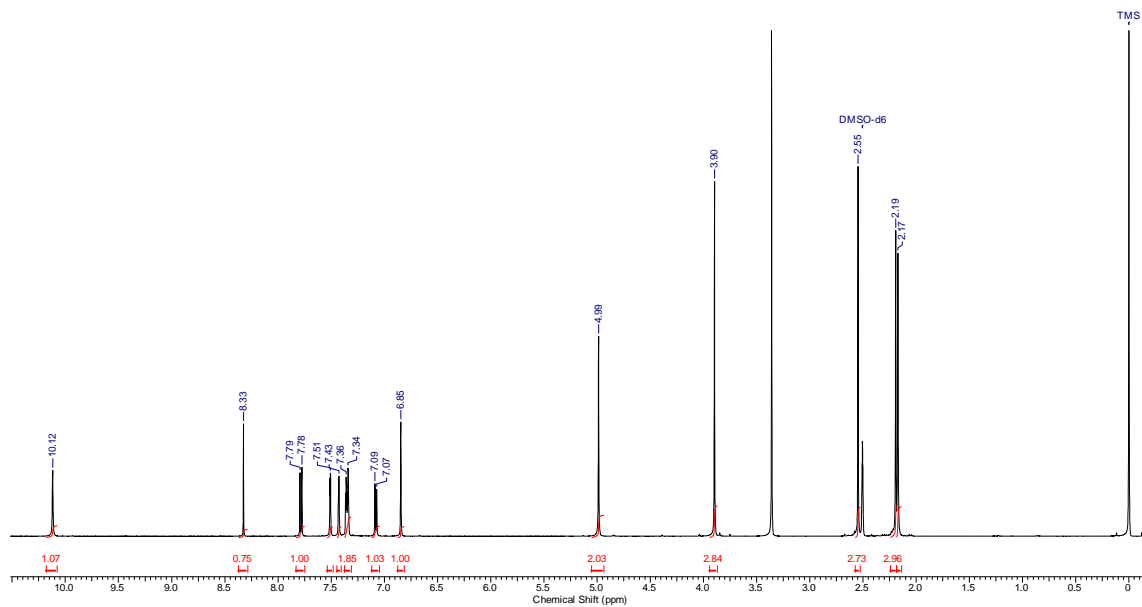
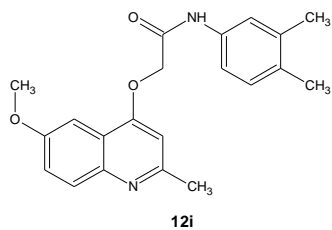


Figure S43. ^1H RMN spectrum of 2-[(6-methoxy-2-methylquinolin-4-yl)oxy]-*N*-(3,4-dimethylphenyl)acetamide (**12i**) in $\text{DMSO-}d_6$.

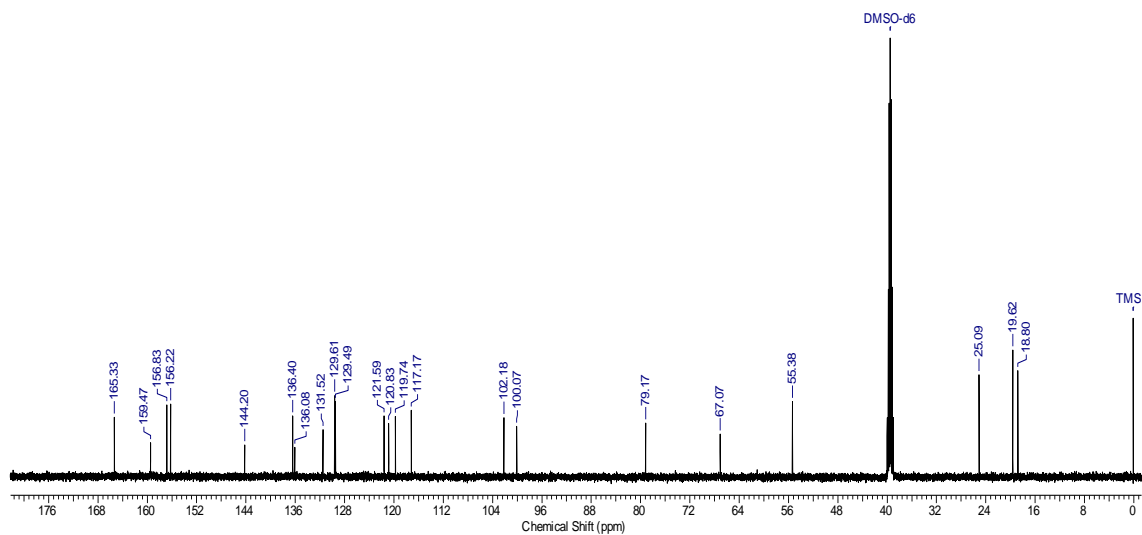


Figure S44. ^{13}C RMN spectrum of 2-[(6-methoxy-2-methylquinolin-4-yl)oxy]-*N*-(3,4-dimethylphenyl)acetamide (**12i**) in $\text{DMSO-}d_6$.

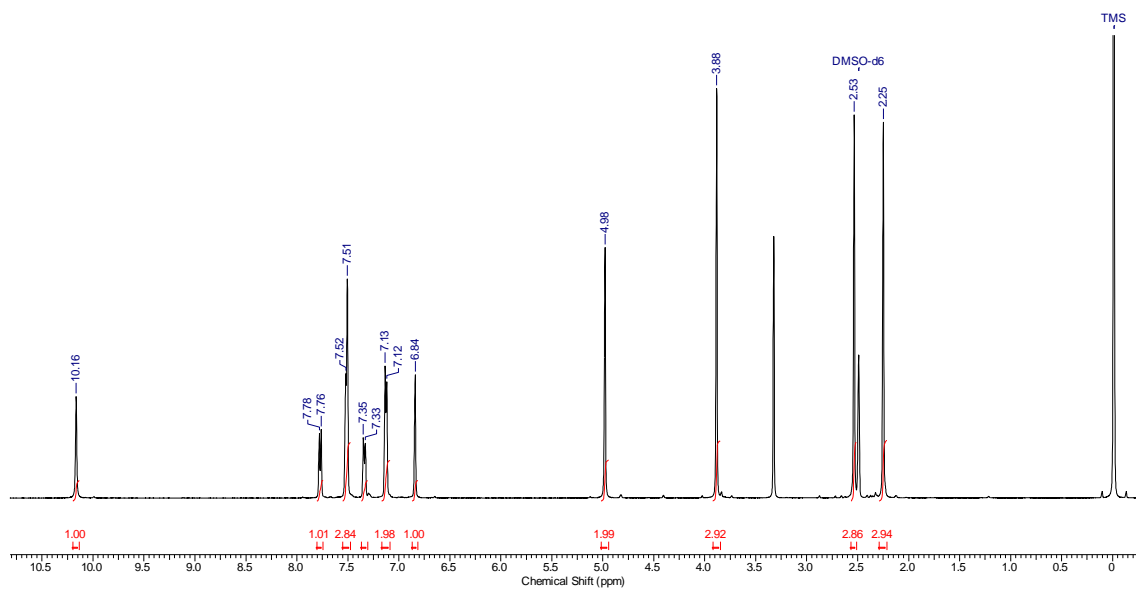
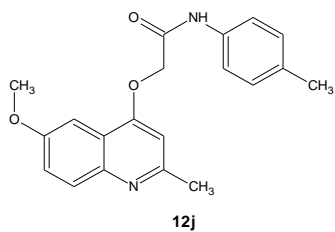


Figure S45. ^1H RMN spectrum of 2-[(6-methoxy-2-methylquinolin-4-yl)oxy]-*N*-(4-methylphenyl)acetamide (**12j**) in $\text{DMSO-}d_6$.

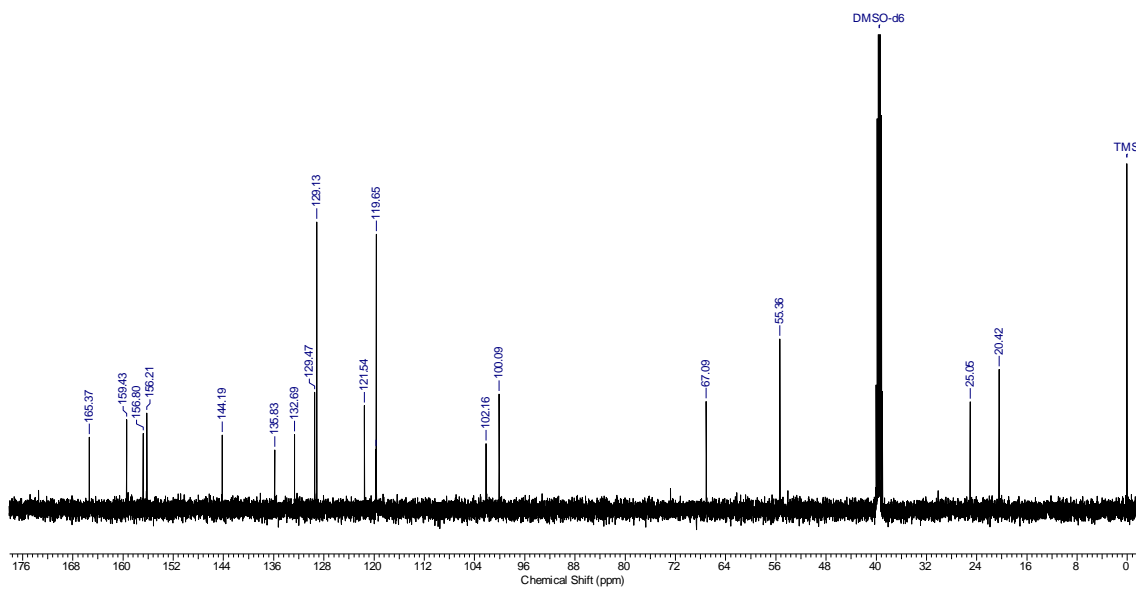


Figure S46. ^{13}C RMN spectrum of 2-[(6-methoxy-2-methylquinolin-4-yl)oxy]-*N*-(4-methylphenyl)acetamide (**12j**) in $\text{DMSO-}d_6$.

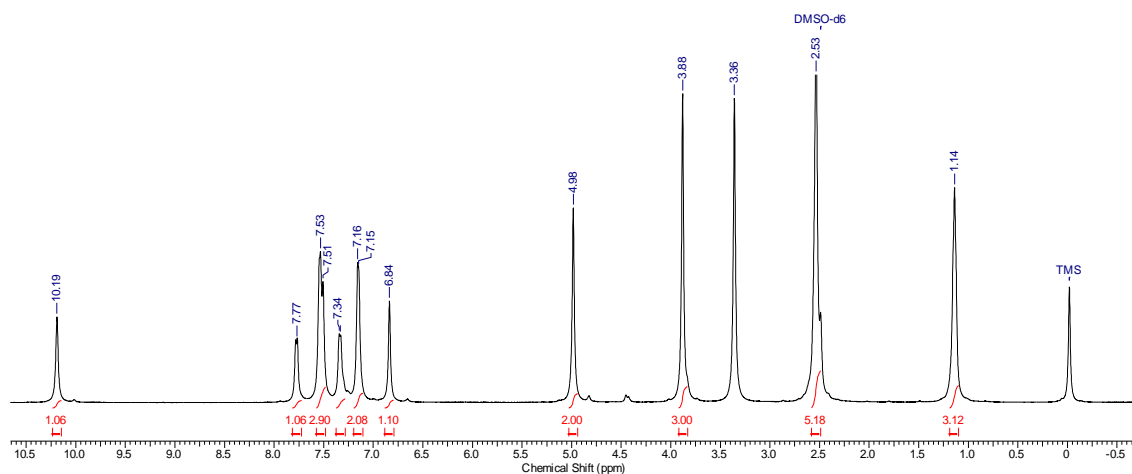
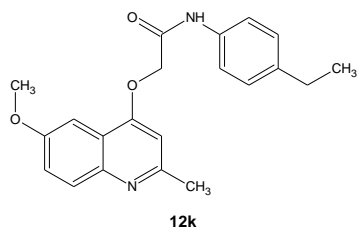


Figure S47. ^1H RMN spectrum of 2-[(6-methoxy-2-methylquinolin-4-yl)oxy]-*N*-(4-ethylphenyl)acetamide (**12k**) in $\text{DMSO-}d_6$.

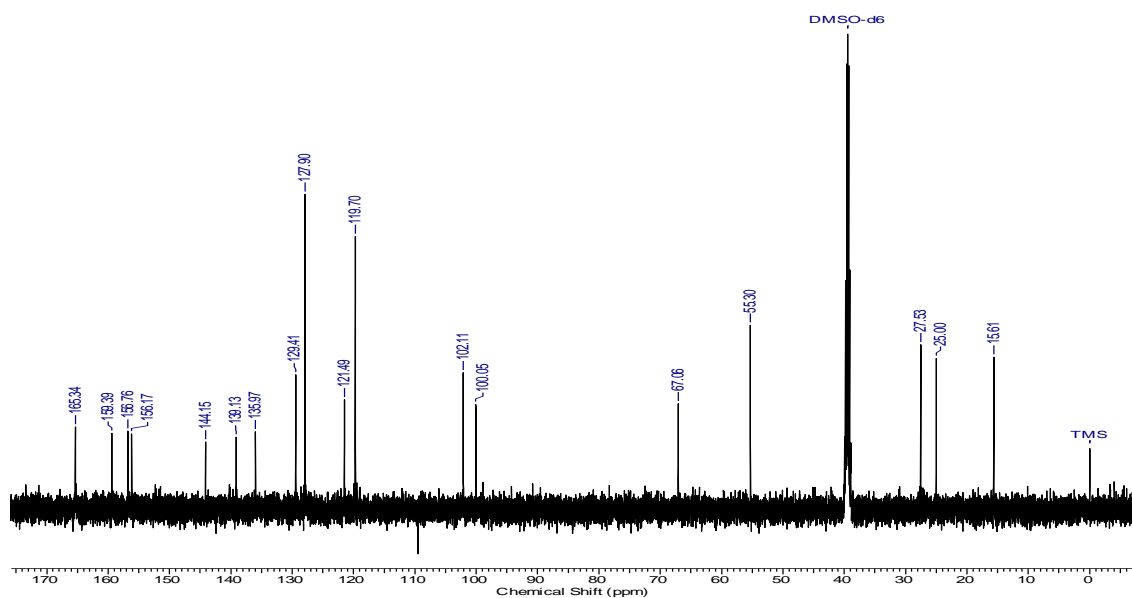


Figure S48. ^{13}C RMN spectrum of 2-[(6-methoxy-2-methylquinolin-4-yl)oxy]-*N*-(4-ethylphenyl)acetamide (**12k**) in $\text{DMSO-}d_6$.

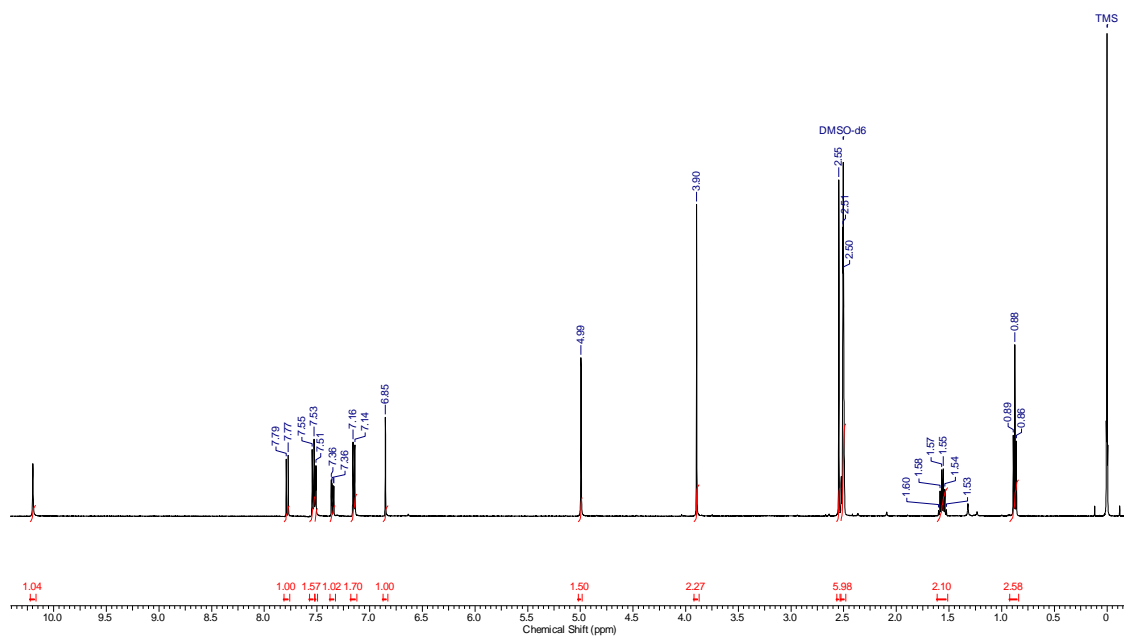
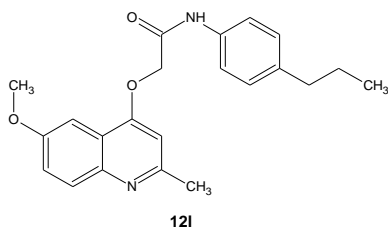


Figure S49. ^1H RMN spectrum of 2-[(6-methoxy-2-methylquinolin-4-yl)oxy]-*N*-(4-propylphenyl)acetamide (**121**) in $\text{DMSO-}d_6$.

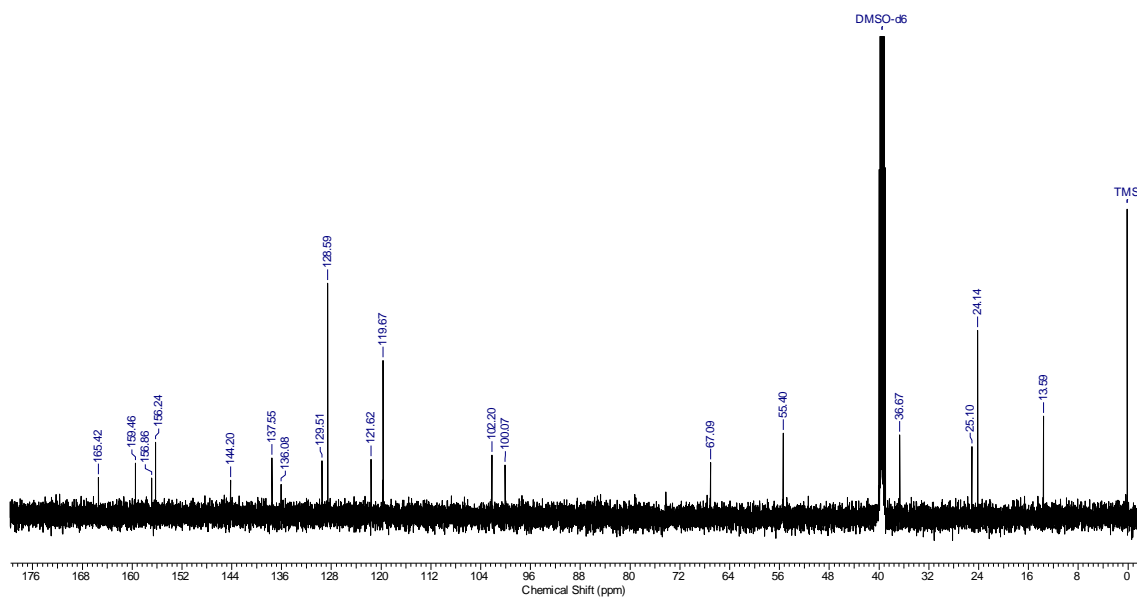


Figure S50. ^{13}C RMN spectrum of 2-[(6-methoxy-2-methylquinolin-4-yl)oxy]-*N*-(4-propylphenyl)acetamide (**121**) in $\text{DMSO-}d_6$.

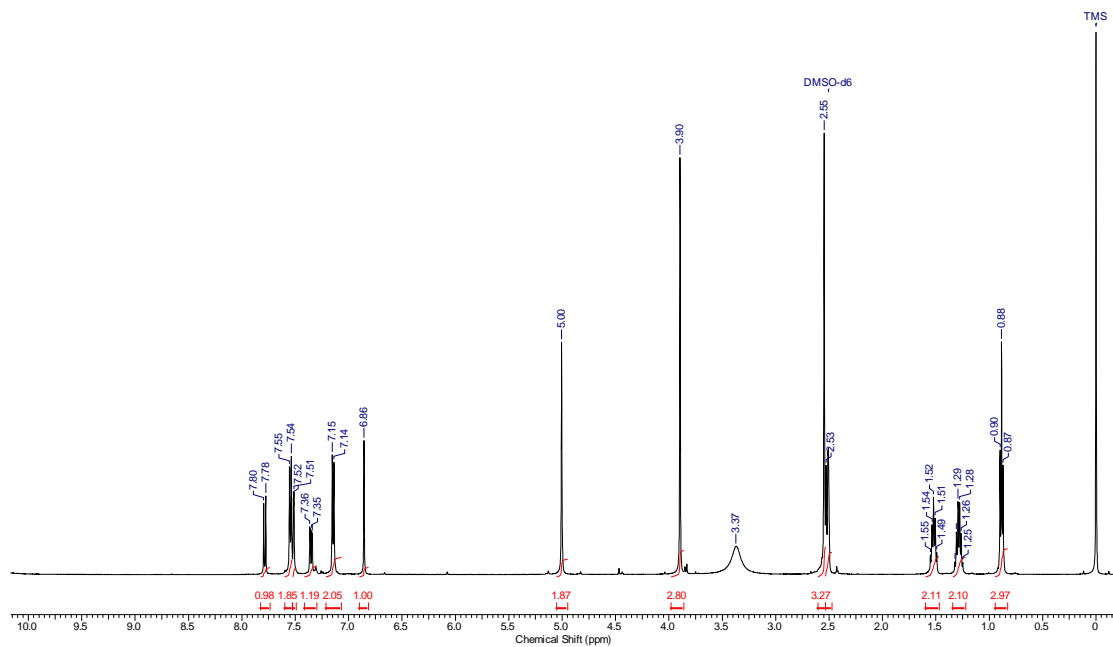
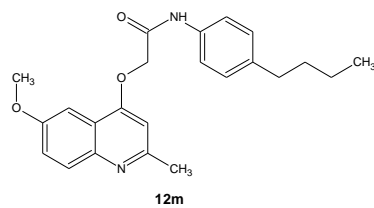


Figure S51. ^1H RMN spectrum of 2-[(6-methoxy-2-methylquinolin-4-yl)oxy]-*N*-(4-butylphenyl)acetamide (**12m**) in $\text{DMSO-}d_6$.

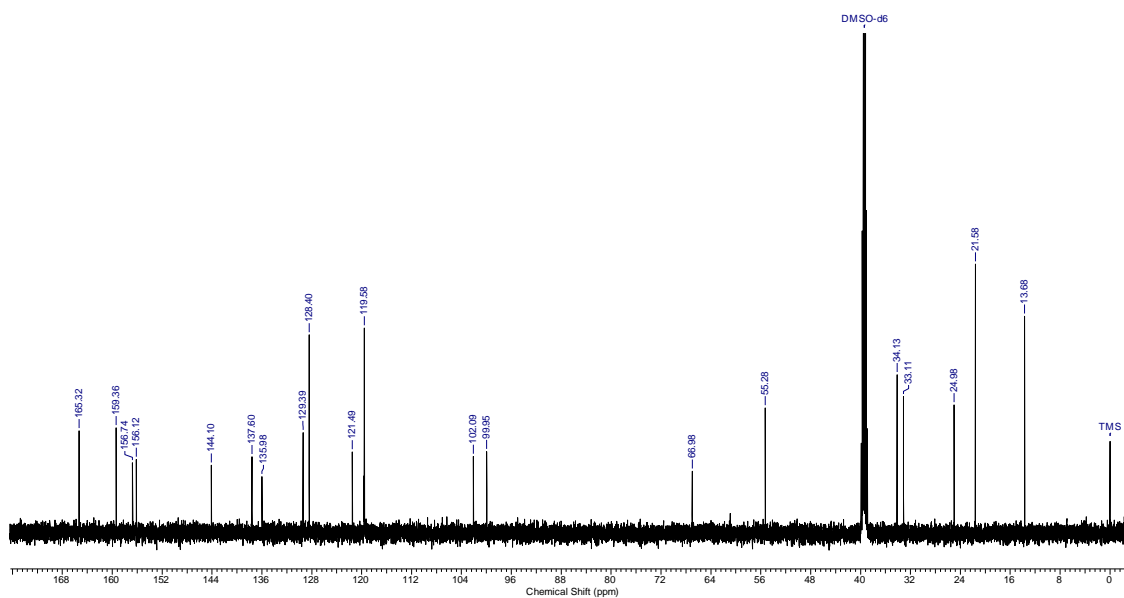


Figure S52. ^{13}C RMN spectrum of 2-[(6-methoxy-2-methylquinolin-4-yl)oxy]-*N*-(4-butylphenyl)acetamide (**12m**) in $\text{DMSO-}d_6$.

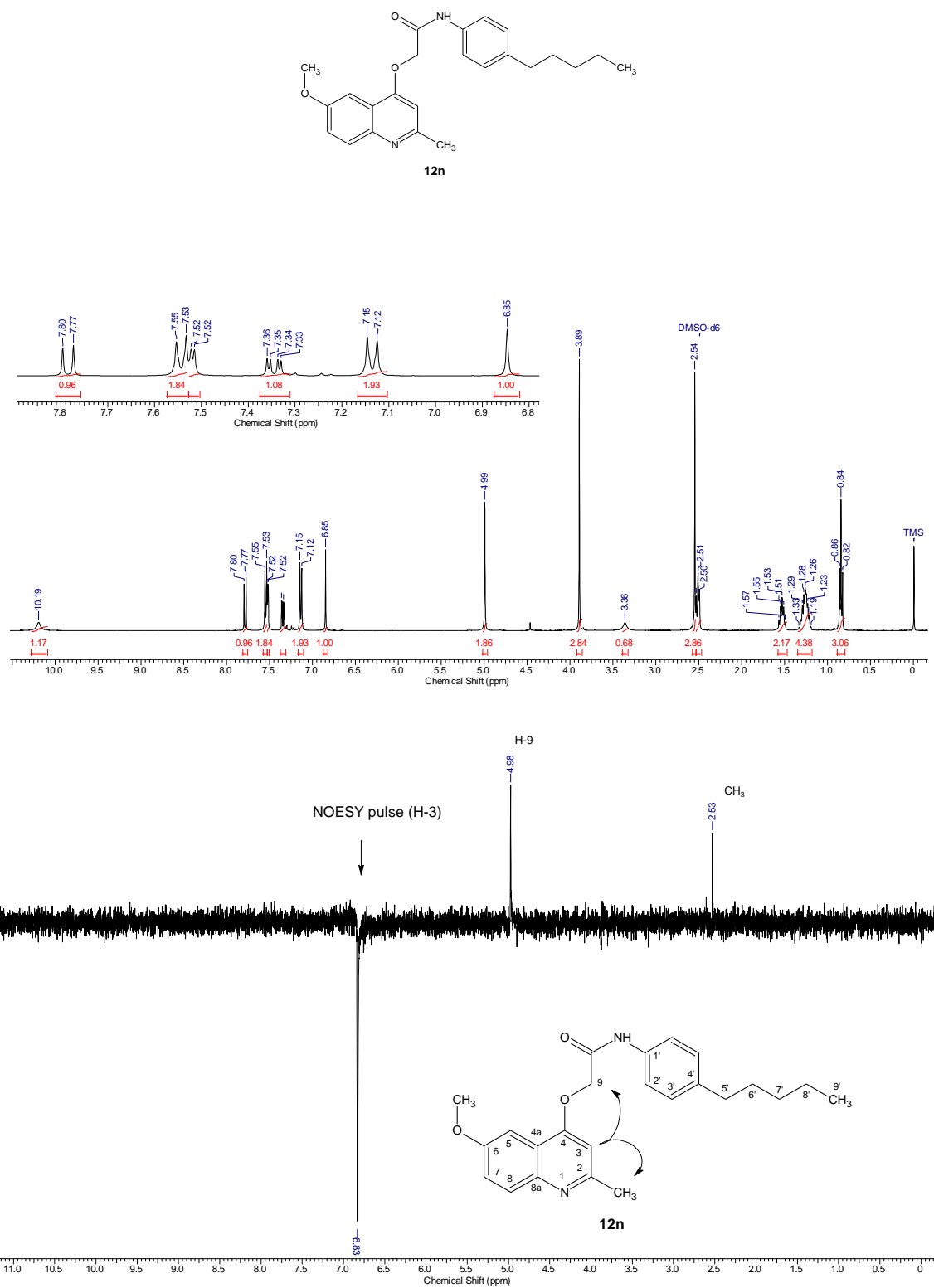


Figure S53. Top: Spectrum of ^1H NMR of 2-[(6-methoxy-2-methylquinolin-4-yl)oxy]-*N*-(4-pentylphenyl)acetamide (**12n**) in $\text{DMSO-}d_6$; Bottom: Selective 1D NOESY irradiation at = 6.83 ppm, the long-range interactions were observed between H-3 with H-9 and CH_3 .

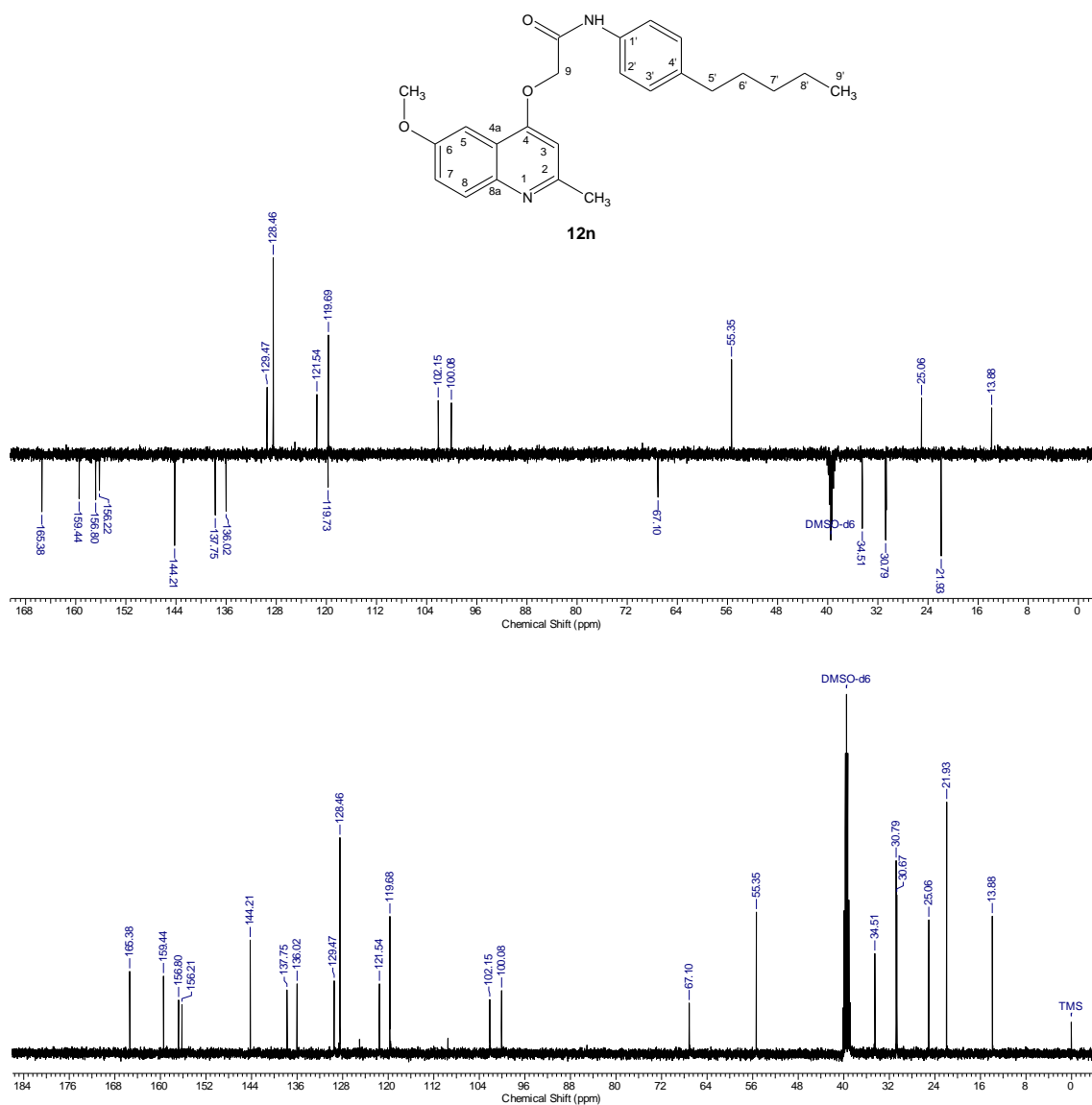
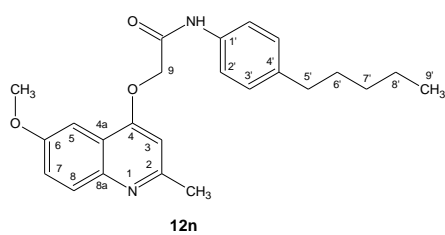


Figure S54. Top: ^{13}C APT NMR spectrum of 2-[(6-methoxy-2-methylquinolin-4-yl)oxy]-*N*-(4-pentylphenyl)acetamide (**12n**) in $\text{DMSO-}d_6$; Bottom: ^{13}C NMR of compound **12n** in $\text{DMSO-}d_6$.

Table S1. ^1H NMR and ^{13}C NMR chemical shift (δ) values for compound **12n**.

Entry	^1H NMR δ (ppm)	^{13}C NMR δ (ppm)
CH ₃	2.54	25.06
2	-	156.22
3	6.85	102.15
4	-	156.80
4 ^a	-	119.73
5	7.52	100.08
6	-	159.44
7	7.34	121.54
8	7.79	128.47
8 ^a	-	144.21
9	4.99	67.10
OCH ₃	3.89	55.35
C=O	-	165.38
1'	-	136.02
2',2''	7.54	119.69
3',3''	7.13	128.46
4'	-	137.75
5'	2.51	34.51
6'	1.55	30.79
7'	1.28	30.67
8'	1.28	21.93
9'	0.84	13.88

2. Biological Experimental Section

2.1 *Mycobacterium tuberculosis* inhibition assay

The measurements of the minimum inhibitory concentrations (MICs) for each tested compound were performed in 96-well U-bottom polystyrene microplates. Isoniazid (INH, control drug) and compound solutions were prepared at concentrations of 1 mg/ml in neat DMSO. They were diluted in Middlebrook 7H9 medium containing 10% ADC (albumin, dextrose, and catalase) to a concentration of 20 µg/mL of each compound containing 5% DMSO. Serial two-fold dilutions of each drug in 100 µl of Middlebrook 7H9 medium containing 10% ADC were prepared directly in 96-well plates at concentration ranges from 10.0 to 0.02 µg/ml. Growth controls without antibiotic and sterility controls without inoculation were included. The MIC was determined for *M. tuberculosis* H37Rv and for clinical isolate (PE-003) strains (see the main text for more information about this strain). Mycobacterial strains were grown in Middlebrook 7H9 containing 10% OADC (oleic acid, albumin, dextrose, and catalase) and 0.05% tween 80, and cells were vortexed with sterile glass beads (4 mm) for 5 min to disrupt clumps and then allowed to settle for 20 min. The supernatants were measured spectrophotometrically at an absorbance of 600 nm. The *M. tuberculosis* suspensions were aliquoted and stored at -20 °C. Each suspension was appropriately diluted in Middlebrook 7H9 broth containing 10% ADC to achieve an optical density of 0.006 at 600 nm, and 100 µl was added to each well of the plate except to the sterility controls. The plates were covered, sealed with parafilm, and incubated at 37 °C. After 7 days of incubation, 60 µl of 0.01% resazurin solution was added to each well, and the plate was incubated for an additional 48 hours at 37 °C.³ A change in color from blue to pink indicated bacterial growth, and the MIC was defined as the lowest drug concentration that prevented the color change. Three tests were conducted independently for each compound and each strain, and the MIC values reported here were either observed in at least two experiments or were the highest value observed among the three assays.

2.2 Cytotoxicity investigation

Cellular viability was determined after incubation with the test compounds essentially as previously described.⁴ The results were expressed as percentage of cell viability, in which the untreated control wells were considered as 100% of cell viability. Briefly, Vero cells were grown in DMEM media (Dulbecco's Modified Eagle Medium) supplemented with 10% inactivated fetal bovine serum and 1% antibiotics (penicillin-streptomycin). The cells were maintained in culture bottles at 37 °C in a humidified atmosphere with 5% CO₂. Cells were seeded at 3×10^4 cells/well (Vero) in a 96-well microtiter plate and incubated for 24 hours to adhere. The medium was carefully aspirated and replaced with 190 µL of DMEM and 10 µL of treatment drugs, resulting in concentration of 20 µM (DMSO 0.5%, v/v). After 72 h at 37 °C under 5% CO₂, the

cultures were incubated with MTT (1 mg/mL) for 2 h. The formazan crystals were dried at room temperature for at least 24 h and dissolved in DMSO. The absorbance was measured at 595 nm (Spectra Max M2e, Molecular Devices, USA). The precipitated purple formazan crystals were directly proportional to the number of live cells with active mitochondria. The percentage of cell viability for the treated groups was reported, in which the control wells (DMSO 0.5%-treated) were considered as 100% of cell viability: cell viability (%) = (absorbance of treated wells/absorbance of control wells) × 100. Data were expressed as the means of cell viability ± standard error of the means of three independent experiments performed in triplicate. Statistical analysis was performed by one-way analysis of variance followed by Bonferroni's post-test using GraphPad Prism 5.0 (San Diego, CA, USA). Differences were considered significant at the 95% confidence level.

References:

18. Thomas KD, Adhikari AV, Shetty NS. Design, synthesis and antimicrobial activities of some new quinoline derivatives carrying 1,2,3-triazole moiety. *Eur. J. Med. Chem.* **2010**, *45*, 3803-3810.
19. Sahu NP, Pal C, Mandal NB, Banerjee S, Raha M, Kundu AP, Basu A, Ghosh M, Roy K, Bandyopadhyay S. Synthesis of a novel quinoline derivative, 2-(2-methylquinolin-4-ylamino)-*N*-phenylacetamide: a potential antileishmanial agent. *Bioorg. Med. Chem.* **2002**, *10*, 1687-1693.
20. Palomino, J. C.; Martin, A.; Camacho, M.; Guerra, H.; Swings, J.; Portaels, F. Resazurin microtiter assay plate: Simple and inexpensive method for detection of drug resistance in *Mycobacterium tuberculosis*. *Antimicrob. Agents Chemother.* **2002**, *46*, 2720-2722.
21. Renck, D.; Machado, P.; Souto, A.A.; Rosado, L.A.; Erig, T.; Campos, M.M.; Farias, C.B.; Roesler, R.; Timmers, L.F.S.M.; de Souza, O.N.; Santos, D.S.; Basso, L.A. Design of novel potent inhibitors of human uridine phosphorylase-1: synthesis, inhibition studies, thermodynamics, and in vitro influence on 5-fluorouracil cytotoxicity. *J. Med. Chem.* **2013**, *56*, 8892-8902.

5 CONSIDERAÇÕES FINAIS

Este trabalho foi realizado buscando aprimorar características farmacêuticas do composto 5s (Pissinate et al. 2016), previamente desenvolvido pelo Centro de Pesquisa em Biologia Celular e Molecular. Podemos observar que o aumento da lipofilicidade dos compostos levou a uma melhora no MIC, chegando ao composto 12n com MIC de 5,1 nM frente à cepa H37Rv sendo definido como o novo composto líder.

Mais trabalhos ainda serão necessários para avaliar melhor as características farmacêuticas do composto 12n, assim como caracterizar sua farmacodinâmica e farmacocinética.

6 REFERÊNCIAS BIBLIOGRÁFICAS

Alimuddin Zumla, Payam Nahid, Stewart T. Cole. Advances in the development of new tuberculosis drugs and treatment regimens. *Nature reviews* 2013, 12(5):388-404

Andries K, Verhasset P, Guillemont J, Göhlman HW, Neefs JM, Winkler H, Van Gestel J, Timmerman P, Zhu M, Lee E, Williams P, de Chaffoy D, Huitric E, Hoffner S, Cambau E, Truffot-Pernot C, Lounis N, Jarlier V. A diarylquinoline drug active on the ATP synthase of *Mycobacterium tuberculosis*. *Science* 2005 14; 307: 223-7.

Balganesh TS, Alzari PM, Cole ST. Rising standards for tuberculosis drug development. *Trends Pharmacol Sci.* 2008;29(11):576-81.

Ballell L, Bates RH, Young RJ, Alvarez-Gomez D, Alvarez-Ruiz E, Barroso V, Blanco D, Crespo B, Escribano J, Gonzáles R, Lozano S, Huss S, Santo-Villarejo A, Martín-Plaza JJ, Mendoza A, Rebollo-Lopez MJ, Remuñan-Blanco M, Lavandera JL, Pérez-Herran E, Gamo-Benito FJ, García-Bustos JF, Barros D, Castro JP, Cammack N. Fueling open-source drug discovery: 177 small-molecule leads against Tuberculosis. *ChemMedChem.* 2013 Feb;8(2):313-21.

Barreiro, Eliezer J, Fraga, Carlos Alberto Manssour. *Química Medicinal: As bases moleculares da ação dos fármacos.* 2. ed. São Paulo: Artmed, 2005. 536 p.

Basso LA, Blanchard JS. Resistance to antitubercular drugs. *Adv Exp Med Biol* 1998; 456:115-44.

Beena, Rawat, DS. Antituberculosis Drug Research: A Critical Overview. *Med Res Rev.* 2013 Jul;33(4):693-764.

Bleicher KH, Böhm HJ, Müller K, Alanine AI. Hit and lead generation: beyond high-throughput screening. *Nature Rev Drug Discov* 2003; 2: 369-378.

Denny WA. Anti-cancer 2,3-dihydro- 1H-pyrrolo[3,2-f]quinoline complexes of cobalt and chromium. U.S. Patent 2006, 7064117.

Dhillon J, Andriez K, Phillips PP, Mitchison DA. Bactericidal activity of the diarylquinoline TMC207 against *Mycobacterium tuberculosis* outside and within cells. *Tuberculosis* 2010;90:301– 305.

Dorman SE, Chaisson RE. From magic bullets back to the Magic Mountain: the rise of extensively drug-resistant tuberculosis. *Nature Med* 2007; 13: 295-8.

Drlica K, Zhao X. Dna gyrase, topoisomerase IV and the 4-quinolones. *Microbiol Mol Biol Rev* 1997 Sep; 61 (3) :377-92.

- Drlica K. Mechanism of fluoroquinolone action. *Curr Opin Microbiol* 1999; 2 (5): 504-8
- Ducati RG, Ruffino-Netto A, Basso LA, Santos DS. The resumption of consumption -- a review on tuberculosis. *Mem Inst Oswaldo Cruz* 2006; 101 (7): 697-714.
- Duncan K. Progress in TB drug development and what is still needed. *Tuberculosis* 2003; 83: 201-7.
- Elston JW, Thaker HK. Co-infection with human immunodeficiency virus and tuberculosis. *Indian J Dermatol Venereol Leprol* 2008; 74 (3): 194-9.
- Ernst JD. The immunological life cycle of tuberculosis. *Nat Rev Immunol*. 12. England 2012. p. 581-91.
- Flynn JL, Chan J. Immunology of tuberculosis. *Annu Rev Immunol* 2001; 19:93-129.
- Gandhi NR, Moll A, Sturm AW, Pawinski R, Govender T, Lallo U, Zeller K, Andrews J, Friedland G. Extensively drug-resistant tuberculosis as a cause of death in patients co-infected with tuberculosis and HIV in a rural area of South Africa. *Lancet* 2006; 368: 1575-80.
- Global Tuberculosis Control: a short update to the 2009 report. Geneva: World Health Organization, 2010.
- Global Tuberculosis Report 2012. Geneva: World Health Organization, 2012.
- Hoshino K. ET AL antimicrob. Agents Chemother 2008, 52 (1) , 65-76.
- Jarlier V, Nikaido H. Mycobacterial cell wall: structure and role in natural resistance to antibiotics. *FEMS Microbiol Lett* 1994; 123 (1-2): 11-8.
- Jassal M, Bishai WR. Extensively drug-resistant tuberculosis. *Lancet Infect Dis* 2009; 9 (1): 19-30.
- Kaufmann SH. Recent findings in immunology give tuberculosis vaccines a new boost. *Trends Immunol*. 26. England 2005. p. 660-7.
- Kaufmann SHE. How can immunology contribute to the control of tuberculosis? *Nature Reviews Immunology* 2001; 1: 20-30.
- Kawai V, Soto G, Gilman RH, Bautista CT, Caviedes L, Ticona E, Ortiz J, Tovar M, Chavez V, Rodriguez R, Escombe AR, Evans CA. Tuberculosis mortality, drug resistance, and infectiousness in patients with and without HIV infection in Peru. *Am J Trop Med Hyg*. 2006;75(6):1027-33.
- Koul A, Arnoult E, Lounis N, Guillemont J, Andries K. The challenge of new drug discovery for tuberculosis. *Nature*. 469. England 2011. p. 483-90.

Kumar R, Madhumathi BS, Nagaraja V. Molecular basis for the differential quinolone susceptibility of mycobacterial DNA gyrase. *Antimicrob Agents Chemother* 2014; 58 (4): 2013-20.

Lamichhane G. Novel targets in *M. tuberculosis*: search for new drugs. *Trends Mol Med* 2010 Elsevier Ltd; 2010.

Lienhardt C, Glaziou P, Uplekar M, Lönnorth K, Getahun H, Raviglione M. Global tuberculosis control: lessons learnt and future prospects. *Nat Rev Microbiol*. 10. England 2012. p. 407-16.

Lilienkampf A, Mao J, Wan BY, Franzblau SG, Kozikowski AP. Structure-activity relationships of quinoline-based compounds active against replicating and nonreplicating *Mycobacterium tuberculosis*. *J Med Chem* 2009 9; 52 (7): 2109-18.

Loewenberg S. India reports cases of totally drug-resistant tuberculosis. *Lancet* 2012; 379:205.

MacPherson IS, Kirubakaran S, Gorla SK, Riera TV, D'Aquino JA, Zhang M, Cuny GD, Hedstrom L. The structural basis of Cryptosporidium -specific IMP dehydrogenase inhibitor selectivity. *J Am Chem Soc* 2010 3; 132: 1230-1.

Mahamoud A, Chevalier J, Davin-Regli A, Barbe J, Pagès JM. Quinoline derivatives as promising inhibitors of antibiotic efflux pump in multidrug resistant *Enterobacter aerogenes* isolates. *Curr Drug Targets* 2006; 7: 843–847.

Mathew B, Ross L, Reynolds RC. A novel quinoline derivative that inhibits mycobacterial FtsZ. *Tuberculosis* 2013; 398-400.

Ministério da saúde. Boletim Epidemiológico. Volume 43, março 2012.

Mitchison DA, Davies G. The chemotherapy of tuberculosis: past, present and future. *Int J Tuberc Lung Dis* 2012; 16: 724-732.

Multidrug and extensively drug-resistant TB (M/XDR-TB): 2010 global report on surveillance and response. Geneva: World Health Organization, 2010.

Muscia GC, Buldain GY, Asís SE. Design, synthesis and evaluation of acridine and fused-quinoline derivatives as potential anti-tuberculosis agents. *European Journal of Medicinal Chemistry* 2014, 12; 73: 243-9.

Nasveld P, Kitchener S. Treatment of acute vivax malaria with tafenoquine. *Trans R Soc Trop Med Hyg* 2005; 99: 2–5.

O'Brien RJ, Nunn PP. 2001. The need for new drugs against tuberculosis - Obstacles, opportunities, and next steps. *Am J Respir Crit Care Med* 2001; 163: 1055-1058.

Pabloz-Mendez A, Gowda D, Friden T. Controlling multidrug-resistant tuberculosis and access to expensive drugs: a rational framework. Bull World Health Organization 2002; 80 (6): 489-495.

Palomino JC, Martin A. TMC207 becomes bedaquiline, a new anti-TB drug. Future Microbiology 2013; 10, 2217

Parrish NM, Dick JD, Bishai WR. Mechanisms of latency in *Mycobacterium tuberculosis*. Trends Microbiol. 6. England 1998. p. 107-12.

Pissinate K, Villela AD, Rodrigues-Junior R, Giacobbo BC, Grams ES, Abbadi BL, da Trindade RV, Back DF, Campos MM, Basso LA, Santos DS, Machado P. Synthesis and structure-activity relationships for a series of 4-quinoloxycetamides active against drug-susceptible and drug resistant *Mycobacterium tuberculosis* strains. DOI:10.1021/acsmedchemlett.5b00324.

Ramakrishnan L. Revisiting the role of the granuloma in tuberculosis. Nat Rev Immunol. 12. England 2012. p. 352-66.

Ramaswamy S, Musser JM. Molecular genetic basis of antimicrobial agent resistance in *Mycobacterium tuberculosis*: 1998 update. Tuberc Lung Dis. 1998; 79 (1): 3-29.

Renck D, Machado P, Souto AA, Rosado LA, Eriq T, Campos MM, Farias CB, Roesler R, Timmers LF, de Souza ON, Santos DS, Basso LA. Design of novel potent inhibitors of human uridine phosphorylase-1: Synthesis, inhibition studies, thermodynamics and in vitro influence of 5-Fluorouracil cytotoxicity. J Med Chem 2013, 16; 56, 8892-8902.

Russell DG. WHO puts the tubercle in tuberculosis? Nat Rev Microbiol. 2007;5(1):39-47.

Rustomjee R, Diacon AH, Allen J, Venter A, Reddy C, Patientia RF, Mthiyane TC, De Marez T, van Heeswijk R, Kerstens R, Koul A, De Beule K, Donald PR, McNeeley DF. Early bactericidal activity and pharmacokinetics of the diarylquinoline TMC207 in treatment of pulmonary tuberculosis. Antimicrob Agents Chemother 2008; 52: 2831–2835.

Sacchettini JC, Rubin EJ, Freundlich JS. Drugs versus bugs: in pursuit of the persistent predator *Mycobacterium tuberculosis*. Nat Rev Microbiol. 6. England 2008. p. 41-52.

Singh JA, Upshur R, Padayatchi N. XDR-TB in South Africa: no time for denial or complacency. PLoS Med 2007; 4 (1): e50.

Strekowski L, Mokrosz JL, Honkan VA, Czarny A, Cegla MT, Wydra RL, Patterson SE, Schinazi RF. Synthesis and quantitative structure-activity relationship analysis of 2-(aryl or heteroaryl)quinolin-4-amines, a new class of anti-HIV-1 agents. J Med Chem 1991; 4: 1739–1746.

Treatment of Tuberculosis: guidelines for national programmes. Geneva: World Health Organization, 2003.

Tuberculosis Antimicrobial Acquisition & Coordinating Facility (TAACF), 2001.

Udwadia ZF, Amale RA, Ajbani KK, Rodrigues C. 2011. Totally drug-resistant tuberculosis in India. *Clin Infect Dis* 2011; 54: 579-581.

Umeijiego NN, Gollapalli D, Sharling L, Voulfstun A, LU J, Benjamin NN, Stroupe AH, Riera TV, Striepen B, Hedstrom L. Targeting a prokaryotic protein in a eukaryotic pathogen: identification of lead compounds against cryptosporidiosis. *Chem Biol* 2008; 15: 70-77.

Velayati AA, Farnia P, Masjedi MR, Ibrahim TA, Tabarsi P, Haroun RZ, Kuan HO, Ghanavi J, Farnia P, Varahram M. Totally drug-resistant tuberculosis strains evidence of adaptation at cellular level. *European Respiratory Journal* 2009; 34, 1202-1203.

Wilson WD, et al. Design of RNA interactive anti-HIV-1 agents: Unfused aromatic intercalators. *Med Chem Res* 1992; 2: 102-110.

World Health Organization. Multidrug and extensively drug-resistant TB (M/XDR-TB): 2010 global report on surveillance and response. 2010. (http://whqlibdoc.who.int/publications/2010/9789241599191_eng.pdf)

World Health Organization. Guidelines for the programmatic management of drug-resistant tuberculosis, Emergency update 2008. 2008. (http://whqlibdoc.who.int/publications/2008/9789241547581_eng.pdf?ua=1)

World Health Organization. WHO report 2015: Global tuberculosis report. 2015. (apps.who.int/iris/bitstream/10665/191102/1/9789241565059_eng.pdf?ua=1)

Wu WN, Yuan WB, Tang N, Yang RD, Yan L, Xu ZH. Synthesis, characterizations and luminescent properties of three novel aryl amide type ligands and their lanthanide complexes. *Spectrochimica Acta Part A* 65 2006, 912-918.

Yew WW, Leung CC. Management of multidrug-resistant tuberculosis: Update 2007. *Respirology* 2008; 13 (1): 21-46.

Zager EM, McNerney R. Multidrug-resistant tuberculosis. *BMC Infect Dis* 2008; 8: 10.

Zahrt TC. Molecular mechanisms regulating persistent *Mycobacterium tuberculosis* infection. *Microbes Infect.* 5. France 2003. p. 159-67.

Zahrt TC. Molecular mechanisms regulating persistent *Mycobacterium tuberculosis* infection. *Microbes Infect.* 5. France 2003. p. 159-67.